

UCLA-ENG-7371

September 1973

CATALYSTS FOR AUTOMOTIVE
POLLUTION CONTROL DEVICES

Final Report - ARB Project No. 2-009-1a

Ken Nobe, Principal Investigator
George L. Bauerle, Project Engineer

Project Staff:

J. D. Pinkerton
L. L. C. Sorensen
N. T. Thomas
S. C. Wu
R. A. Orsini
S. A. Tunick
J. Kuo
K. Barry
K. Kiisel

LIBRARY
AIR RESOURCES BOARD
P. O. BOX 2015
SACRAMENTO, CA 95812

School of Engineering and Applied Science
University of California
Los Angeles

FOREWORD

The work in this project was supported by the Air Resources Board of the State of California under ARB Project No. 2-009-1a.

ABSTRACT

Over a hundred catalysts have been screened for potential use in automobile exhaust converters for removal of CO, hydrocarbons or NO_x. The studies consisted of laboratory tests using dry gases as well as actual auto exhaust tests with the more promising catalysts. For CO and hydrocarbon oxidation only the noble metals showed sufficient activity to attain cold-start emissions standards. For reduction of NO_x only ruthenium and mixed ruthenium oxide catalysts showed satisfactory low temperature activity and low production of undesired ammonia. Strontium yttrium ruthenium oxide shows considerable promise. Since warmup problems are not as severe for NO_x control as for CO and hydrocarbon control, cheaper catalysts which have NO_x-removal capability only at high temperatures may be tolerable; several base metal catalysts are promising for such operation. By using strontium yttrium ruthenium oxide catalyst in the first stage of a two-stage converter, over 90% NO removal has been achieved. The fuel economy loss was about 11%. Extended testing of platinum catalyst in the second stage showed no appreciable deterioration for about 150 hours. Total removal of CO was observed up to that time. Degradation that occurred after that time was caused by a trace lead contamination of the unleaded gasoline supply.

SUMMARY

Catalytic converters for control of hydrocarbons and carbon monoxide (CO) in automobile exhaust have been considered the most promising method to meet 1975 emissions standards. Up to the present time only the noble metals have demonstrated adequate activity and durability for use as oxidation catalysts. Catalysis has also been considered for the control of oxides of nitrogen (NO_x) by the reduction of NO_x with CO and hydrogen (H_2) in the first stage of a two-stage converter (the second stage would contain the oxidation catalyst). Little published data exist describing two-stage converter performance.

This program was undertaken to provide information about the performance of two-stage converters. The development of active, inexpensive and durable catalysts for either oxidation or reduction was of primary emphasis.

Over one hundred catalysts were tested for activity in the oxidation of CO and in the reduction of NO_x by CO and H_2 . The more promising catalysts were evaluated further in actual exhaust gases in a small reactor simulating either the oxidation or reduction converter. Finally, several catalysts were tested in full-scale devices.

Some of the more promising catalysts in the laboratory studies for oxidation of CO were:

The noble metals	Cobalt oxide
Rare earth cobalt oxides	Monel
Lanthanum rhodium oxide	

For reduction of NO with CO or H_2 the following catalysts were most promising:

- Ruthenium
- Strontium ruthenium oxide
- Strontium yttrium ruthenium oxide

Monel
Nickel chromium spinels
Rare earth nickel oxide
Copper nickel oxide
Lanthanum nickel ruthenium oxide
Lanthanum rhodium oxide
Nickel oxide

In the latter group, the criteria used was both high activity for NO reduction as well as low ammonia (NH_3) production during reduction with H_2 in the temperature range, 100°C to 500°C .

When tested in automobile exhaust in the small reactor with injection of secondary air to simulate oxidation converter operation, several of the more promising catalysts showed very poor activity. Only noble metal catalysts exhibited CO and hydrocarbon oxidation activity sufficient to attain emissions standards by cold-start driving schedules. For NO_x reduction in simulated first stage converter operation, only ruthenium and mixed ruthenium oxides performed satisfactorily. These catalysts appear to exhibit true selectivity for reduction of NO_x to nitrogen rather than to NH_3 .

Strontium yttrium ruthenium oxide showed particular promise since it showed the smallest difference in NO_x reduction activity between the dry, synthetic gas experiments and the actual auto exhaust tests. Other catalysts showed substantial loss of activity; in some instances temperatures several hundred degrees higher were required to develop NO_x conversion levels equivalent to those observed in the laboratory.

Copper chromite, monel, stainless steel and strontium yttrium ruthenium oxide were evaluated as first-stage catalysts in a full-scale, two-stage converter. Platinum catalysts were used in the second stage for all full-scale two-stage converter tests. Strontium yttrium ruthenium oxide was particularly effective for NO_x removal. Copper chromite was moderately active while monel and stainless steel required very high temperatures for adequate performance. With the mixed ruthenium oxide catalyst, 90% NO_x removal was achieved with the A/F ratio set to give

3% CO in the exhaust. Fuel economy loss was 11% with such operation.

The platinum catalyst was operated for 150 hours with no loss in activity. Essentially total CO removal was achieved under controlled, steady-state test conditions. Deterioration in activity occurred subsequent to that time and has been attributed to lead contamination of the unleaded gasoline used after the original supply was depleted at about 120 hours operation.

TABLE OF CONTENTS

	Page
1. Introduction	1
1.1 Laboratory Development of Catalysts	1
1.2 Automotive Exhaust Studies	1
1.2.1 Prototype Exhaust Converter	1
1.2.2 Small Scale Exhaust Reactor	1
1.2.3 Construction and Test of a Two-Stage Device	2
2. Background	3
3. Experimental Procedure	7
3.1 Laboratory Screening Tests	7
3.2 Catalysts Studied in Screening Tests	12
3.3 Automotive Exhaust Tests	21
3.3.1 Small-Scale Exhaust Reactor	22
3.3.2 Prototype Exhaust Converter	27
3.3.3 Two-Stage Catalytic Converter	31
4. Results and Discussion	35
4.1 Screening Studies	35
4.1.1 Catalytic NO Reduction with CO	35
4.1.2 Catalytic Oxidation of CO	49
4.1.3 Catalytic NO Reduction with H ₂	59
4.2 Automotive Exhaust Tests	85
4.2.1 Auto Exhaust Tests with a Small Reactor	85
4.2.2 Prototype Full-Scale Converter	95
4.2.3 Automotive Tests of a Two-Stage Platinum Converter	113
4.2.4 Auto Exhaust Tests with Full-Scale, Two-Stage Reactor	122
5. References	147
6. Appendix	149

LIST OF FIGURES

Figure		Page
3-1	Schematic of Screening Reactor.	8
3-2	Screening Studies Test System.	9
3-3	Typical Mixing Manifold and Reactor Assembly.	10
3-4	Analytical Equipment Used in Automotive Tests.	23
3-5	Schematic of Small-Scale Exhaust Reactor.	25
3-6	Small Exhaust Reactor Test System.	26
3-7	View of Disassembled Axial-Flow Reactor.	29
3-8	Axial-Flow Converter Mounted on Engine Exhaust Line.	30
3-9	Schematic of Two-Stage Catalytic Converter.	32
3-10	Two-Stage Converter Mounted on Engine Exhaust Line.	34
4-1	Reduction of NO with CO on Noble Metal Catalysts.	41
4-2	Reduction of NO with CO on Rh-Based Catalysts.	43
4-3	Reduction of NO with CO on Ru-Based Catalysts.	44
4-4	Protruded Metal Hollow Semi-Cylindrical Catalyst.	45
4-5	Reduction of NO with CO on Metal Catalysts.	46
4-6	Reduction of NO with CO on NiO·Cr ₂ O ₃ Spinel Catalysts.	48
4-7	Oxidation of CO on Noble-Metal Catalysts.	54
4-8	Oxidation of CO on Metal Catalysts.	55
4-9	Oxidation of CO on Cobalt Oxide Catalysts.	57
4-10	Oxidation of CO on Impregnated Rare Earth Cobalt Oxide Supported on Various Carriers.	60
4-11	Oxidation of CO on LaRhO ₃ Catalysts.	61
4-12	Oxidation of CO on NiO·Cr ₂ O ₃ Catalysts.	62
4-13	Reduction of NO with H ₂ and Production of NH ₃ on Pressed Nickel-Chromium Spinel Catalysts.	75
4-14	Reduction of NO with H ₂ and Production of NH ₃ on Impregnated Nickel-Chromium Catalysts.	76

LIST OF FIGURES (cont.)

Figure		Page
4-15	Reduction of NO with H ₂ and Production of NH ₃ on Impregnated Nickel-Copper Catalysts.	78
4-16	Reduction of NO with H ₂ and Production of NH ₃ on LaRhO ₃ Catalysts.	80
4-17	Reduction of NO with H ₂ and Production of NH ₃ on Noble Metal Catalysts.	81
4-18	Reduction of NO with H ₂ and Production of NH ₃ on Ruthenium-Based Catalysts.	83
4-19	Reduction of NO with H ₂ and Production of NH ₃ on NiO catalysts.	84
4-20	Oxidation of CO in Auto Exhaust using Small Reactor.	89
4-21	Reduction of NO in Auto Exhaust using Small Reactor.	90
4-22	Production of NH ₃ During Reduction of NO in Small Reactor.	91
4-23	NO Reduction and NH ₃ Production in Auto Exhaust using Small Empty Reactor.	93
4-24	Engelhard PTX Converter and a Monolithic Structure as Typically Incorporated.	98
4-25	Incipient Burnout of PTX After Less than 10 Hours Operation.	101
4-26	Exhaust Gas Concentration over FTP Cycle (Time x 1.5) with Two-Stage PTX Converter and High-Performance Carburetion and Ignition Systems.	115
4-27	Exhaust Gas Concentration over FTP Cycle with Two-Stage PTX Converter and Standard Carburetion and Timing.	118
4-28	Comparison of Exhaust Gas Concentration over FTP Cycle with Exhaust Thermal Reactor and Two-Stage PTX Converter.	120
4-29	Damage to PTX Converter after Less than 2000 Miles Operation.	121

LIST OF FIGURES

Figure		Page
4-30	Flow Diverting Tube Installed in Inlet Plenum Chamber.	125
4-31	Pressure Drop through Two-Stage Converter Girdler G-43 Used as Second Stage.	126
4-32	Effect of Initial CO Concentration on NO Conversion with Copper Chromite Catalyst. Normal Spark Advance.	127
4-33	Effect of Initial CO Concentration on NO Conversion with 304 Stainless Steel Catalyst. Normal Spark Advance.	128
4-34	Effect of Initial CO Concentration on Conversion of NO using Monel Chips. Tests run with Retarded Spark.	129
4-35	Effect of CO Concentration of Conversion of NO using Sr-Y-Ru Monolith. Standard Spark Advance.	130
4-36	Effect of CO Initial Concentration on NO Conversion on Sr-Y-Ru Monolith. Tests Run with Spark Retarded.	131
4-37	Comparison of Sr-Y-Ru Monolith and Monel Catalysts with Two Different Spark Settings.	133
4-38	Effect of Spark Advance and CO Concentration on Fuel Economy.	134
4-39	Effect of Manifold Afterburning on NO Reduction on Sr-Y-Ru Monolithic Catalyst. Spark Retarded.	136
4-40	Effect of Manifold Afterburning on Reactor Temperatures.	137
4-41	Transient Operation of Two-Stage Converter. Sr-Y-Ru Monolith in First Stage, G-43 in Second Stage. Normal Spark Advance, 25% Secondary Air.	139
4-42	Transient Operation of Two-Stage Converter. Sr-Y-Ru Monolith in First Stage, G-43 in Second Stage. Spark Retarded, 25% Secondary Air.	140
4-43	Transient Operation of Two-Stage Converter. Monel in First Stage, G-43 in Second Stage, 25% Secondary Air.	142
4-44	Effect of Running Time on CO and Hydrocarbon Conversion.	143
4-45	Influence of CO Concentration on CO Conversion for Platinum Catalyst at Start and End of Two-Stage Tests.	144

LIST OF TABLES

Table		Page
3-1	Catalyst Description.	13
3-2	Approximate Composition of Rare Earth Mixtures.	20
3-3	Typical Exhaust Compositions Used in Small Reactor Studies.	27
3-4	Typical Test Modes with a Prototype Converter.	28
4-1	Summary of Results of Screening Studies-Reduction of NO with CO.	36
4-2	Summary of Results with Catalysts Promoting 80% Conversion of NO or Higher at 275°C or Less with CO.	40
4-3	Summary of Results of Screening Studies-Oxidation of CO in Air.	50
4-4	Summary of Results with Catalysts Promoting 80% Conversion of CO or Higher at 110°C or Less.	53
4-5	Summary of Activity Tests of NO Reduction with H ₂ .	63
4-6	Summary of Results with Catalysts Producing High Yields of NH ₃ and Higher than 90% Conversion of NO.	72
4-7	Summary of Results with Catalysts Producing Low Yields of NH ₃ and Higher than 90% Conversion of NO.	73
4-8	List of Catalysts Tested in Small Reactor.	87
4-9ab	Catalytic Oxidation and Reduction of Auto Exhaust in the Small Reactor.	88
4-10	Baseline Emissions for 170 CID, Six-Cylinder Engine.	97
4-11	Performance of Platinum Oxidation Converter.	99
4-12	Inhibition Effects on CO Oxidation over Rare Earth Cobalt Oxide on Cordierite Monolith Carrier.	103
4-13	Performance of Rare Earth-Cobalt Oxide Monolith Converter (small scale).	105
4-14	Performance of Pelletized Ni-Pt-Al ₂ O ₃ and Pelletized Rare Earth Cobalt Oxide-Al ₂ O ₃ Converters.	106
4-15	Performance of Pelletized Ni-Pt-Al ₂ O ₃ (G-43) Converter. Emissions with Variable Secondary Air Flow.	108
4-16	Performance of Large-Scale Catalytic Converters.	110

LIST OF TABLES (Contd.)

Table		Page
4-17	Exhaust Concentration During Various Driving Modes with Modified Carburetion and Ignition Systems and Two-Stage Platinum Exhaust Reactors.	117
4-18	Exhaust Concentrations During Various Driving Modes with Stock Carburetor and Ignition Systems and Two-Stage Platinum Exhaust Reactor.	117
A-1	Cross-Reference Listing of Catalysts.	149

1. INTRODUCTION

This report describes work performed on Air Resources Board Project ARB No. 2-009-1a, covering the period May 1, 1971 through June 30, 1973. The overall objective of this project was the investigation of catalytic methods for control of automotive exhaust emissions. The specific aims of the program were divided into two broad areas of study: (a) laboratory development of catalysts and (b) automotive testing of the more promising catalysts including those commercially available. The automotive tests involved two versions of a full-scale converter and a smaller exhaust reactor capable of parametric variation of test conditions.

1.1 Laboratory Development of Catalysts.

In this phase, an extensive laboratory investigation was made of new and improved catalysts for use in the reduction of NO by CO or H₂. In addition, catalysts were sought for use in oxidation converters for removal of CO and hydrocarbons. Several commercial catalysts, including noble metals, were also screened.

1.2 Automotive Exhaust Studies.

1.2.1 Prototype Exhaust Converter

At the outset of the project, a prototype exhaust converter was built and tested using several known catalysts and carriers as well as catalysts showing promise during the initial screening studies. The converter consisted of a single catalyst bed which served to study both oxidation and reduction reactions by alteration of engine operating conditions.

1.2.2 Small Scale Exhaust Reactor.

A small reactor employing laboratory-scale quantities of catalyst was designed and built to study parametric effects on converter operation in a rapid, economical manner. Although the reactor used only part of the exhaust from the test engine, flow rates and catalyst quantities were such that reasonable "scale down" conditions were employed. As in the

previous sub-task, each catalyst was studied for its potential as either a first or second-stage catalyst.

1.2.3 Construction and Test of a Two-Stage Device.

Some promising catalysts were tested in a two-stage catalytic converter. Although not of "road-weight" because of features incorporated into the design permitting rapid changes in catalyst loading and the use of instrumentation devices attached to the unit, extensive testing was done on a dynamometer-mounted engine.

2. BACKGROUND

Catalytic afterburners have been shown to be practical for the control of CO and hydrocarbons in automobile exhausts (Cannon, 1957; Sourirajan and Accomazzo, 1961; Andersen et al., 1961). Extensive research and development in catalysis was carried out in the early 1960's by auto and catalyst manufacturers, and intensified with the passage of the 1970 Clean Air Act. However, to meet the first emissions standards for hydrocarbons and CO emissions in 1966, automobile manufacturers found that carburetion and timing modifications and/or manifold thermal reactors were adequate.

Thus far, no catalyst has been shown to even approach the effectiveness of the noble metals for CO and hydrocarbon oxidation. Removal of NO by a catalytic process is much more difficult than the control of CO and hydrocarbons. On presently known catalysts dissociation of NO is far too slow to be of practical use (Shelef et al., 1969; Shelef and Kummer, 1969; Bartok et al., 1969). A more promising approach is the reduction of NO by the CO, hydrogen and hydrocarbons normally present in exhaust gases (Sourirajan and Blumenthal, 1961; Baker and Doerr, 1964; Taylor, 1959; Aye and Ng, 1966). Unfortunately, there has been little success in meeting the goal of NO removal from normally-operating engines because of the detrimental effect of oxygen since there must be enough reductant in the exhaust to remove all the O₂ and to reduce the NO.

The NO, CO and hydrocarbons can be removed catalytically from auto exhausts by the use of the two-stage converter suggested in 1961 by Sourirajan and Blumenthal (1961). In this device, the exhaust from the engine, which is adjusted for rich operation (i. e., exhaust O₂ is minimized), is passed through the first stage in which NO is reduced by the excess CO. In the second stage oxygen is admitted to oxidize the remaining CO and hydrocarbons. It was just at the start of this project that the first data related to two-stage converter operation were reported (primarily by the IIEC group, e. g., Meguerian and Lang 1971, and by workers at Esso, Bernstein et al., 1971, and Lunt et. al., 1972).

The ultimate goal in the development of catalytic exhaust converters is the discovery of materials capable of promoting the reduction of NO in the presence of large amounts of O₂; thus, optimum economic operation of the engine could be maintained. A more realistic goal would be the development of catalysts that would accelerate the reduction of NO with reductants in fuel-rich atmospheres to a greater extent than that presently observed on known catalysts.

A potential problem in the use of catalysis for NO control is that NO may be only partially reduced to ammonia (NH₃) by hydrogen in the exhaust and not completely reduced to the desired N₂ and O₂. Such production of NH₃ was observed some time ago (Sourirajan and Blumenthal, 1961).

Hydrogen is normally present in exhaust in concentrations ranging from 1/5 to 1/2 that of CO. In addition, in converters, hydrogen can be formed from the reaction between water and CO (the "water-gas shift" reaction) under some conditions. Regardless of the source of hydrogen, ammonia formed by partial reduction of NO can be easily oxidized back to NO in the second, oxidation stage of a dual converter on most catalysts.

For use in NO reduction, most known non-noble metal catalysts must be in a reduced state to be effective (Baker and Doerr, 1965). A mechanism postulated for the reduction of NO (Shelef et al., 1968) is that NO does not react directly with CO but is reduced by the catalyst surface which is then itself reduced by CO. Thus, the lack of activity in the presence of O₂ is due to the fact that the O₂ selectively reacts with the surface, thereby excluding participation of NO in the reaction (unless there are sufficient reductants present to react with all the O₂ first). Unfortunately, even if the catalyst is given appropriate pre-treatment to put it in the required reduced state, and if the carburetor of the engine is adjusted for overall, rich operation, the exhaust can still become oxidizing at times leading to changes in the surface properties and activity of the catalyst (Roth, 1972). Such changes can be due to the interaction between catalyst and carrier. Ideally, a catalyst for NO reduction would be one that does

not rely on pre-treatment for activity or, at least, if pre-treatment is needed, does not undergo drastic surface property changes upon cyclical oxidizing and reducing conditions of the exhaust.

The present program was undertaken with several primary aims. In view of the paucity of published data on the operation of two-stage catalytic converters, it was felt desirable to explore such operation, principally in terms of species distribution between the stages.

It was of interest to determine the importance of the ammonia problem. In this latter area, the NO-reduction system has one advantage. During engine warmup, NO production is relatively low. Attainment of proper temperatures in the second stage indirectly implies that the first stage must reach elevated temperatures equally rapidly. Since decomposition of NH_3 is favored at elevated temperatures it is possible that relatively small amounts of NH_3 may be transmitted from the first to the second stage throughout an overall driving cycle. Description of such effects was a goal of the present research.

Laboratory studies in the development of catalysts for reduction of NO by CO and H_2 were performed. Catalysts were sought which do not promote extensive production of NH_3 . A critical comparison of the activities of noble metals and non-noble metals for the oxidation of CO was also made.

Particular emphasis was placed on the development of catalysts that do not experience severe activity change after exposure to cyclic exhaust environments. In particular, catalysts which maintain high activity for NO reduction after exposure to oxidizing atmospheres were sought.

3. EXPERIMENTAL PROCEDURE

The equipment and procedures used in the performance of the experimental work are described in the following sub-sections.

3.1 Laboratory Screening Tests.

A vertical pyrex glass reactor tube (1.9 cm i. d. x 75 cm length) was used as an up-flow reactor (see Figure 3-1). The reaction zone itself was a 6-cm section in the central portion of the tube. Within the catalyst bed thermowells were blown inward from the walls and thermocouples inserted (up to 7). The thermocouple leads were connected to a multipoint recorder. These thermocouples enabled, through manual adjustment of two preheater tapes and meter-relay control of a reaction zone heater tape, approximation of isothermal conditions. The catalysts, usually 14 gm, were supported on either end by 5-mm pyrex glass beads. The assembly was enclosed in tubular block insulation.

In tests in which monolithic catalysts were used a quartz reactor (19 mm i. d.) which was not equipped with the radial thermowells was used. Instead, a single stainless steel, longitudinal thermowell (1/8-in o. d.), which contained two thermocouples, one placed at the end of the well and the other about 2.5 cm higher, was used. The longitudinal well enabled insertion of the monoliths in the reactor and placement of the thermocouples in a hole previously drilled in the center of the upper face of the monolith and into about two-thirds of the length of the monolith. Gas samples were taken at the ends of the reactor tube with this reactor. Monoliths were about 16 mm diameter and were wrapped with Fiberfrax ceramic fiber (Carborundum Company) before insertion to prevent gas by-pass between the monolith wall and the tube.

Figure 3-2 is a schematic of the the test apparatus. Feed gases were mixed in the manifold after individual adjustment of flow rates using metering valves and bead-type flowmeters. At times during the course of this project up to four individual screening systems were in simultaneous use. Figure 3-3 shows a typical manifold-reactor assembly.

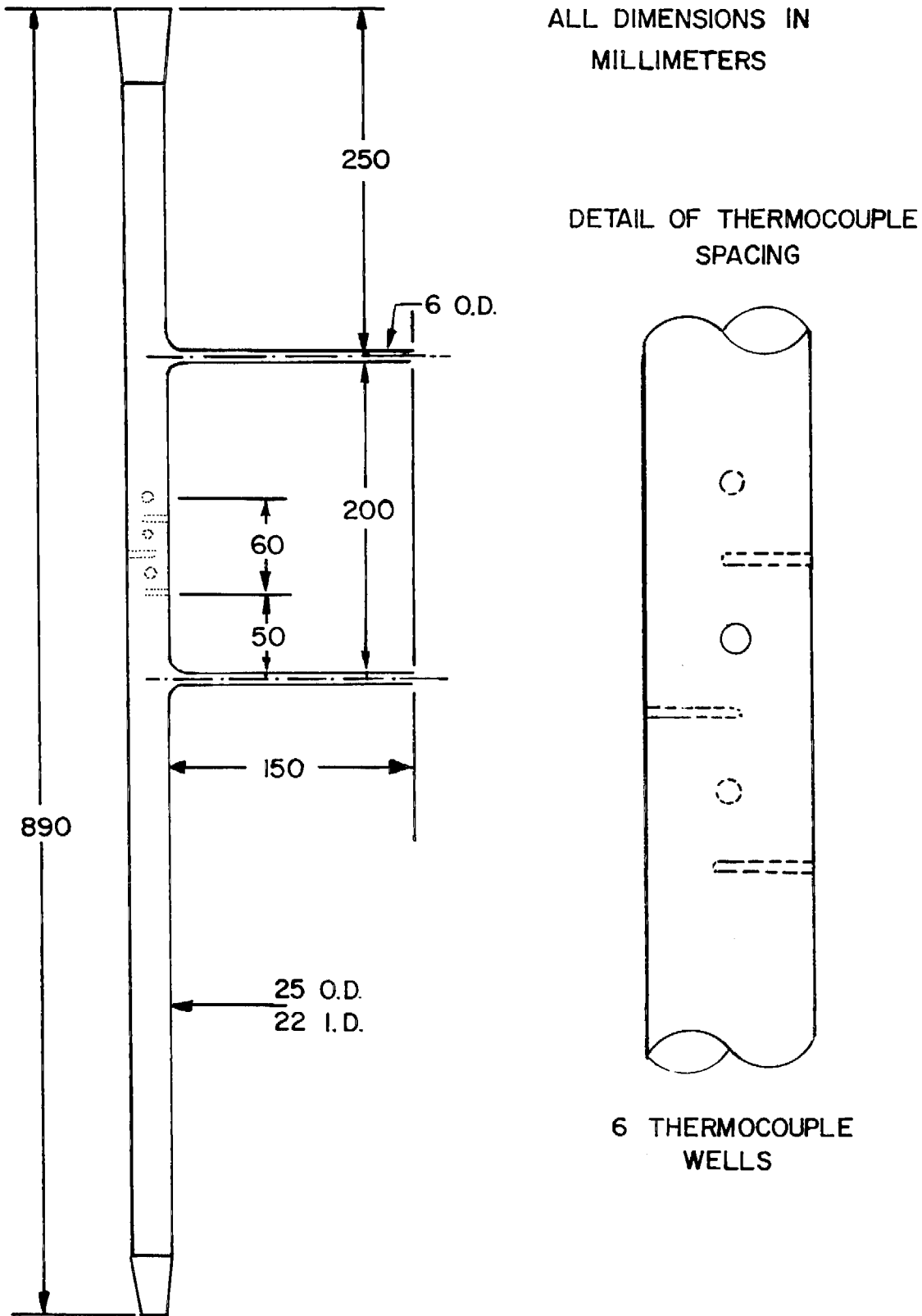


Figure 3-1 Schematic of Screening Reactor.

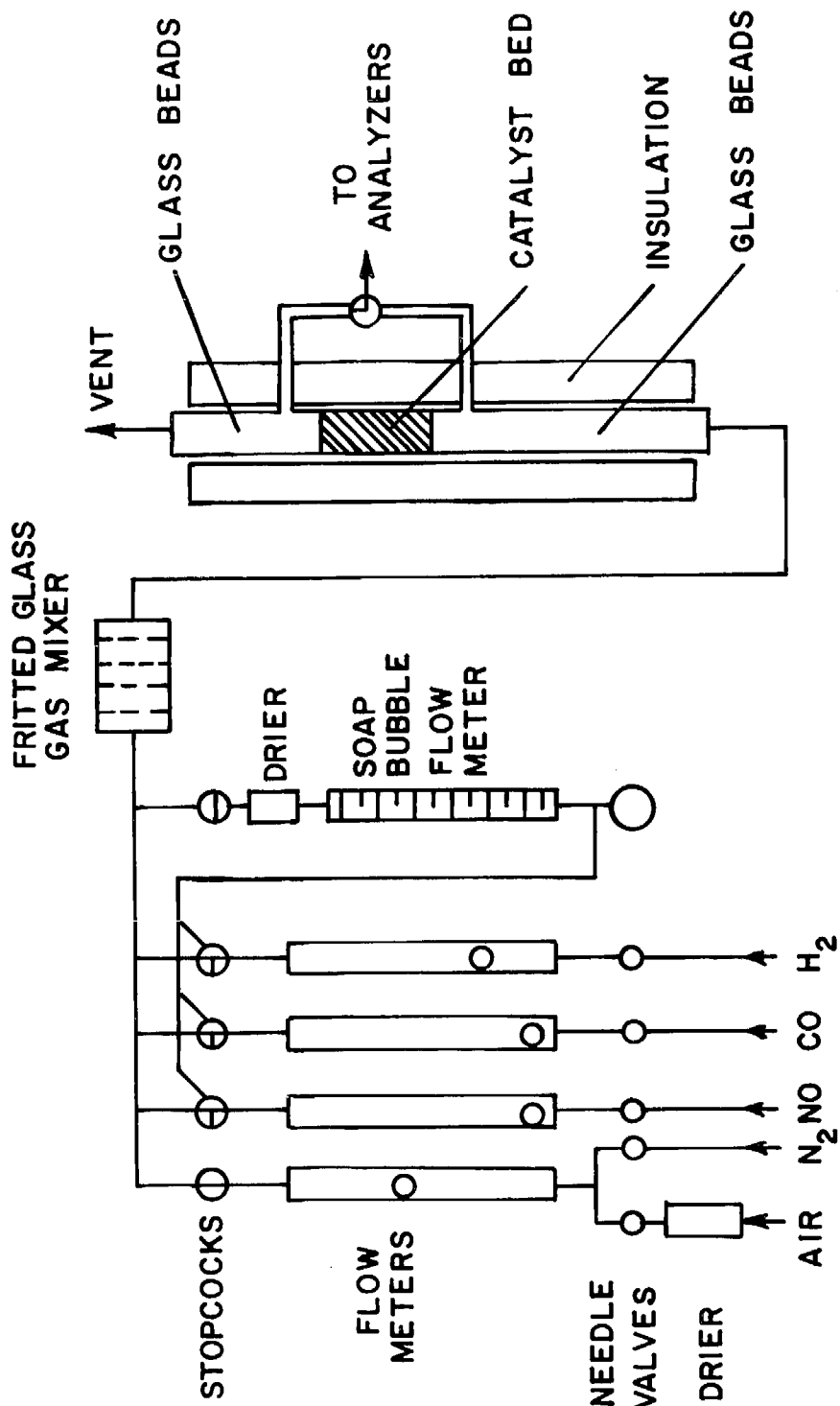


Figure 3-2 Screening Studies Test System.

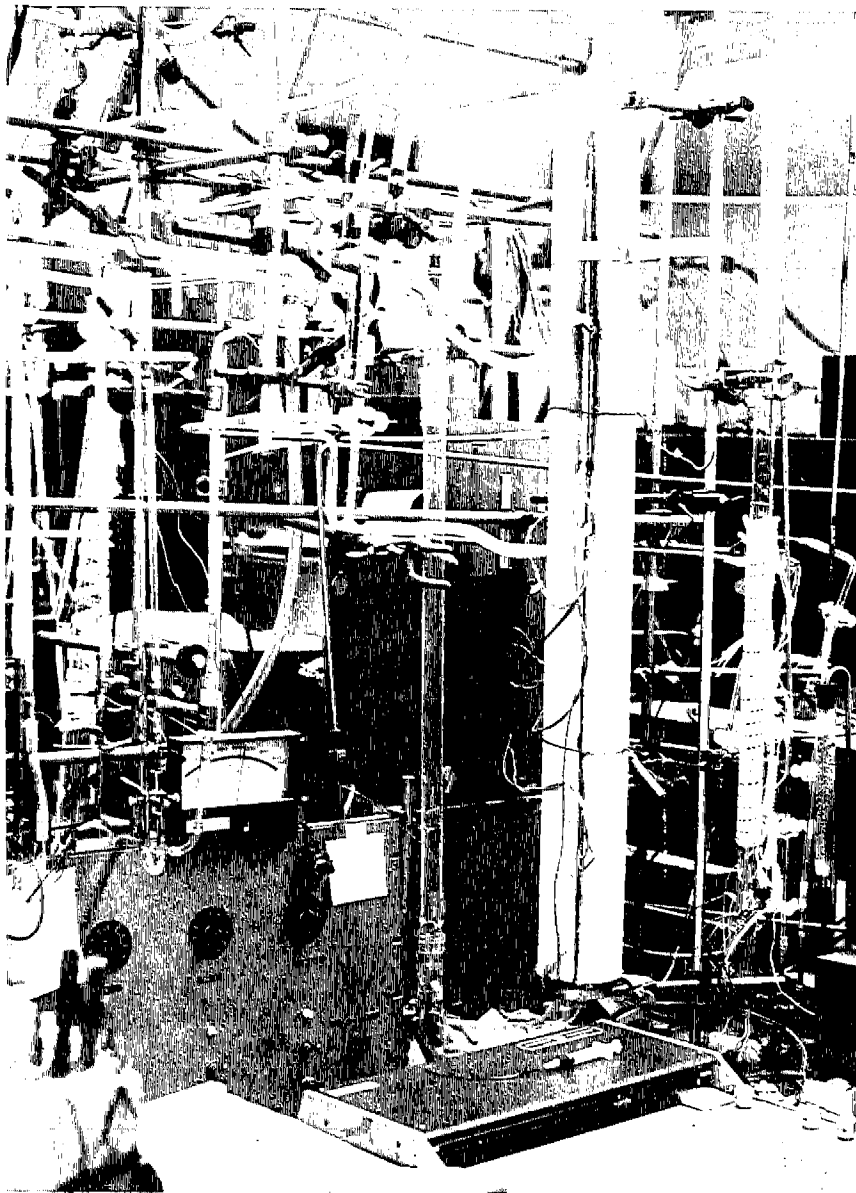


Figure 3-3. Typical Mixing Manifold and Reactor Assembly.

Nitric oxide was analyzed using Beckman Model 315 non-dispersive infrared (NDIR) analyzers. Carbon monoxide was determined using Mine Safety appliances LIRA 300 NDIR analyzers, and carbon dioxide was analyzed using either Beckman Model 15A or Mine Safety Appliance LIRA 300 analyzers. Nitrogen dioxide was analyzed on some tests using a Beckman Model 77 flow colorimeter. Nitrous oxide was determined by gas chromatography using a 3.3-m column (3.2 mm o. d.) of stainless steel containing Porapak Q; with the column, cross-checks of CO₂ concentration were also possible. In isolated tests, O₂ concentration was determined using a 3.3-m column of Molecular Sieves (13X).

Ammonia was determined by two methods. Early tests involved the absorption of ammonia into water with the subsequent determination of NH₃ by the addition of Nessler's reagent and spectrophotometric measurement of the optical density of the solution. Later, NH₃ analyses were conducted by absorption in 5% boric acid solution and titration with 0.04N HCl using bromocresol green as an indicator. Both techniques involved total sample gas flow measurement through a series of absorption flasks using either timed flow through a calibrated flowmeter or a wet-test meter located at the end of the chain.

In the screening tests, 14 gm of catalyst were used in general; however, economic or availability considerations required the use of slightly lower amounts in a few tests. In the case of monolithic catalysts, the final catalyst weights were somewhat higher. In the next section, where catalysts are described in detail, the actual catalyst charge amounts are given in a table.

The standard test flow rate was 300 liters/hr. In the NO reduction tests with CO, 520 ppm NO and 5200 ppm CO were used in a N₂ carrier. For NO reduction with H₂ the concentrations were 520 ppm and 3000 ppm, respectively, in a N₂ carrier. For oxidation of CO, 2000 ppm CO in air were employed. Tests were performed on a dry basis only (i. e., no H₂O was added).

3.2 Catalysts Studied in Screening Tests.

Table 3-1 lists the catalysts that were tested in the laboratory screening studies.* The majority of the catalytic materials were prepared by solid-state reaction, at 1000°C in air, of appropriate mixtures of oxides or carbonates. Compound formation was verified by X-ray diffraction for a number of catalysts including LaCoO₃, GdCoO₃, NdCoO₃, DyCoO₃, the spinel NiO·Cr₂O₃, LaNiO₃, SrRuO₃, SrY_{0.5}Ru_{0.5}O_{2.75}, and LaRhO₃. In general, the candidate catalytic materials were not soluble and the majority were highly acid-resistant.

The use of the catalytic materials in powdered form in the screening tests was not considered practical in the present project. Carrier material was used to support and disperse uniformly the catalytic material with subsequent formation into uniform pellets.

It is well known in catalysis that the support material may, in many cases, affect the reaction process; in fact, the carrier may have significant catalytic properties or may even result in synergistic improvement of the catalytic properties of the basic, active component. Alumina was selected as the standardized carrier material for use in this project. It is known that alumina itself can be an active catalyst for many reactions, especially those important in the petrochemical industry. However, it was established in this laboratory that alumina was quite inactive for those reactions under study in the screening tests. The catalysts were prepared for test in the following fashion: After the solid state reaction step, the resulting material was ground with alumina (Filtrol Grade 90) to prepare, in most cases, a mixture of 15% active material and 85% Al₂O₃. About 5% excess stearic acid was added as a die lubricant. The powder was formed into cylinders (3.2-mm dia x 3.2-mm long) in a motor driven pellet press. The stearic acid was burned off in flowing air at 550°C for a minimum of 15 hours in a calcination tube. Departing from the standardized preparation scheme in a few isolated cases, some catalysts were prepared by impregnation of single

* A cross-reference listing of the catalysts is given in the Appendix.

Table 3-1. Catalyst Description^{††}

<u>Catalyst Number</u>	<u>Catalyst</u>	<u>Description</u> [*]
<u>Cobalt based Catalysts</u>		
2	Lanthanum Cobalt Oxide	La:Co = 1:1 (LaCoO ₃) ^{**}
18	Lanthanum Cobalt Oxide	La:Co = 1:1 (LaCoO ₃)
9	Lanthanum Cobalt Oxide	La:Co = 1:1 (LaCoO ₃) (50%)
20	Lanthanum Strontium Cobalt Oxide	La:Sr:Co = 0.85:0.15:1.0 (La _{0.85} Sr _{0.15} CoO ₃)
7	Lanthanum Oxide-Strontium Oxide-Cobalt Oxide	La:Sr:Co = 0.85:0.15:1.0 ^{**} (La _{0.85} Sr _{0.15} CoO ₃)
27	Lanthanum Oxide-Strontium Oxide-Cobalt Oxide	La:Sr:Co = 0.85:0.15:1.0 (La _{0.85} Sr _{0.15} CoO ₃)
8	Lanthanum Strontium Cobalt Oxide	La:Sr:Co = 0.85:0.15:1.0 (La _{0.85} Sr _{0.15} CoO ₃) (50%)
1	Lanthanum Strontium Cobalt Oxide	La:Sr:Co = 0.98:0.02:1.0 (La _{0.98} Sr _{0.02} CoO ₃) [†]
19	Lanthanum Barium Cobalt Oxide	La:Ba:Co = 0.85:0.15:1.0 (La _{0.85} Ba _{0.15} CoO ₃)
15	Lanthanum Barium Cobalt Oxide	La:Ba:Co = 1.7:0.15:1.0 (La _{0.85} Ba _{0.15} CoO ₃ + 0.425 La ₂ O ₃)
22	Gadolinium Cobalt Oxide	Gd:Co = 1:1 (GdCoO ₃)
30	Neodymium Cobalt Oxide	Nd:Co = 1:1 (NdCoO ₃) ^{**}
31	Dysprosium Cobalt Oxide	Dy:Co = 1:1 (DyCoO ₃) ^{**}
11	Cerium Oxide-Cobalt Oxide	Ce:Co = 1:1 (2CeO + Co ₂ O ₃)
24	Rare Earth Cobalt Oxide	R. E. :Co = 1:1
24B	Rare Earth Cobalt Oxide	R. E. :Co = 1:1, Pellets calcined at 1000°C.
38	Rare Earth Cobalt Oxide	R. E. :Co = 1:1, Impregnated on AlSiMag monolith, calcined at 1000°C. 30 gm
39	Rare Earth Cobalt Oxide	R. E. :Co = 1:1, Impregnated on Cercor monolith, calcined at 1000°C, 25 gm.
37	Rare Earth Cobalt Oxide	R. E. :Co = 1:1, Impregnated calcined at 1000°C.

Table 3-1 (cont.)

<u>Catalyst Number</u>	<u>Catalyst</u>	<u>Description*</u>
40	Rare Earth Cobalt Oxide	R. E. : Co=1:1, Impregnated on Cercor monolith (Al ₂ O ₃ -coated), calcined at 1000°C, 21 gm.
41	Rare Earth Cobalt Oxide	R. E. : Co=1:1, Impregnated on β - spodumene pellets
42	Rare Earth Cobalt Oxide	R. E. : Co=1:1, Impregnated on β -spodumene pellets, calcined at 1000°C.
3	Copper Cobalt Oxide	Cu:Co=1:2 (CuO · Co ₂ O ₃)
29	Strontium Cobalt Oxide	Sr:Co = 1:1 (SrCoO ₃)
32	Cobalt Oxide	Co ₃ O ₄
33	Cobalt Oxide	Co ₂ O ₃ , Prepared from CoCO ₃ at 500°C, may have some Carbonate remaining.
34A	Cobalt Oxide	Co ₂ O ₃ , Impregnated
34B	Cobalt Aluminate	CoAlO ₃ Impregnated, Calcined at 1000°C
5	Cobalt Titanium Oxide	Co:Ti = 2:1 (Co ₂ TiO ₄)
60	Cobalt Manganese Oxide	Co:Mn = 1:1 (Ni MnO ₃)

Rare Earth Oxide Catalysts

23	Rare Earth Oxide	From mixed nitrates (American Potash & Chemical)
71	Rare Earth Oxide	From mixed nitrates (Molycorp.)
43	Bastnasite	Commercial mixed oxides (Molycorp.)
111	Cerium Oxide	CeO (Impregnated), 25 gm.

Chromium-Based Catalysts

56	Rare Earth-Chromium Oxide	R. E. : Cr = 1:1
131	Chromium Oxide	Cr ₂ O ₃ , Impregnated
113	Copper Chromium Oxide	Cu:Cr = 1:2 (CuCr ₂ O ₄) (Girdler G - 22, Chemetron unsupported)
63	Vanadium Chromium Oxide	V:Cr = 1:1

Table 3-1 (cont.)

<u>Catalyst Number</u>	<u>Catalyst</u>	<u>Description*</u>
<u>Nickel-Chromium Catalysts</u>		
84	Nickel Chromium Oxide Spinel	Ni:Cr = 1:3 ($\text{NiO} \cdot \text{Cr}_2\text{O}_3 + 1/2 \text{Cr}_2\text{O}_3$)
86	Nickel Chromium Oxide Spinel	Ni:Cr = 1:2 ($\text{NiO} \cdot \text{Cr}_2\text{O}_3$)
87	Nickel Chromium Oxide Spinel	Ni:Cr = 1:1 ($\text{NiO} \cdot \text{Cr}_2\text{O}_3 + \text{NiO}$)
81	Nickel Chromium Oxide Spinel	Ni:Cr = 1:1 ($\text{NiO} \cdot \text{Cr}_2\text{O}_3 + \text{NiO}$)
61	Nickel Chromium Oxide Spinel	Ni:Cr = 1:1 ($\text{NiO} \cdot \text{Cr}_2\text{O}_3 + \text{NiO}$)
85	Nickel Chromium Oxide Spinel	Ni:Cr = 3:2 ($\text{NiO} \cdot \text{Cr}_2\text{O}_3 + 2\text{NiO}$)
98	Nickel Chromium Oxide Spinel	Ni:Cr = 1:2 ($\text{NiO} \cdot \text{Cr}_2\text{O}_3$) (30%)
97	Nickel Chromium Oxide Spinel	Ni:Cr = 1:2 ($\text{NiO} \cdot \text{Cr}_2\text{O}_3$) 3% deposited from slurry on AlSiMag monolith, 23 gm.
91	Nickel Chromium Oxide Spinel Lithium-doped	Ni:Cr:Li = 49.8:49.8:0.4 ($\text{NiO} \cdot \text{Cr}_2\text{O}_3 + \text{NiO}$)
83A	Bastnasite Nickel Chromium Oxide	R. E. :Ni:Cr = 2:1:1
83B	Bastnasite Nickel Chromium Oxide	R. E. :Ni:Cr = 2:1:1 (No carrier used)
127	Nickel Oxide-Chromium Oxide	Ni:Cr = 1:1 (Impregnated) (27%)
128	Nickel Oxide-Chromium Oxide	Ni:Cr = 3:1 (Impregnated) (23%)
<u>Other Nickel-Based Catalysts</u>		
35	Lanthanum Nickel Oxide	La:Ni = 1:1 (LaNiO_3)
73	Lanthanum Nickel Oxide	La:Ni = 1:1 (LaNiO_3) (48 hour preparation period)
50	Rare Earth Nickel Oxide	R. E. :Ni = 1:1
68	Bastnasite Nickel Oxide	R. E. :Ni = 1:1
47	Lanthanum Iron Nickel Oxide	La:Fe:Ni = 85:15:100
49	Rare Earth Iron Nickel Oxide	R. E. :Fe:Ni = 92:8:100 (Impregnated 11% on AlSiMag monolith, 16.2 gm)
89	Rare Earth Nickel Oxide	R. E. :Ni = 1:1, made from "Lanthanum-Rare Earth" carbonate (cerium-free)
129	Nickel Oxide	NiO (from NiCO_3)

Table 3-1 (cont.)

<u>Catalyst Number</u>	<u>Catalyst</u>	<u>Description</u> *
94	Nickel Oxide	("Black" nickel oxide reagent, 77% Ni)
46	Nickel Manganese Oxide	Ni:Mn = 1:1 (Ni MnO ₃)
65	Nickel Vanadium Oxide	Ni:V = 1:2 (NiO · V ₂ O ₅)
58U	Nickel Metal	4.8 mm x 4.8 mm hollow, perforated semi-cylinders, pretreated by calcining in air at 1000°C.
58	Nickel Metal	same as above - uncalcined
57	Rare Earth Nickel Cobalt Oxide	R. E. :Ni:Co = 2:1:1
6	Nickel Zinc Ferrite	
<u>Copper-Nickel Catalysts</u>		
54	Copper-Nickel Oxide	Cu:Ni = 1:1
123	Copper Oxide-Nickel Oxide	Cu:Ni = 3:1 (Impregnated)
124	Copper Oxide-Nickel Oxide	Cu:Ni = 1:1 (Impregnated)
125	Copper Oxide-Nickel Oxide	Cu:Ni = 1:3 (Impregnated)
126	Copper Oxide-Nickel Oxide	Cu:Ni = 1:99 (Impregnated)
52U	Monel Metal	Cu:Ni = 30:70, 4.8 mm x 4.8 mm hollow perforated semi-cylinders
52	Monel Metal	Cu:Ni = 30:70, 4.8 mm x 4.8 mm hollow, perforated semi-cylinders, pretreated by calcining in air at 1000°C.
<u>Other Copper-Based Catalysts</u>		
53	Lanthanum Copper Oxide	La:Cu = 1:1
62	Rare Earth Copper Oxide	R. E. :Cu = 1:1
44	Copper Molybdenum Oxide	Du:Mo = 1:1 (Cu MoO ₄)
64	Copper Vanadium Oxide	Cu:V = 1:2 (CuO · V ₂ O ₅)
67	Copper Nickel Vanadium	Cu:Ni:V = 1:1:2
66	Copper Chromium Oxide	Cu:Cr = 1:2

Table 3-1 (cont.)

<u>Catalyst Number</u>	<u>Catalyst</u>	<u>Description</u> *
<u>Tungsten Bronze Catalysts</u>		
116	Copper Tungsten Bronze	Cu:W = 1:2 ($\text{Cu}_{0.5}\text{WO}_3$)
117	Cerium Tungsten Bronze	Ce:W = 1:2 ($\text{Ce}_{0.5}\text{WO}_3$)
118	Sodium Tungsten Bronze	Na:W = 1:5 ($\text{Na}_{0.2}\text{WO}_3$)
<u>Other Non-Noble Metal Catalysts</u>		
28	Tin Oxide	SnO
51	Lanthanum Iron Oxide	La:Fe = 1:1
4	Barium Titanium Oxide	Ba:Ti = 1:1 (BaTiO_3)
45	Lanthanum Manganese Oxide	La:Mn = 1:1
112	Copper Iron Oxide	Cu:Fe = 1:1 (CuFeO_2)
115	Unspecified	Water-gas shift catalyst (Girdler G-66A, Chemetron Corp.)
103	Zirconium Vanadium Oxide	Unknown composition**
104	Cerium Tungsten Oxide	Unknown composition**
106	Cerium Molybdenum Oxide	Unknown composition**
110	Stainless Steel	4.8 mm x 4.8 mm hollow, perforated semi-cylinders.
<u>Noble Metal-Based Catalysts</u>		
119	Palladium	0.5% Pd (Engelhard Industries)
120	Ruthenium	0.5% Ru (Engelhard Industries)
121	Platinum	0.5% Pt (Engelhard Industries)
122	Rhodium	0.5% Rh (Engelhard Industries)
78	Strontium Ruthenium Oxide	Sr:Ru = 1:1 (SrRuO_3) 5%
82	Strontium Ruthenium Oxide	Sr:Ru = 1:1 (SrRuO_3) 0.25%
90	Strontium Yttrium Ruthenium Oxide	Sr:Y:Ru = 2:1:1 ($\text{SrY}_{0.5}\text{Ru}_{0.5}\text{O}_{2.75}$)
96	Lanthanum Nickel Ruthenium Oxide	La:Ru:Ni = 2:1:1 ($\text{LaNi}_{0.5}\text{Ru}_{0.5}\text{O}_3$)
99	Nickel Chromium Oxide Spinel Platinum-doped	Ni:Cr = 1:2 with 0.1% excess Pt
76	Lanthanum Rhodium Oxide	La:Rh = 1:1 (LaRhO_3) (11gm)
77	Lanthanum Rhodium Oxide	La:Rh = 1:1 (LaRhO_3) (5%)

Table 3-1 (cont.)

<u>Catalyst Number</u>	<u>Catalyst</u>	<u>Description</u> *
79	Lanthanum Rhodium Oxide	La:Rh = 1:1 (LaRhO ₃) (1%)
80	Lanthanum Rhodium Oxide	La:Rh = 1:1 (LaRhO ₃) (0.25%)
114	Platinum-doped Nickel	3% Ni with 1% Pt Girdler G-43 (Chemetron Corp.)

*Component ratios are in molar units; catalyst weights are 14 gm unless noted; impregnated catalysts 15% by weight on Al₂O₃ unless noted; all other catalysts pressed 15% (active oxides) with Al₂O₃ unless noted; active material for pressed catalysts prepared at 1000°C for 16 hours unless noted; pressed pellets calcined at 550°C unless noted; impregnated catalysts made from nitrates and calcined at 500°C unless noted.

**Catalyst supplied by Prof. W. F. Libby.

†Prepared by calcination of lanthanum cobalticyanide.

†† A cross-reference listing of the catalysts is given in the Appendix.

or mixed aqueous nitrate solutions on pre-formed carrier pellets or monoliths (e. g., alumina or β -spodumene pellets or Cercor or AlSiMag monoliths). The nitrates were decomposed by calcination in flowing air at 500°C. The nominal loading with these catalysts was 15% active material as with the pressed catalysts. Variations in the preparation scheme outlined above were used in a few cases. With some pressed catalysts the active material was prepared from nitrates at 500°C rather than at 1000°C; in addition, to determine if reaction between carrier and active material can occur at elevated temperatures some pelletized catalysts were calcined at 1000°C rather than at the normal 550°C (for pressed catalyst) or 500°C (for impregnated catalyst).

As seen in Table 1, most of the binary oxides consisted of a 1:1 molar ratio of the metals. Several of the catalysts are listed as consisting of rare earth metal (i. e., not specified as Ce, La, Gd, etc.). These catalysts were prepared using a commercial mixture of rare earths (American Potash and Chemical Co.). In addition, several catalysts were prepared from bastnasite, another commercial mixture of rare earths (Molycorp) and from a cerium-free mixture of rare earth carbonates of bastnasite origin called "lanthanum rare earth" (Molycorp). Table 3-2 shows typical compositions for these mixtures. In any case, the catalysts were prepared so that the transition metals involved were in the molar ratios shown in Table 3-1 with the rare earth metals in the starting mixture.

Three tungsten bronzes were prepared following a preparation scheme by Broyde (1968) involving firing mixtures of tungstic oxide, tungsten powder and the metal tungstate or oxide in vacuum at 1000°C. Functional formulae were $\text{Cu}_{0.5}\text{WO}_3$, $\text{Ce}_{0.5}\text{WO}_3$ and $\text{Na}_{0.2}\text{WO}_3$.

Nickel metal and monel alloy were also tested for catalytic activity. These metals were in the form of perforated, hollow semi-cylinders (4.8-mm dia x 4.8-mm long) which are normally sold commercially as distillation packing. Catalysts obtained from commercial suppliers included a series of supported noble metals, a platinum-promoted nickel catalyst and a water-gas shift catalyst.

Table 3-2. Approximate Composition of Rare Earth Mixtures

	Rare Earth Oxide (American Potash and Chemical Corp.)	Bastnasite (Molycorp)	Lanthanum Rare Earth Oxide
Percentage as oxides			
CeO ₂	45.6	27.6	1.0 or less
La ₂ O ₃	22.8	41.3	45.9
Nd ₂ O ₃	16.2	11.6	12.9
Pr ₆ O ₁₁	4.7	4.3	4.8
Sm ₂ O ₃	2.8	0.4	0.4
Gd ₂ O ₃	1.9	0.3	0.3
Y ₂ O ₃	0.2	0.3	0.3
Other Rare Earth Oxides	0.8	0.4	0.4
Total Rare Earth Oxides	95.0	86.2	66.0
SO ₃	2.0	--	--
P ₂ O ₅	0.5	0.5	--
Na ₂ O+K ₂ O	0.1	1.0	0.03
CaO+MgO	1.0	0.8	0.03
Fe ₂ O ₃ +Al ₂ O ₃	1.5	0.1	0.004
Fluorine	--	6.0	--
SrO ₂	0.1	--	0.03
BaO	--	1.5	--
SrO	--	0.9	0.03
SiO ₂	--	3.0	--

Several of the more promising catalysts were selected, on the basis of the screening studies, for further investigation in the automotive tests. In addition, there were a few isolated tests in the exhaust studies of catalysts that were not initially examined in the screening studies. These latter catalysts were selected for study following indications in the literature that certain performance features might be expected. These catalysts will be described in the appropriate section of this report.

3.3 Automotive Exhaust Tests.

Several commercially available and promising laboratory-prepared catalysts were evaluated for performance using actual engine exhaust. Three areas of study were involved: (a) testing with a prototype full-scale converter, (b) testing of research quantities of catalyst in a scaled-down exhaust converter and (c) testing with a full-scale, two-stage converter. The engine-dynamometer systems used in the three studies are described below.

The engine used in all the experiments was a 1967 Ford six cylinder, 170 cu in displacement engine. This engine was factory equipped with an exhaust manifold air reactor. This reactor was used in its stock configuration for some of the early evaluations of prototype, full-scale reactors. Later the air pump was removed and air was supplied in measured quantities from a laboratory air supply system. The engine was dynamometer-mounted and was instrumented for measurement of air and fuel flow. The engine air flow was measured either with a Miriam 100 cfm laminar flow meter or with a 400 cfm laminar flow meter. The fuel flow was determined with an automatic fuel-weighing apparatus and during extended runs by weighing the fuel supply on a beam balance. The engine torque was measured by the dynamometer load. The speed was measured with a Standard tachometer which was controlled by the fuel weighing apparatus. This measured the time to consume a given amount of fuel and the engine revolutions during this time.

In addition to engine oil pressure and water temperature the inlet manifold vacuum was monitored. The condition of the ignition system was

checked with a Dumont Engine Scope. Standard spark timing of 5 degrees before top dead center, as measured with the vacuum disconnected was used throughout these tests. The methods used for analysis of exhaust gases were similar to those employed in the laboratory screening tests. Inlet and outlet sample analyses of NO were made using a Mine Safety Appliances LIRA 200 NDIR analyzer. Analyses of CO, CO₂, and hydrocarbons were made with Mine Safety Appliances LIRA 300 NDIR units. In addition, a Beckman Model 109 flame ionization analyzer for hydrocarbons and a Beckman Model F-3 paramagnetic O₂ analyzer were incorporated in the analysis. Figure 3-4 is a photograph of the analytical test system.

In the full-scale tests using the two-stage catalytic reactor the stock carburetor was removed and a Carter model W-I carburetor was substituted. This change was made to permit variation of the air-fuel ratio in order to study its effect on catalyst performance. This particular carburetor was chosen because it had a very similar bolt mounting pattern to the stock carburetor and because the flow through the main jet was controlled by a tapered plunger in the carburetor body. By simply disconnecting this plunger from the throttle linkage and constructing a thumb-screw mechanism to raise and lower it, it was possible to alter manually the air-fuel ratio from approximately 16 to 12:1 continuously during operation. The test procedures differed for the three types of converters and are given in subsequent sections.

3.3.1 Small-Scale Exhaust Reactor.

Not long after the project was in progress it became apparent that the automobile exhaust tests with the prototype converter could not keep pace with the growing list of promising catalysts. Time-consuming preparation of kilogram quantities of catalyst with the equipment available was the major deterrent to rapid testing. In addition, in some cases, the promising catalysts contained expensive materials.

To provide a logical intermediate step between the laboratory screening tests and full-scale evaluation, a small exhaust reactor was designed and built. The catalyst quantity employed and the flow rates used were such that typical automotive space velocity (the primary criterion for scale-up or

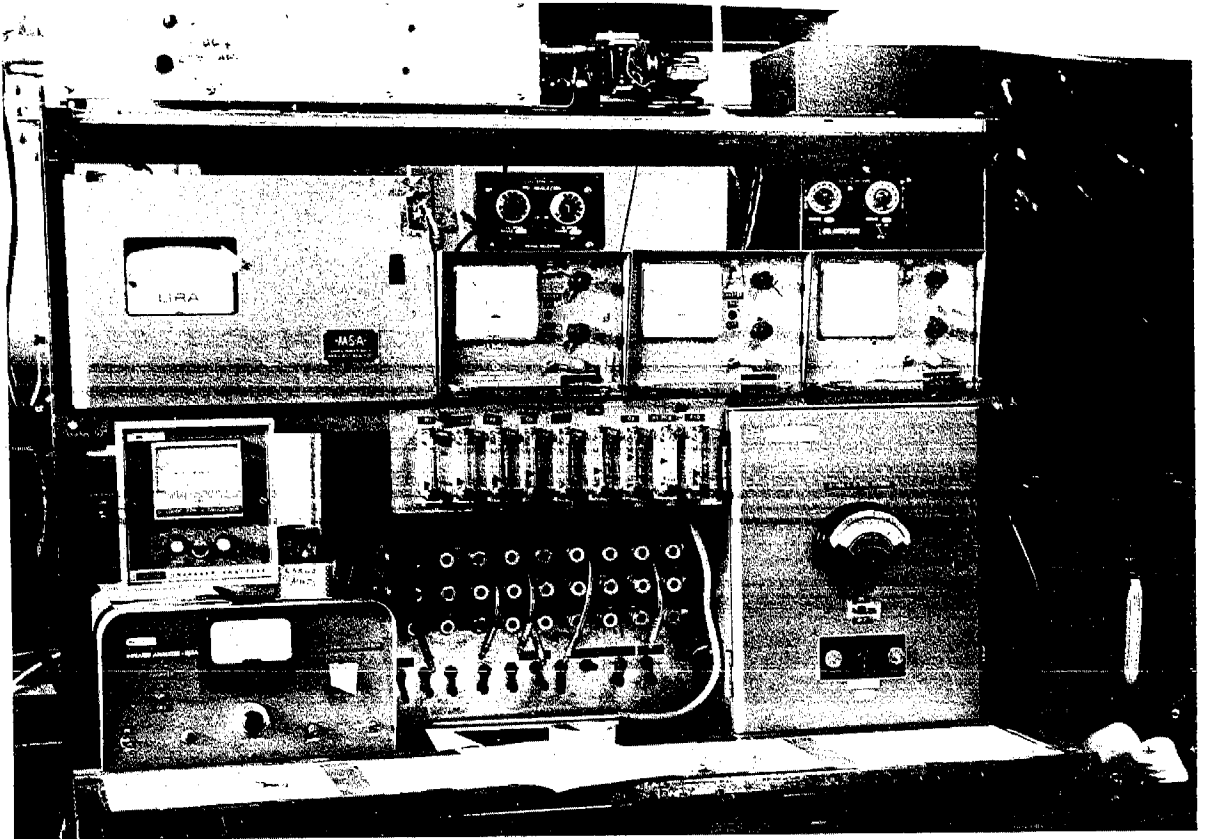


Figure 3-4. Analytical Equipment Used in Automotive Tests.

scale-down in catalytic reactors, defined as the volumetric flow rate of gas per volume of catalyst) could be simulated. Capability for temperature adjustment was another important feature with the small reactor, enabling operation at temperatures typical of full scale converters.

The reactor was constructed of 304 stainless steel tubing (1-inch o.d. x 0.065-inch wall thickness). Figure 3-5 is a schematic of the reactor. The reactor was placed in a horizontal furnace with two independently-controlled heating sections.

A preheating section, approximately 10 inches in length, contained quartz chips to facilitate heat transfer. A stainless-steel screen separated the chips from the catalyst section. The catalyst section was about 3 inches in length providing space velocities over the flow rates used from about 8000 hr^{-1} to about $45,000 \text{ hr}^{-1}$. Additional quartz beads were placed downstream of the reactor section. Figure 3-6 shows the assembled reactor in the furnace, along with the temperature controllers and recorder. Longitudinal thermowells (1/16-in o.d.) extended from both end fittings to provide for temperature measurement and controller signal input. A mixing manifold similar to those employed in the screening studies can be seen above the reactor. By using the manifold, either first or second-stage operation could be simulated by addition of various components to the exhaust. In fact, since the change from a reducing to an oxidizing atmosphere could be done easily the catalysts were tested for use in both stages.

Analyses were made of the inlet and outlet gases using the equipment described above. In tests simulating first stage operation, ammonia was analyzed using the absorption titration method described in Section 3.1. Due to the large amount of water present, drying of the sample gases was necessary; reduction of the dew point to 32°C (0.6% H_2O) was accomplished in an ice bath followed by final water removal in a drying tube filled with Drierite absorbent. Since ammonia would be retained in the drying system, a separate ammonia sample outlet was required. The sample line was heated to a temperature above the dew point of the reactor effluent to prevent water condensation.

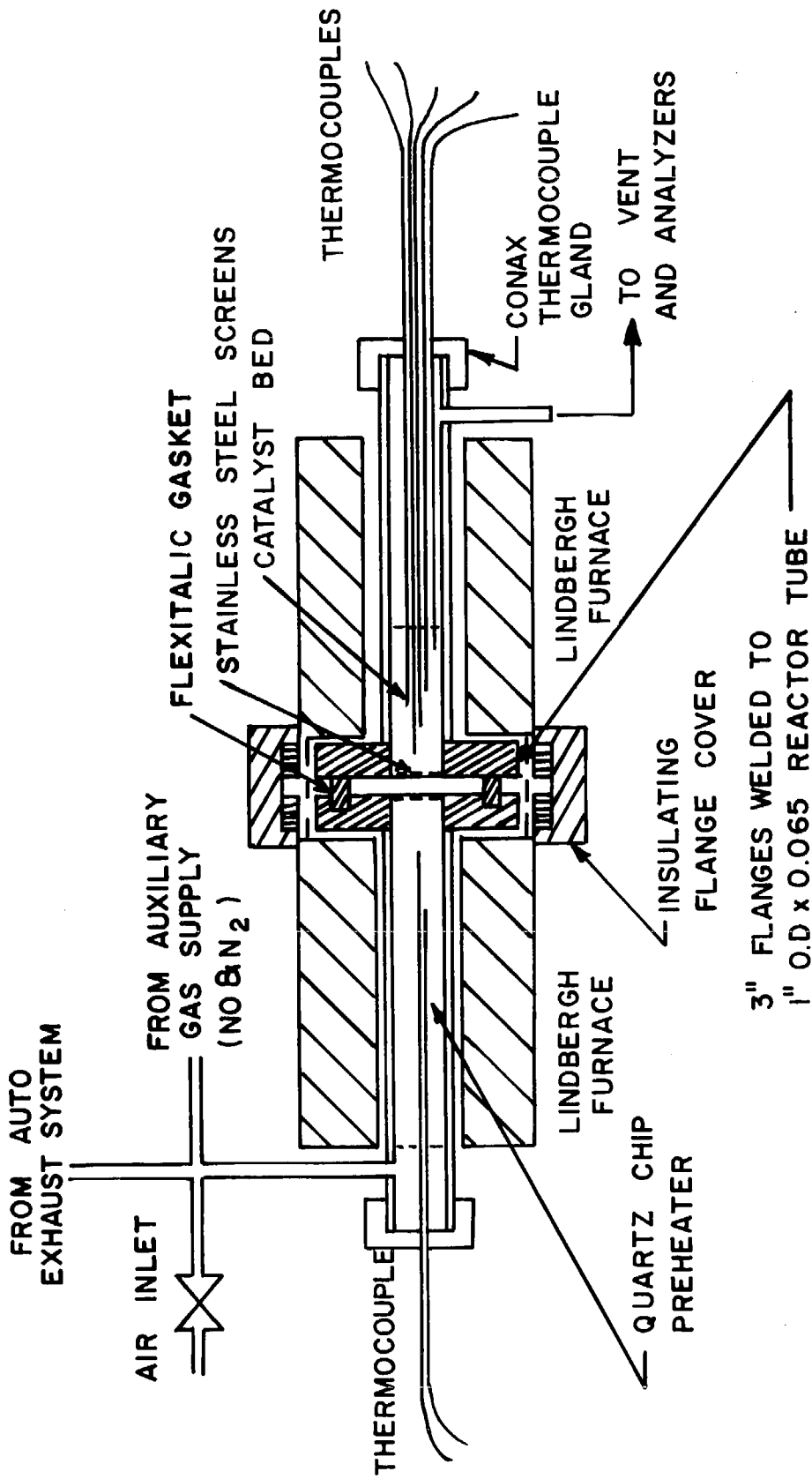


Figure 3-5 Schematic of Small-Scale Exhaust Reactor.

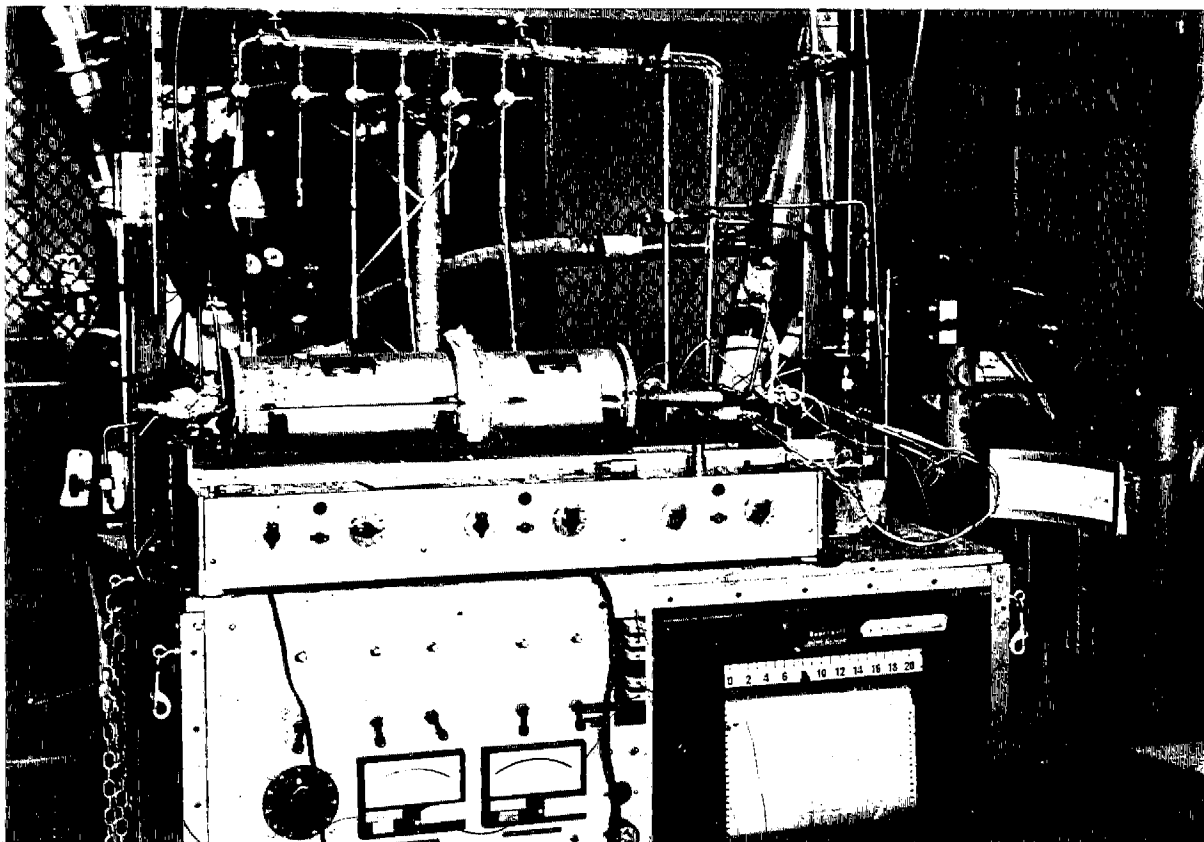


Figure 3-6. Small Exhaust Reactor Test System.

The exhaust feed to the reactor was taken from the 170 cu. in., 6-cylinder engine mounted on a stationary dynamometer. The engine was operated at near-idle conditions to provide for a fuel-rich exhaust. Nitric oxide was added to the exhaust, using the mixing manifold for those tests in which first stage operation was simulated. Air was added to the exhaust to simulate effluent from a first stage converter plus secondary air in order to study second-stage operation.

Typical exhaust composition is given in Table 3-3 for the two cases.

Table 3-3. Typical Exhaust Compositions used in Small Reactor Studies.

Species	First Stage Studies	Second Stage Studies
	Concentration	
CO	3%	3%
CO ₂	11%	11%
HC	500 ppm	500 ppm
NO	1200 ppm	100 ppm
O ₂	0.2%	2-4%

In addition to those species given, it is estimated that hydrogen was present at concentration levels from 25 to 50% that of CO.

3.3.2 Prototype Exhaust Converter.

Tests with automobile exhaust began shortly after the start of this project using several commercial catalysts, as well as catalysts showing promise based on the initial laboratory screening studies. The converter employed was constructed from a standard automobile muffler. The converter body was 5 inches in diameter and 21 inches long. The perforated internal baffles were removed from the stock muffler and a bolted flange was constructed at one end.

The converter contained a diffuser consisting of several layers of

18-mesh stainless steel screen and two screen catalyst supports. The supports were retained by steel rings to which 1/4-inch threaded studs were attached. The studs at the entrance end rested on the front face of the muffler, while the studs at the exit end of the muffler extended through the opening flange. By adjustment of locknuts the catalyst bed could be set at any desired length. Figure 3-7 is a view of the disassembled reactor.

Several bosses were welded to the converter body for attachment of thermocouples as well as for sampling and pressure-drop measurements. The thermocouples were chromel-alumel with 1/16-inch Inconel sheaths. Lava glands were used to seal the thermocouples in the bosses. Output was recorded on a multipoint recorder calibrated to 2400°F. Figure 3-8 shows the converter mounted on a 6-cylinder GMC engine.

In actual tests the converter was mounted on the exhaust line of a 1967 Ford, six-cylinder 170 CID engine which was equipped with a manifold air injection reaction system and an anti-backfire valve. The air flow to the manifold was provided by a belt-driven pump in the stock configuration. In some tests, the pump was disconnected and the air was supplied from the laboratory air system. The actual flow rate was measured with a large, calibrated rotameter.

The engine was operated at several power-rpm combinations to simulate typical driving modes (e. g., idle, street-driving, cruise, and full-power modes). The simulated modes, speed and horsepower levels selected for testing are given in Table 3-4.

Table 3-4. Typical Test Modes with a Prototype Converter.

Mode	Speed (rpm)	Power (bhp)
idle	615	0
street	1500	20
cruise	2600	36
power	300	60

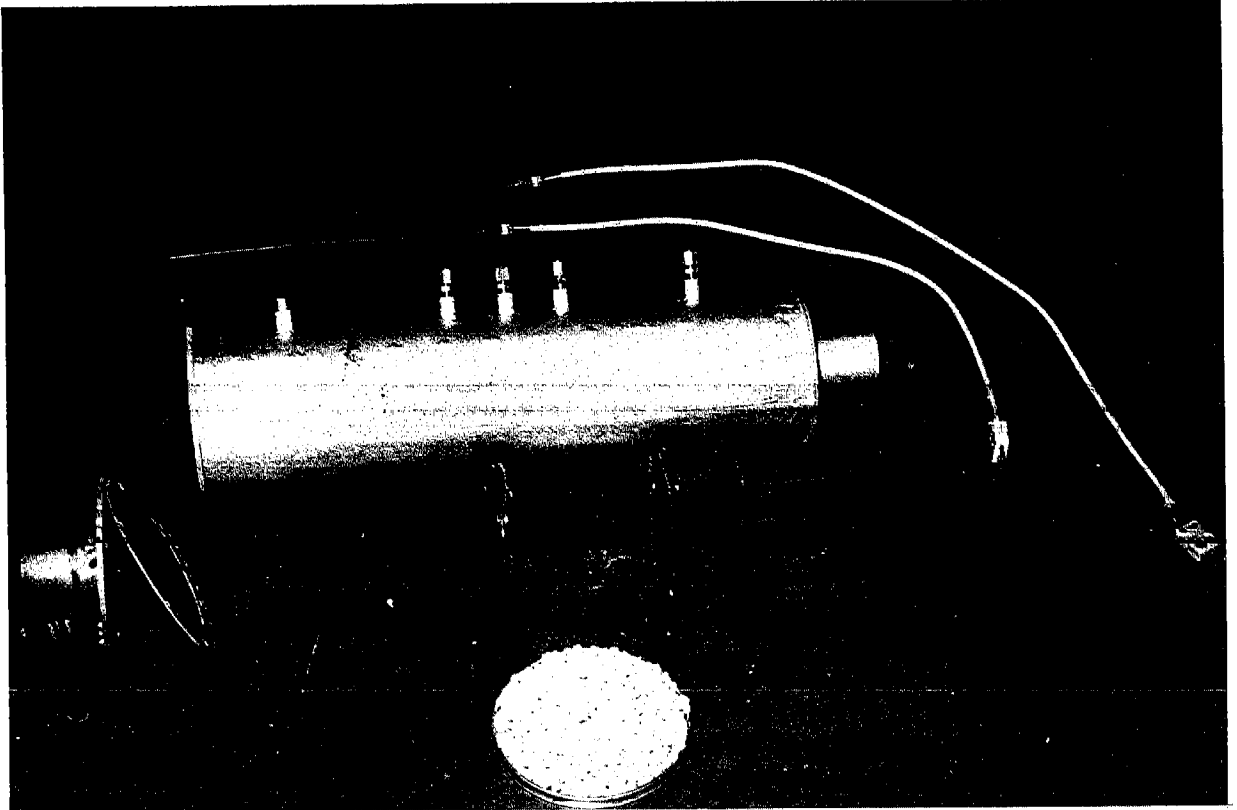


Figure 3-7. View of Disassembled Axial-Flow Reactor.

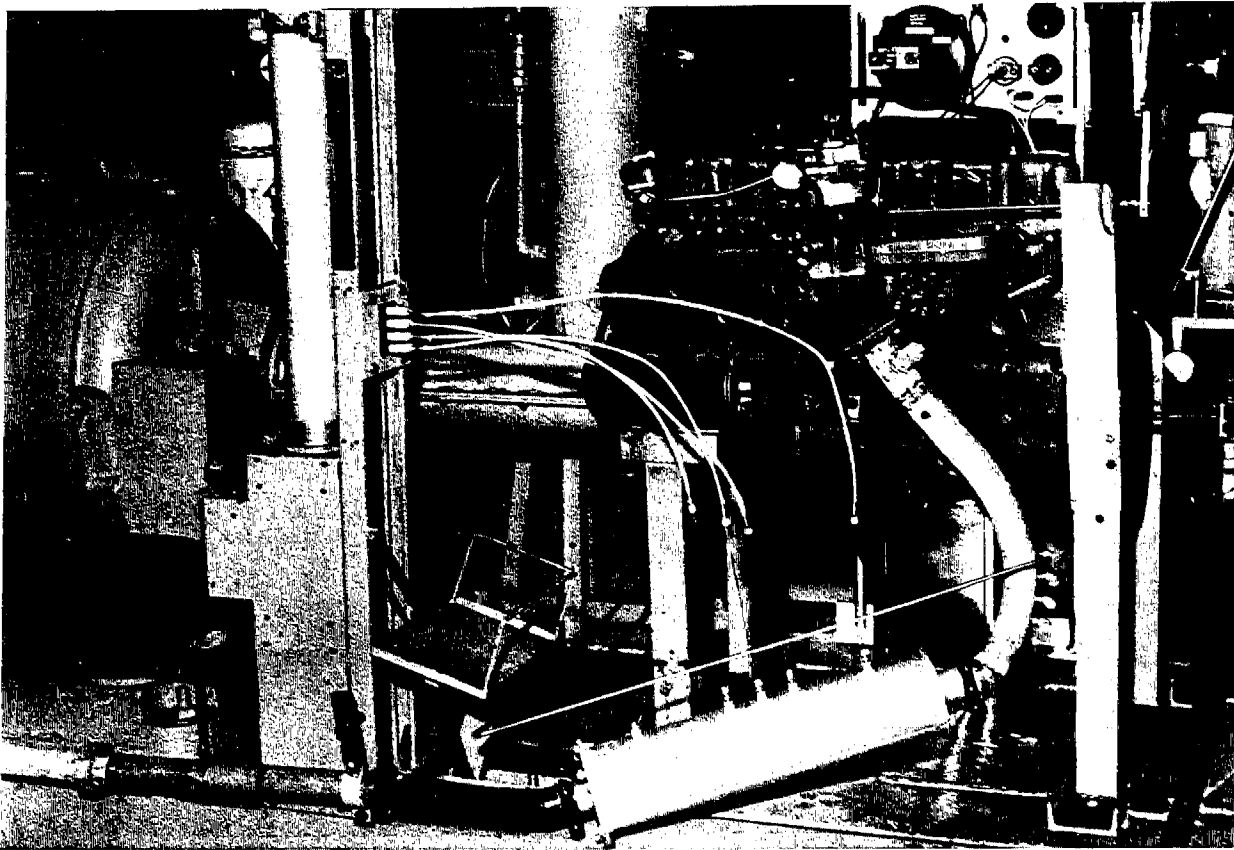


Figure 3-8. Axial-Flow Converter Mounted on Engine Exhaust Line.

By using either the pump or the laboratory air system or by not employing air injection at all a broad range of exhaust conditions simulating either stage of a two-stage converter could be obtained.

3.3.3 Two-Stage Catalytic Converter.

Based on results of the screening and the small-scale exhaust reactor studies, several catalysts were selected for further evaluation in a full-scale, two-stage converter.

Design of the converter was based on the following desired features:

- (1) Fairly rapid removal and replacement of catalyst must be possible.
- (2) The converter must be equipped with interstage sampling ports.
- (3) Both pelleted and monolithic catalysts must be accommodated.
- (4) Pressure drop, even with pellets, must not be excessive.

The desired features, even though representing a significant improvement over the prototype axial-flow converter, implied that the second-generation device still would not be of road-weight construction. However, a certain amount of care was taken in the design to enable such mobile use later if desired (e. g., completely welded with no instrumentation, etc.)

Figure 3-9 is a schematic of the converter showing major dimensions. A lid was employed, equipped with lever clamps for rapid catalyst removal. Bosses for Swagelok-held thermowells were welded at several points.

Secondary air injection was accomplished through a perforated tubing (1/2-inch o. d.) placed between stages. A baffle between the stages enhanced mixing with the secondary air. The injection tube was removable for alteration of hole pattern and could be rotated for optimum orientation of the air injection pattern. In initial tests the optimum direction for air injection and subsequent mixing was found by observing maximum conversion of CO and hydrocarbons. Interestingly, the optimum direction was in a slightly upstream direction as indicated by the arrow in Figure 3-9.

Perforated stainless steel plates were placed at the entrance and exit planes of each catalyst stage. To prevent blow by between the catalyst bed and the lid, the converter was operated in a downflow fashion. Such a position would be inconvenient for actual automotive use; a suitable compressible gasket between catalyst and upper converter surface would then be necessary.

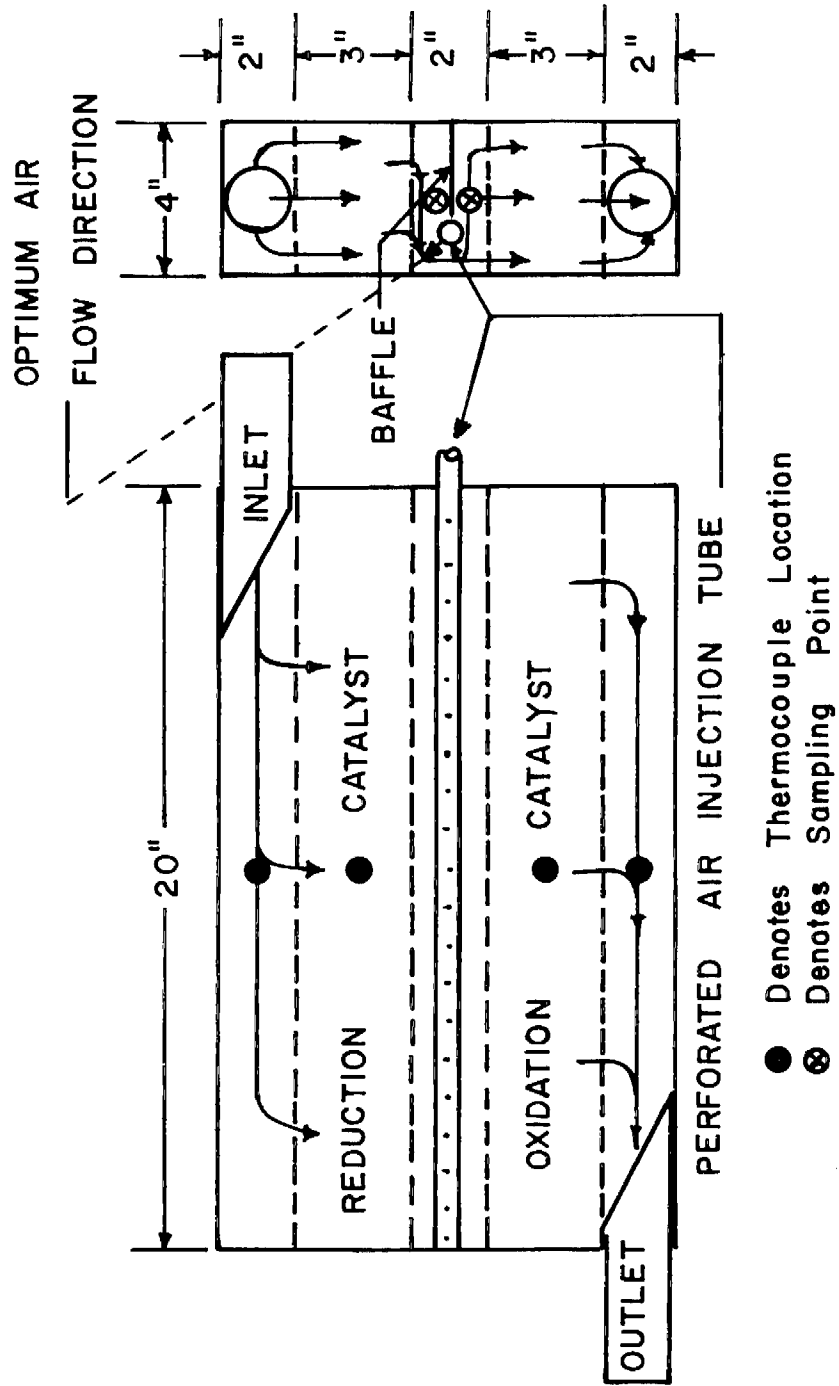


Figure 3-9 Schematic of Two-Stage Catalytic Converter.

Figure 3-10 shows the converter mounted on the Ford engine exhaust line. The secondary air line is shown entering the converter at the middle right.

In designing the cross-flow reactor, it was assumed that the maximum allowable pressure drop through the converter would be limited to 4 inches Hg. The maximum bed length for a pressure drop of 2 in Hg was calculated for flow rates of 100 and 120 scfm at 1160^oF assuming the gaseous properties for nitrogen were applicable. The two flow rates would apply to first and second stages, respectively.

It was assumed that a maximum space velocity of 50,000 hr⁻¹ was allowable. Thus, for 120 scfm flow rate, catalyst volume (per bed) would be about 240 cu in. Using a graphical correlation of the Ergun equation for pelletized beds (Bauerle and Nobe, 1971) it was determined that a reasonable combination of cross-sectional area and length would be 80 sq. in. and 3 in, respectively, in each bed. The calculations were made for the rigorous conditions of 1/8-inch pellets and only 30% voids. Larger pellets and/or a larger void fraction would lead to lower pressure drops. The use of monolithic beds would result in even lower pressure drops.

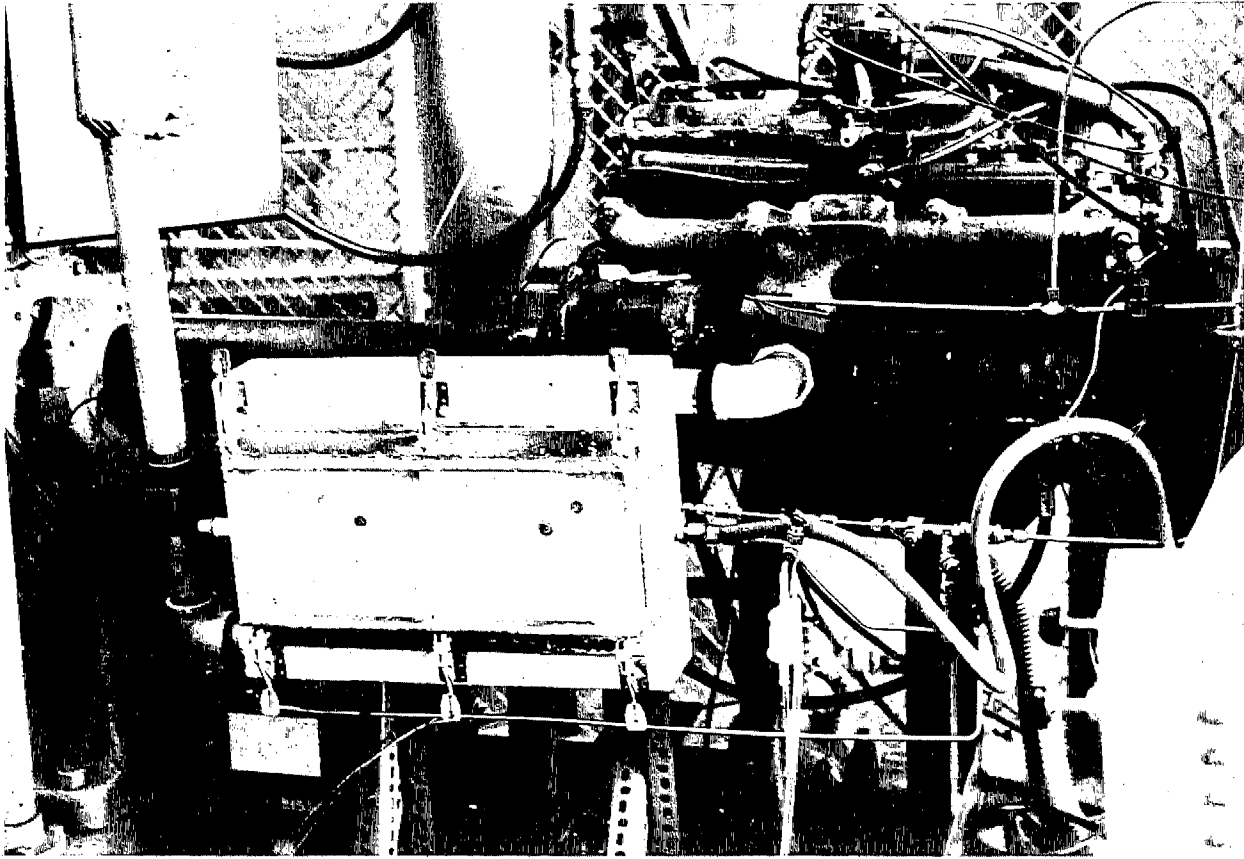


Figure 3-10. Two-Stage Converter Mounted on Engine Exhaust Line.

4. RESULTS AND DISCUSSION

The presentation of project results is delineated into each of the individual work tasks. The results of the screening studies have been subdivided further in terms of the particular reaction under study.

4.1 Screening Studies.

4.1.1 Catalytic NO Reduction with CO.

Table 4-1 presents a summary of data for NO reduction with CO.

Using the temperature for 80% conversion of NO as a criterion for classification, a condensed listing of the more active catalysts is given in Table 4-2. Included are the temperatures necessary to attain 100% conversion with each of the catalysts.

It can be seen that activity of the catalyst requiring the lowest temperature for 80% conversion, No. 83B, bastnasite nickel chromium oxide (carrier free), was very insensitive to temperature above 80% conversion. The noble metal catalysts, on the other hand, all showed moderately high sensitivity to temperature, as did the rare earth nickel iron oxide catalyst, No. 49.

There were some catalysts that reached 100% conversion below 500°C, but temperatures for 80% conversion were somewhat higher than those listed in Table 4-2. The nickel chromium spinel catalysts, activated monel (No. 52) and the lanthanum oxide-strontium oxide-cobalt oxide catalyst (No. 7) were of interest.

Figure 4-1 gives the conversion of NO with the noble metal catalysts. The order of decreasing activity for the four noble catalysts is Rh > Ru > Pd > Pt. It is interesting to note that the Ni-Pt catalyst (Girdler G43) which contains 0.1% platinum and the Engelhard catalyst (0.5% Pt) had approximately equivalent activity. The data for the Pt, Ru and Rh are in good agreement with data reported previously (Bauerle et al., 1972). In that study it was shown that the NO-CO reaction produced up to 100 ppm N₂O under the test conditions employed.

Table 4-1. Summary of Results of Screening
Studies-Reduction of NO with CO.

Catalyst No.	Temperature ($^{\circ}$ C) for Conversion of:				
	20%	40%	60%	80%	100% +
<u>Cobalt Based Catalysts</u>					
2	315	375	410	435	500
18	380	440	480	--	(67)
9*	--	360	470	--	(66)
20	450	--	--	--	(22)
7	--	180	255	330	430
27	180	365	400	435	500
8*	--	--	382	455	(92)
1++	395	460	--	--	(53)
19	380	445	480	--	(67)
15	355	410	480	--	(62)
22	350	425	460	--	(77)
30	325	390	420	445	500
31	330	395	450	490	(87)
11	280	370	430	475	(90)
24	345	385	420	455	500
37	475	--	--	--	(34)
38	435	480	500	--	(60)
39	--	--	--	--	(10)
40	490	--	--	--	(21)
41	330	390	440	500	(80)
42	--	--	--	--	(10)
3	350	376	405	460	(91)
5	500	--	--	--	(20)
29	460	--	--	--	(30)
60	400	465	500	--	(60)
32	100	235	355	410	455
34A	100	180	250	310	440
34B	350	--	--	--	(39)
<u>Rare Earth Oxide Catalysts</u>					
23	360	447	--	--	(55)
71	340	375	414	--	(76)
43	425	500	--	--	(40)
111***	--	260	315	380	400

Table 4-1 (cont.)

Catalyst No.	Temperature ($^{\circ}\text{C}$) for Conversion of:				
	20%	40%	60%	80%	100%
<u>Chromium-Based Catalysts</u>					
63	--	--	--	--	(10)
56	403	445	476	495	(84)
131	282	400	460	490	(97)
<u>Nickel-Chromium Catalysts</u>					
84	220	340	403	437	500
86	270	325	360	410	(95)
87	285	350	385	402	485
81	200	265	320	375	490
61	300	350	380	410	490
85**	280	310	350	380	430
98	440	560	--	--	(40 at 560°C)
97	390	450	500	--	(60)
91	317	347	357	360	400
83A	374	410	450	--	(75)
83B**	104	110	118	150	(96)
<u>Nickel-Based Catalysts</u>					
35	100	190	230	270	370
73	--	175	200	237	380
50	250	315	375	408	500
68	--	220	300	405	(95)
47	180	240	295	365	480
49	195	200	200	205	230
89	260	285	305	335	490
57	246	277	310	340	410
46	115	140	175	270	500
65*	475	--	--	--	(28)
6	305	405	500	--	(60)
94	410	485	--	--	(44)
58U	403	437	460	485	510
58	--	--	--	--	(2)

Table 4-1 (cont.)

Catalyst No.	Temperature ($^{\circ}\text{C}$) for Conversion of:				
	20%	40%	60%	80%	100%
<u>Copper-Nickel Catalysts</u>					
54*	245	294	345	400	480
52u	490	--	--	--	(24)
52	230	283	305	330	400
<u>Copper-Based Catalysts</u>					
62	360	420	460	--	(75)
44	365	400	415	430	(97)
64	345	385	410	430	(95)
67	340	405	460	485	(87)
66	310	375	435	465	500
113	110	130	145	170	300
<u>Tungsten Bronze Catalysts</u>					
116	270	290	300	320	390
117	325	350	370	395	410
118	--	--	--	--	(2% at 400°C)
<u>Other Non-Noble Metal Catalysts</u>					
28	390	445	480	500	(80)
51	265	335	380	420	500
45	473	--	--	--	(30)
112	285	335	370	413	500
115	115	143	174	240	500
103	400	470	--	--	(58)
104	365	395	485	--	(61)
106	474	--	--	--	(37)

Table 4-1 (cont.)

Catalyst No.	Temperature (°C) for Conversion of:				
	20%	40%	60%	80%	100%
<u>Noble Metal-Containing Catalysts</u>					
119	225	248	264	277	295
120	--	205	210	224	265
121	306	318	354	394	(98)
122	157	170	178	194	250
78	200	220	240	257	340
82	270	330	370	400	(82)
90	260	290	305	316	370
96	288	307	326	355	420
76	170	180	190	200	250
77	180	190	195	200	250
79	200	210	217	225	300
80	195	210	220	235	300
114	283	355	407	465	(90)

* Catalyst disintegrated upon reduction in CO; data are for unreduced catalyst.

** Catalyst sintered during testing.

*** 25 gm catalyst, 253 l/hr flow rate.

+ Number in parentheses denotes conversion at designated temperature (otherwise at 500°C).

++ 183 l/hr flow rate instead of standard 300 l/hr.

Table 4-2. Summary of Results with Catalysts Promoting
80% Conversion of NO Higher at 275°C or Less with CO.

Number	Catalyst Type	Temperature (°C)	
		for 80% Conversion	for 100% Conversion
83B	Bastnasite Nickel Chromium Oxide (without carrier)	150	>500
113	Copper Chromium Oxide	170	300
122	Rhodium	194	250
76	LaRhO ₃ (15%)	200	250
77	LaRhO ₃ (5%)	200	250
49	Rare Earth Iron Nickel Oxide	205	230
79	LaRhO ₃ (1%)	225	300
120	Ruthenium	226	265
80	LaRhO ₃ (0.25%)	235	300
73	Lanthanum Nickel Oxide	237	380
115	Commercial Water-gas Catalyst	240	500
78	Strontium Ruthenium Oxide	257	340
46	Nickel Manganese Oxide	270	500
35	Lanthanum Nickel Oxide	270	370
119	Palladium	277	295

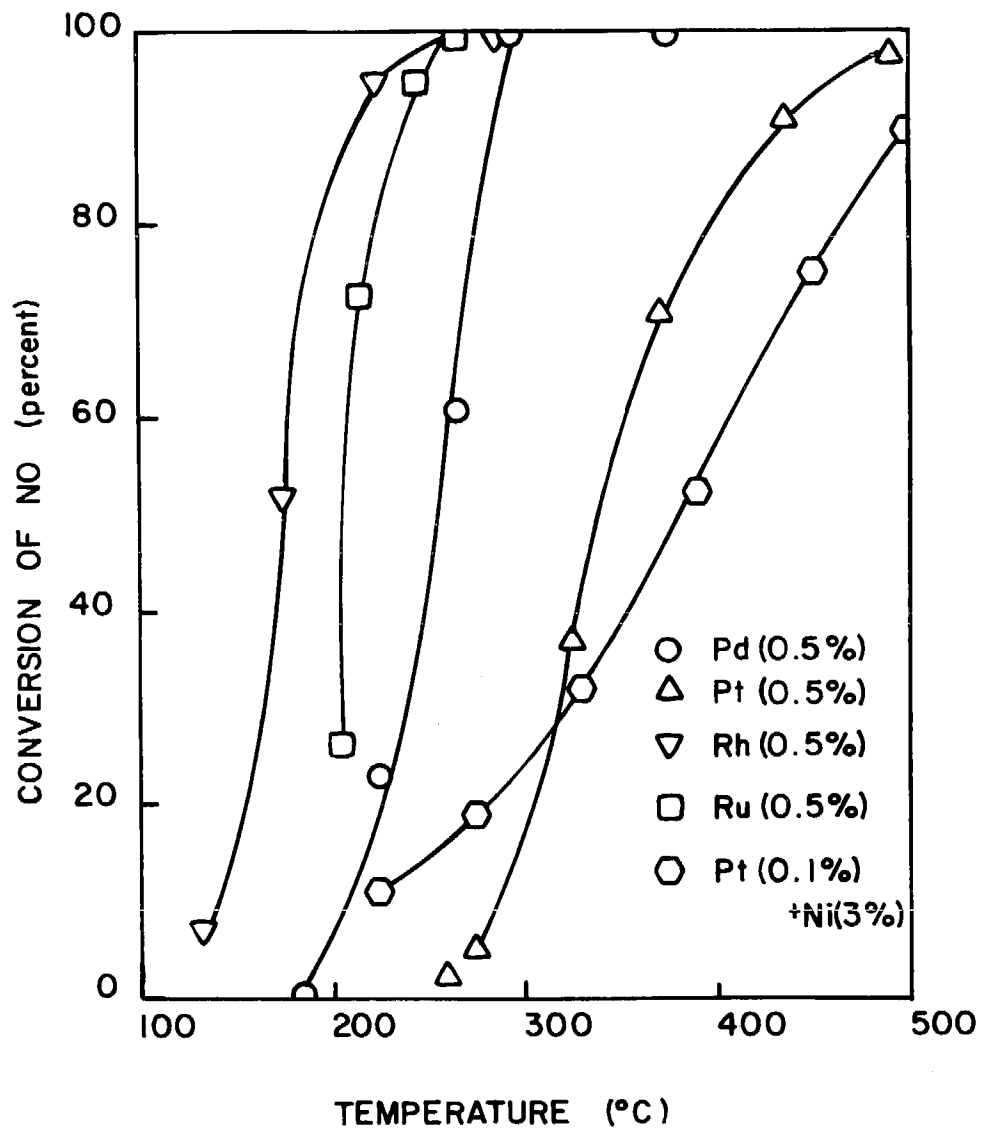


Figure 4-1 Reduction of NO with CO on Noble Metal Catalysts.

The lanthanum rhodium series of catalysts was of interest, particularly, in view of the similarity in activities of Rh and LaRhO_3 (Table 4-2). Figure 4-2 shows conversion of NO for the rhodium-containing catalysts. Of the more dilute catalysts only the 0.25% LaRhO_3 catalyst showed activity significantly lower than that of the 15% LaRhO_3 . No explanation is apparent for the maximum in conversion of NO with the 0.25% LaRhO_3 catalyst at about 400°C.

The amounts of rhodium in 15%, 5%, 1% and 0.25% LaRhO_3 are 5.3, 1.8, 0.4, and 0.09%, respectively. Thus, the 1% LaRhO_3 has a noble metal loading approximately equivalent to that in the platinum PTX converters (Engelhard) proposed for use in Ford automobiles in 1975. At the time of this writing commercial rhodium catalysts were being marketed at 1 1/2 to 2 1/2 times the cost of platinum catalysts.

Another group of promising catalysts were the ruthenium-containing perovskite materials. Reduction of NO with CO on these catalysts is shown in Figure 4-3. Ruthenium (0.5%) catalyst is also shown on the graph for reference. The 5% SrRuO_3 (2% Ru) and the ruthenium catalyst had identical activities.

Dilution of SrRuO_3 to only a 0.25% loading (0.1% Ru) caused a significant decrease in activity. Addition of yttrium to SrRuO_3 ($\text{SrY}_{0.5}\text{Ru}_{0.5}\text{O}_{2.75}$) caused a decrease in activity, also. Activity with the 5% $\text{LaNi}_{0.5}\text{Ru}_{0.5}\text{O}_3$ catalyst (1% Ru) was approximately equivalent to the $\text{SrY}_{0.5}\text{Ru}_{0.5}\text{O}_{2.75}$ (3.3% Ru).

Monel catalyst has been reported to be effective for reduction of NO in auto exhaust (Bernstein et. al., 1971, Meguerian and Lang, 1971). Tests for activity of monel and nickel metal were made using commercially-obtained metals in the form of perforated, hollow semi-cylinders (see Figure 4-4). Figure 4-5 shows the results of the activity tests. It was found that oxidation of monel in air for 16 hours at 1000°C caused a sharp increase in activity. Such an observation was also made by Meguerian and Lang (1971). The improvement with oxidation of the catalyst implies that a higher oxidation state may lead to improved activity. On the other hand, other work in this laboratory has shown that catalysts prepared by

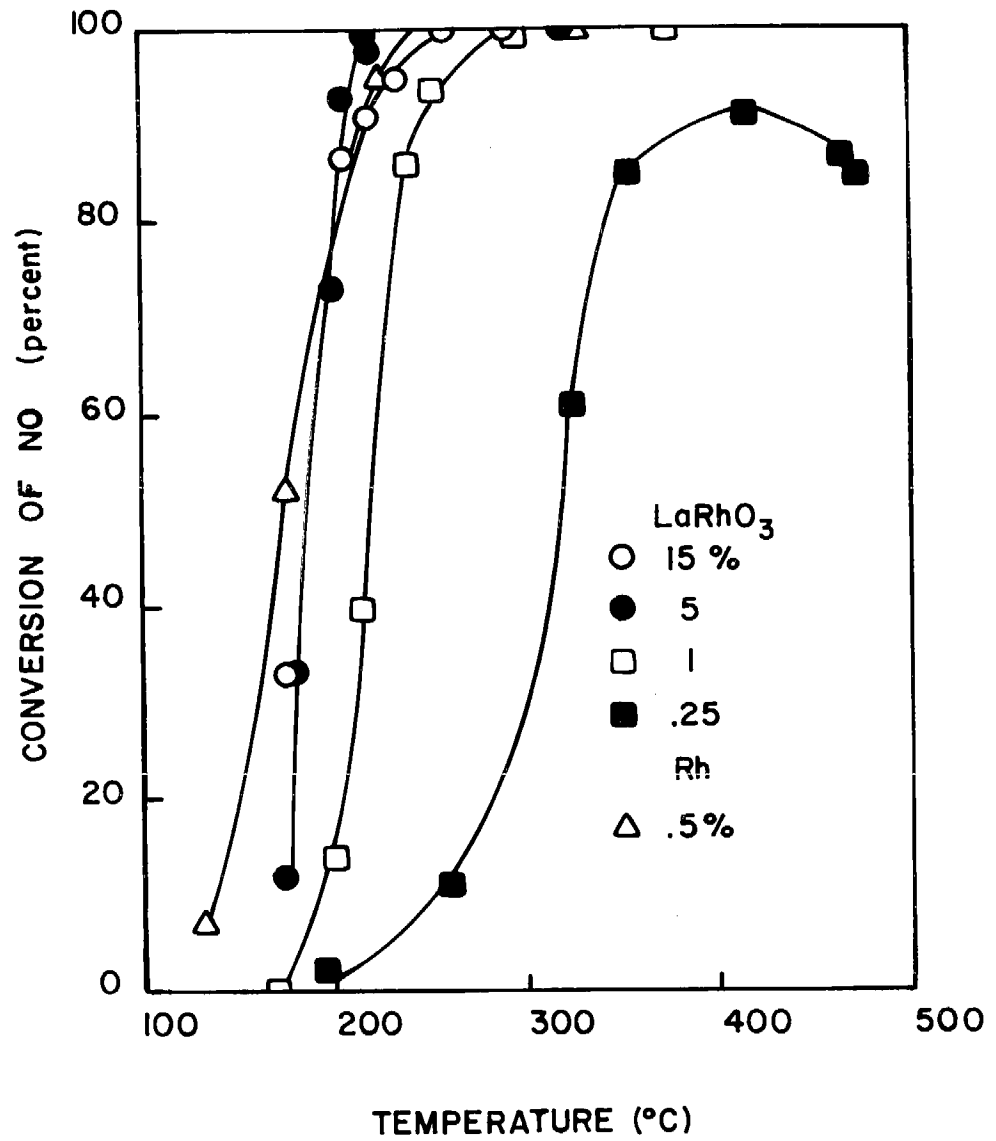


Figure 4-2 Reduction of NO with CO on Rh-Based Catalysts.

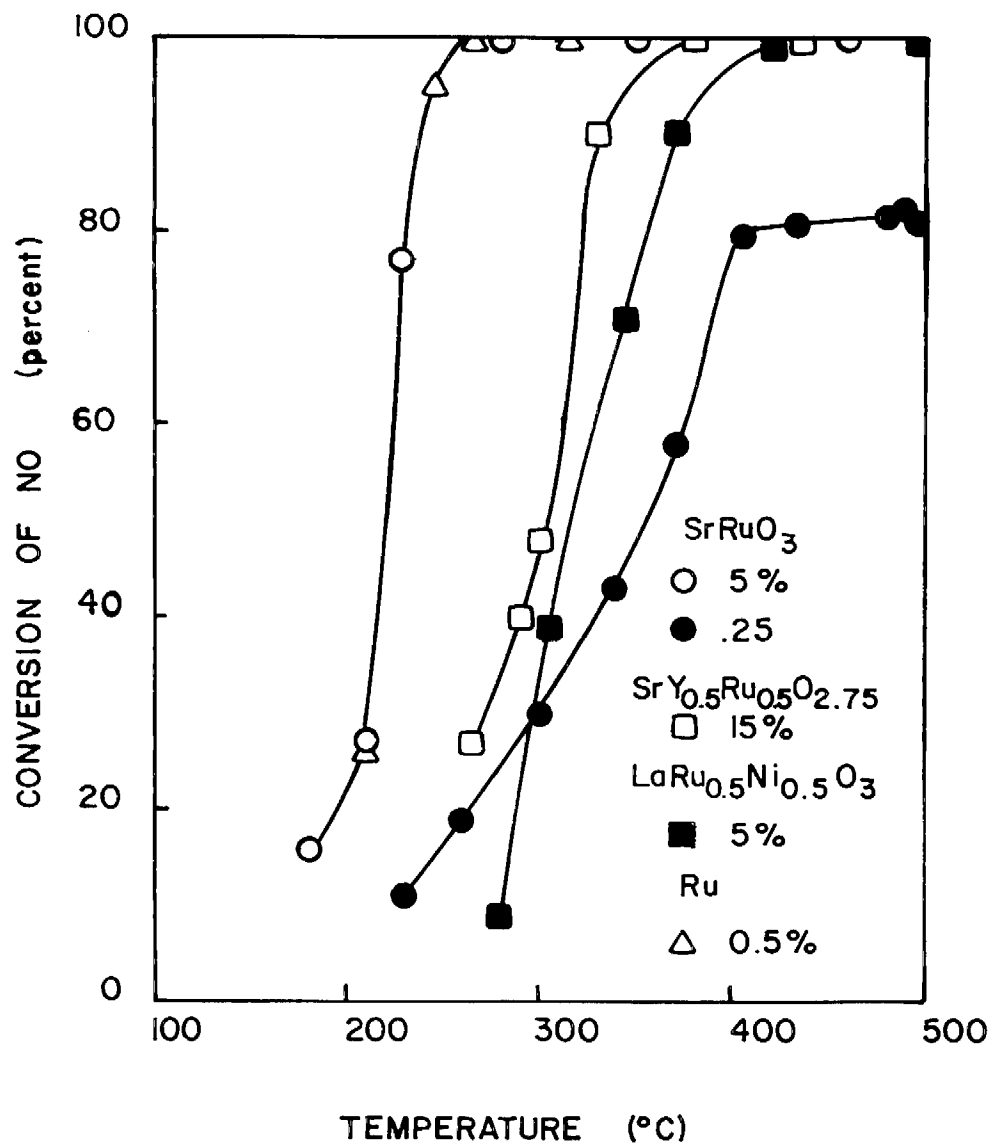


Figure 4-3 Reduction of NO with CO on Ru-Based Catalysts.



Figure 4-4. Protruded Metal Hollow Semi-Cylindrical Catalyst.

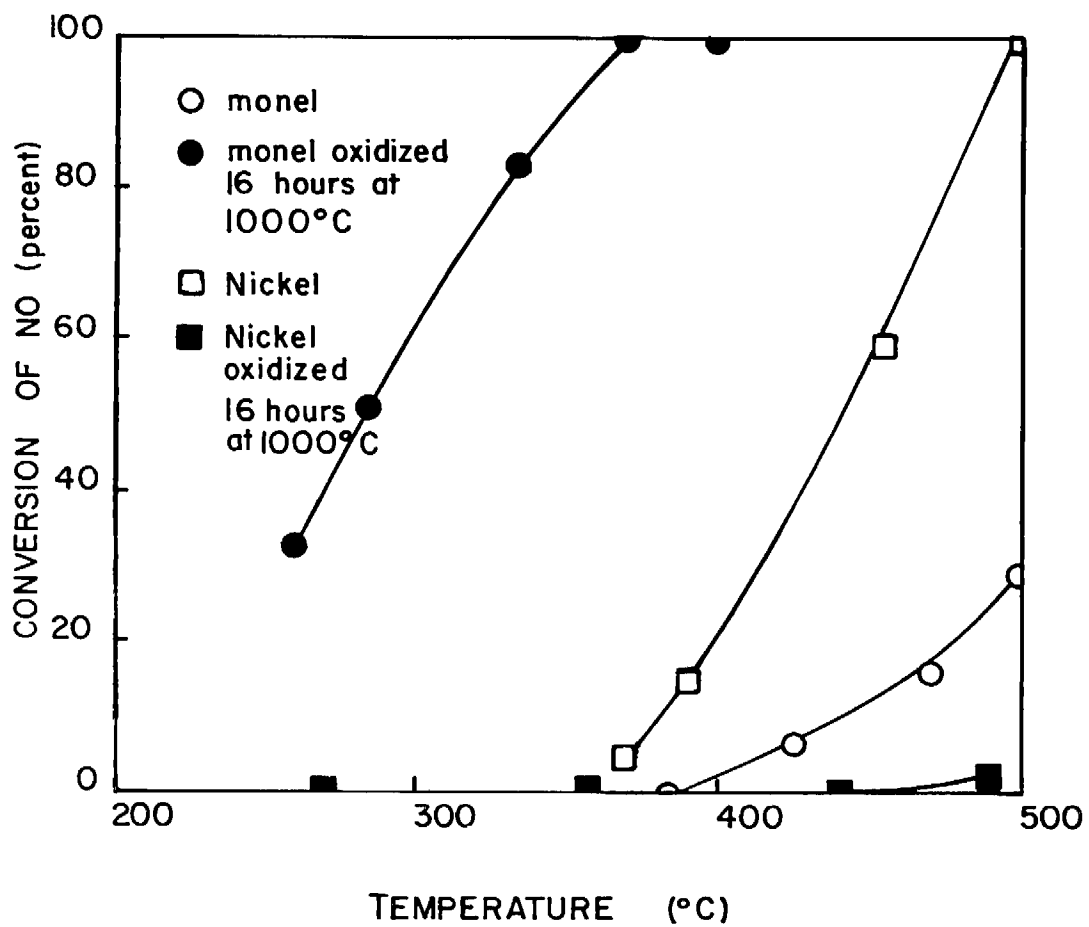


Figure 4-5 Reduction of NO with CO on Metal Catalysts.

reducing mixtures of NiO and CuO to lower oxidation states become less active as the reducing conditions (e. g., temperature and time) are made more severe (Bauerle, et al., 1973). Calcination of nickel metal resulted in a significant activity loss, as seen in Figure 4-5.

Activity of the series of catalysts containing the spinel $\text{NiO} \cdot \text{Cr}_2\text{O}_3$ is shown in Figure 4-6. The spinel composition corresponds to a Ni:Cr rate of 1:2. At about 425°C the activities of the four catalysts containing only nickel and chromium oxides and the spinel can be arranged in descending order:

$$3:2 \text{ Ni:Cr} > 1:1 \text{ Ni:Cr} > 1:2 \text{ Ni:Cr} \approx 1:3 \text{ Ni:Cr}$$

The sequence indicates that excess NiO leads to higher activity. As seen in the figure, doping the 1:1 Ni:Cr catalyst with lithium leads to sharply increased activity and temperature dependence.

Catalyst 83B, bastnasite nickel chromium oxide, the material showing the highest activity up to the 80% conversion level (Table 4-2) was prepared without a carrier. The material was originally prepared by calcining at 1000°C a mixture of bastnasite and a portion of Catalyst 81 ($\text{NiO} \cdot \text{Cr}_2\text{O}_3 + \text{NiO}$) resulting in a ratio R. E. :Ni:Cr = 2:1:1. The spinel portion of No. 81 had already been prepared and verified; however, it is not known if some of the nickel or chromium in the spinel itself reacted with individual rare earth metals (to form, e. g., LaNiO_3). Thus, the composition of bastnasite nickel chromium oxide might be interpreted as consisting of at least some Ni-Cr spinel, some rare earth nickel oxide, and excess bastnasite. The latter material did exhibit some activity itself (catalyst 43) and was certainly more active than the standard carrier (Al_2O_3). During the tests the catalyst disintegrated and subsequent attempts to make strong pellets were not successful. Nevertheless, in view of the high activity of the material, further research in methods to produce strong, unsupported granular catalysts from this material or the production of monoliths made predominantly from the material is desirable.

To summarize the screening studies of NO reduction with CO,

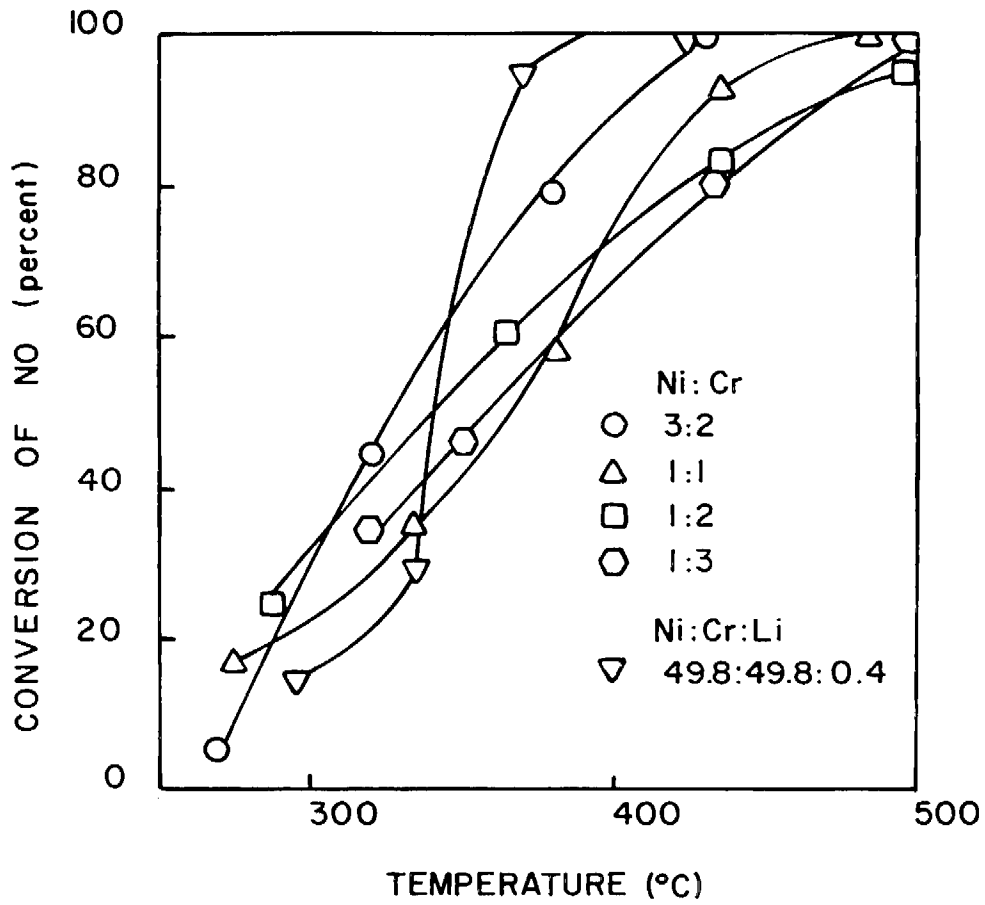


Figure 4-6 Reduction of NO with CO on NiO·Cr₂O₃ Spinel Catalysts.

those catalysts listed in Table 4-2, as well as the metallic catalysts and the nickel-chromium spinel series were considered to be good candidates for the automotive tests. Final selection was based on these results and the NO-H₂ tests to be described later.

4.1.2 Catalytic Oxidation of CO.

Table 4-3 presents results of catalyst tests for oxidation of CO in air. Based on temperature for 80% conversion, Table 4-4 lists the more active catalysts. It can be seen that the lowest temperatures for complete conversion of CO were attained with the noble metals. Several cobalt-containing catalysts and, surprisingly, monel (the oxidized version) showed high activity.

Figure 4-7 shows conversion-temperature data for the four commercial noble metal catalysts and the commercial Ni-Pt catalyst. Very little difference in activity for the four Engelhard noble metal catalysts was seen. The activity of these catalysts was strongly dependent on temperature. In fact, with Pt, Pd and Ru, it was not possible to maintain steady-state conditions between 20 and 90% conversion. Thus, the shape of the conversion curve for Pd may be in error as plotted; a more nearly vertical rise may be the true relationship, and the point for 80% conversion may be closer to 80°C.

The Pt-Ni catalyst was somewhat less active for CO oxidation than the straight platinum catalyst; however, it had only a fifth the amount of platinum in the Engelhard catalyst.

Figure 4-8 shows activity of the metallic catalysts. As in the screening studies of NO reduction by CO, pre-oxidation of monel at 1000°C resulted in a significant improvement in activity. Nickel metal had relatively low activity for CO oxidation and pre-oxidation resulted in a complete loss in activity.

As seen in Table 4-4, several of the active catalysts contain cobalt. Early work in this project was concentrated on cobalt-containing catalysts, in view of preliminary information obtained from Prof. W. F. Libby (1971). Some of the early results were quite encouraging.

Table 4-3. Summary of Results of Screening Studies-
Oxidation of CO in Air.

Catalyst No.	Temperature (°C) for Conversion of:				
	20%	40%	60%	80%	100% ⁺
<u>Cobalt-Based Catalysts</u>					
2	80	90	105	135	300
20	72	105	135	200	320
7	--	--	80	90	200
27	--	60	90	100	160
1	80	115	165	230	350
15	--	180	375	300	(93% at 380°C)
22	50	80	100	120	200
30	--	35	60	80	135
31	25	70	100	125	220
11	110	145	150	175	225
24	65	80	85	90	170
37	260	370	440	495	(82)
38	150	155	160	165	350
39	260	320	355	420	(91)
40	170	180	204	250	(95)
41	110	140	155	175	230
3	105	150	195	255	350
5	97	125	250	--	(66% at 380°C)
29	120	185	235	300	(93)
60	80	90	100	120	250
32	--	42	75	100	200
33	--	350	--	--	(55)
34A	25	35	55	80	200
34B	--	120	180	250	500
42	--	350	--	--	(56)
<u>Rare Earth Oxide Catalysts</u>					
23	215	265	285	370	(85)
71	130	265	380	--	(64% at 420°C)
43	--	110	230	420	(97)
111	290	305	322	400	(80)
<u>Chromium-Based Catalysts</u>					
63	320	343	375	500	(80)
56	280	325	365	425	(89)

Table 4-3 (cont.)

Catalyst No.	Temperature ($^{\circ}\text{C}$) for Conversion of:				
	20%	40%	60%	80%	100%
<u>Nickel-Chromium Catalysts</u>					
84	370	445	495	--	(61)
86	337	390	435	--	(75)
87	177	250	342	--	(79)
81	160	180	215	295	(93)
61	210	295	345	400	(86)
85	--	156	176	223	350
97	390	480	--	--	(44)
91	200	290	308	353	470
83A	320	383	420	450	(97)
83B	294	340	390	470	(84)
<u>Nickel-Based Catalysts</u>					
35	100	140	175	224	350
73	--	170	320	305	(95)
68	--	150	200	295	(97)
49	175	200	210	225	300
89	154	182	230	305	(90)
57	65	85	105	154	300
65	335	410	480	--	(66)
6	300	335	405	--	(70)
94	160	200	226	272	(96)
58U	250	295	314	327	415
58					(0)
<u>Copper-Nickel Catalysts</u>					
54	100	115	140	180	300
52u	205	223	239	256	350
52	87	93	100	110	140
<u>Copper-Based Catalysts</u>					
64	290	375	410	460	(91)
62	80	95	110	135	220
67	190	210	243	330	(91)
66	140	180	200	250	430
<u>Tungsten Bronze Catalysts</u>					
116	180	230	282	330	(92% at 400 $^{\circ}\text{C}$)
117	--	400	--	--	(46% at 440 $^{\circ}\text{C}$)

Table 4-3 (cont.)

Catalyst No.	Temperature (°C) for Conversion of:				
	20%	40%	60%	80%	100%
<u>Other Non-Noble Metal Catalysts</u>					
28	250	275	293	385	(89)
51	--	310	385	435	(88)
112	120	147	178	242	400
115	55	65	73	110	500
103	290	327	--	--	(56)
104	315	--	--	--	(28)
106	--	--	--	--	(19)
110					
<u>Noble Metal-Containing Catalysts</u>					
119	68	57	93	91	105
120	75	80	83	86	100
121	70	72	74	76	92
122	85	100	110	116	135
78	150	180	210	257	360
82	220	228	243	265	(94% at 370°C)
90	240	270	295	353	(97)
96	246	370	--	--	(95)
76	--	125	180	200	280
77	80	105	120	135	220
79	200	210	218	225	310
80	180	205	210	230	310
114	123	130	135	138	175

+ Number in parentheses denotes conversion at designated temperature (otherwise at 500°C).

Table 4-4. Summary of Results with Catalysts Promoting
80% Conversion of CO or Higher at 110°C or Less.

Catalyst	Temperature (°C) for		
	80% Conversion	100% Conversion	
121	Platinum	76	92
30	Neodymium Cobalt Oxide	80	135
34A	Cobalt Oxide (Impregnated)	80	200
120	Ruthenium	86	97
7	Lanthanum-Strontium- Cobalt Oxide Mixture	90	200
24	Rare Earth Cobalt Oxide	90	170
119	Palladium	91	105
27	Lanthanum-Strontium- Cobalt Oxide Mixture	100	160
32	Cobalt Oxide	100	200
52	Monel (oxidized)	110	140
115	Girdler G-66A	110	500

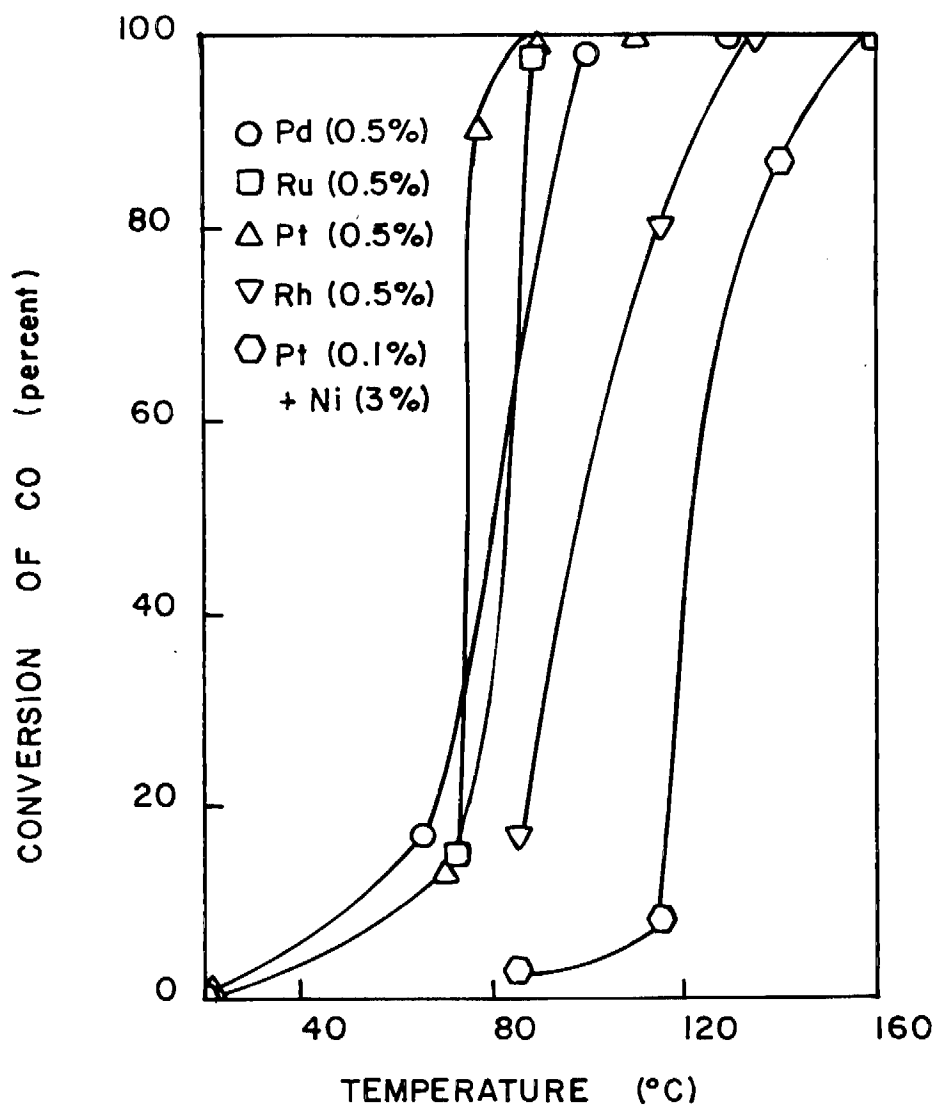


Figure 4-7 Oxidation of CO on Noble-Metal Catalysts.

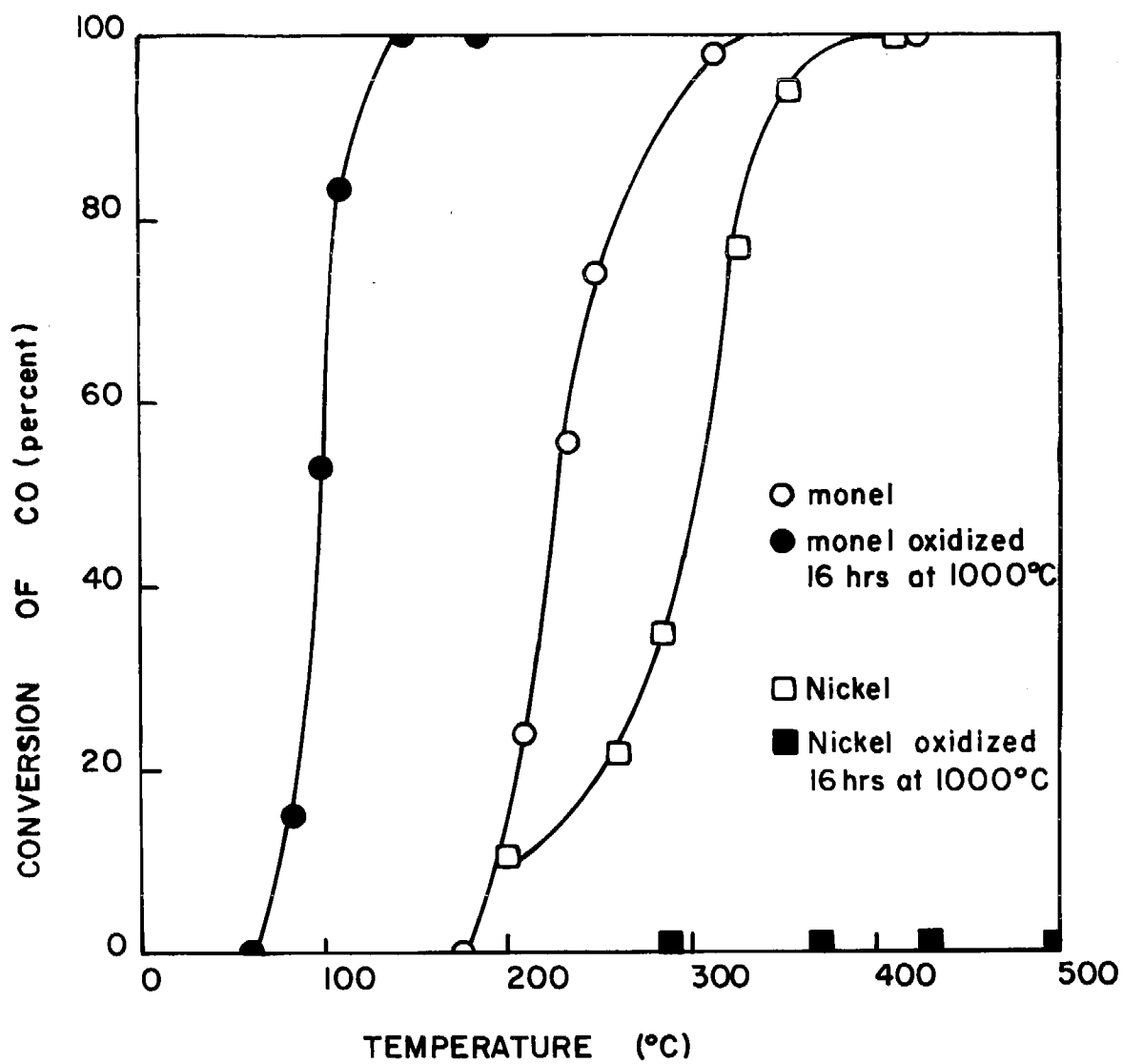


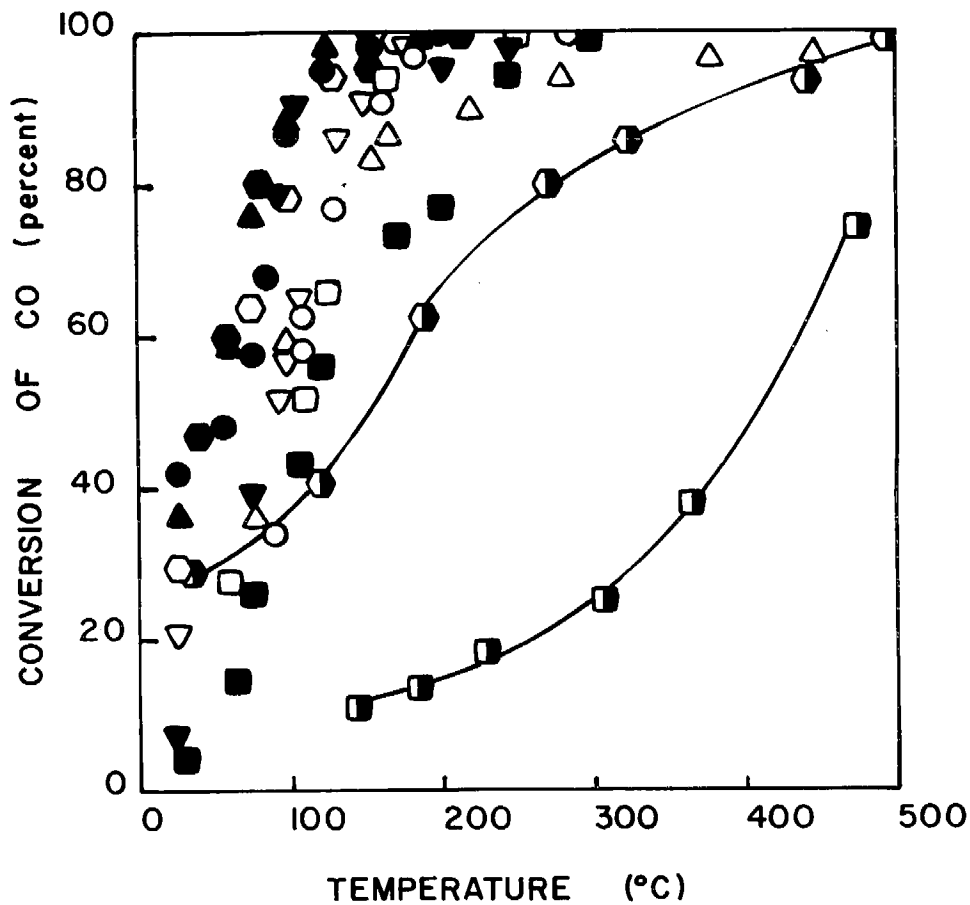
Figure 4-8 Oxidation of CO on Metal Catalysts.

Of interest were oxide compounds of rare earths and cobalt; in particular, those with the perovskite structure. Catalysts 2 and 7 were those initially tested (the catalysts were numbered consecutively in order of preparation and **not** in order of test) and were thought to be LaCoO_3 and $\text{La}_{0.85}\text{Sr}_{0.15}\text{CoO}_3$, respectively. There was a marked, improvement in activity with the addition of strontium as seen in Table 4-3. The beneficial effects of doping LaCoO_3 with Sr for use as an oxygen electrode had been previously reported (Meadowcroft, 1970) and a similar improvement for CO oxidation catalysis was assumed to be the case in the present study.

As mentioned, at the time Catalyst 7 was tested it was assumed that the material was $\text{La}_{0.85}\text{Sr}_{0.15}\text{CoO}_3$. A second batch of the compound was prepared by calcination of La_2O_3 , SrCO_3 and CoCO_3 at 1000°C . This catalyst (No. 20) had significantly lower activity than Catalyst 7 and was similar in activity to the undoped LaCoO_3 (No. 2).

X-ray diffraction spectra were obtained for the three catalysts. It was found that for Catalysts 2 and 20 the x-ray patterns conformed closely with data on file or obtained from the literature. The pattern for Catalyst 7 indicated that the material was a mixture of oxides. It was subsequently determined from Dr. M. Sheridan, who prepared the material that a calcination temperature of 500°C had been employed. Thus, compound formation was not possible at this low temperature. To further test the supposition that a mixture of oxides was present in Catalyst 7, a mixture of the oxides was prepared and pelletized (Catalyst 27). It was seen that activity was the same as Catalyst 7. Cobalt oxide was probably the constituent responsible for the high activity of the oxide mixtures. A cobalt oxide catalyst (No. 32) was prepared and tested. Activity data were, again, very close to those obtained with the oxide mixture. Finally, a cobalt oxide catalyst was prepared by impregnation methods (No. 34A). Activity was approximately equivalent with that of the pressed cobalt oxide catalyst and the mixture of oxides.

Figure 4-9 shows the data for Catalysts 7, 32, and 34A (these points are not connected for clarity). The verified mixed oxides were very close in activity; Nos. 30 (NdCoO_3), 24 (rare earth cobalt oxide), and 31 (DyCoO_3).



○ -#2, LaCoO_3 ; ● -#7, $\text{La}_2\text{O}_3 + \text{SrO} + \text{Co}_2\text{O}_3$; □ -#11, Ce-Co Oxide;
 ■ -#20, $\text{La}_{0.85}\text{Sr}_{0.15}\text{CoO}_3$; △ -#22, GdCoO_3 ; ▲ -#30, NdCoO_3 ;
 ▽ -#31, DyCoO_3 ; ▼ -#24, R.E. Cobalt Oxide; ◐ -#32, Cobalt Oxide;
 ◑ -#34A, Cobalt Oxide (Impregnated); ◒ -#34B, Cobalt Oxide (Impregnated, Calcined at 1000°C); ◓ -#37, R.E. Cobalt Oxide (Calcined at 1000°C).

Figure 4-9 Oxidation of CO on Cobalt Oxide Catalysts.

It should be pointed out that the rare earth cobalt oxide (No. 24), which appeared to be as active as cobalt oxide may have contained free cobalt oxide. The mixed oxide of cobalt and cerium has not been verified, as it has for La, Dy, Gd and Nd. It appears that neodymium may be somewhat superior to lanthanum for preparation of rare earth cobalt catalysts.

Figure 4-9 also shows data for two catalysts that were prepared and then calcined at elevated temperatures. These catalysts were prepared to determine if a blue coloration that had appeared on some of the R. E. cobalt oxide pellets during testing could be due to the formation of cobalt aluminate, CoAlO_3 , and to determine if this aluminate spinel had significant activity itself. In either case, with Catalysts 34B, cobalt oxide (impregnated), and 37, rare earth cobalt oxide the pellets uniformly became bright blue after calcining at 1000°C , indicating the reaction between alumina and cobalt.

As shown in Figure 4-9, the formation of the aluminate leads to drastically reduced activity (compare data for Catalysts 34A and 34B and for Catalysts 24 and 37). Thus, the use of catalysts containing cobalt and alumina may not be practicable if temperatures approaching 1000°C are expected. Some of the blue aluminate was observed to form in the temperature range of the test conditions indicating that formation can, in fact, begin at 500°C .

Other carrier materials were tested to determine if elevated temperatures would lead to reaction between the active material and the catalyst. The catalysts were prepared by impregnation methods using aqueous solutions of cobalt and rare earth nitrates. The carriers were (a) an AlSiMag (American Lava) monolith made of cordierite ($4\text{MgO} \cdot 4\text{Al}_2\text{O}_3 \cdot 10\text{SiO}_2 \cdot \text{H}_2\text{O}$) (b) two Cercor (Corning) monoliths made of β -spodumene ($\text{Li}_2\text{O} \cdot \text{Al}_2\text{O}_3 \cdot 4\text{SiO}_2$), one of these Al_2O_3 -coated and (c) β -spodumene pellets. With the monoliths, the impregnated carriers were calcined at 1000°C , while with the β -spodumene pellets, batches were made at 500°C and 1000°C , respectively.

Figure 4-10 shows the conversion data for these catalysts. The AlSiMag monolith showed activity roughly comparable with earlier data for pelletized R.E. CoO_3 calcined at 550°C after pressing (Figure 4-6). Similarly, the oxide mixture on β -spodumene pellets (500°C calcination) was of comparable activity. Lower activity was observed with the uncoated Cercor monolith. Very low activity was observed with the Al_2O_3 -coated Cercor monolith and with the β -spodumene pellets calcined at 1000°C .

It appears that the aluminum in cordierite is less reactive with cobalt at 1000°C than is the aluminum in β -spodumene. Only in the cases of the Al_2O_3 -coated Cercor and the β -spodumene pellets calcined at 1000°C was the deep blue color characteristic of cobalt aluminate evident.

Figure 4-11 shows data for the oxidation of CO on the LaRhO_3 series of catalysts. There appears to be a maximum in activity at about the 5% loading level, although it cannot be asserted with certainty since the 15% catalyst bed weighed only 11 gm rather than the standard 14 gm.

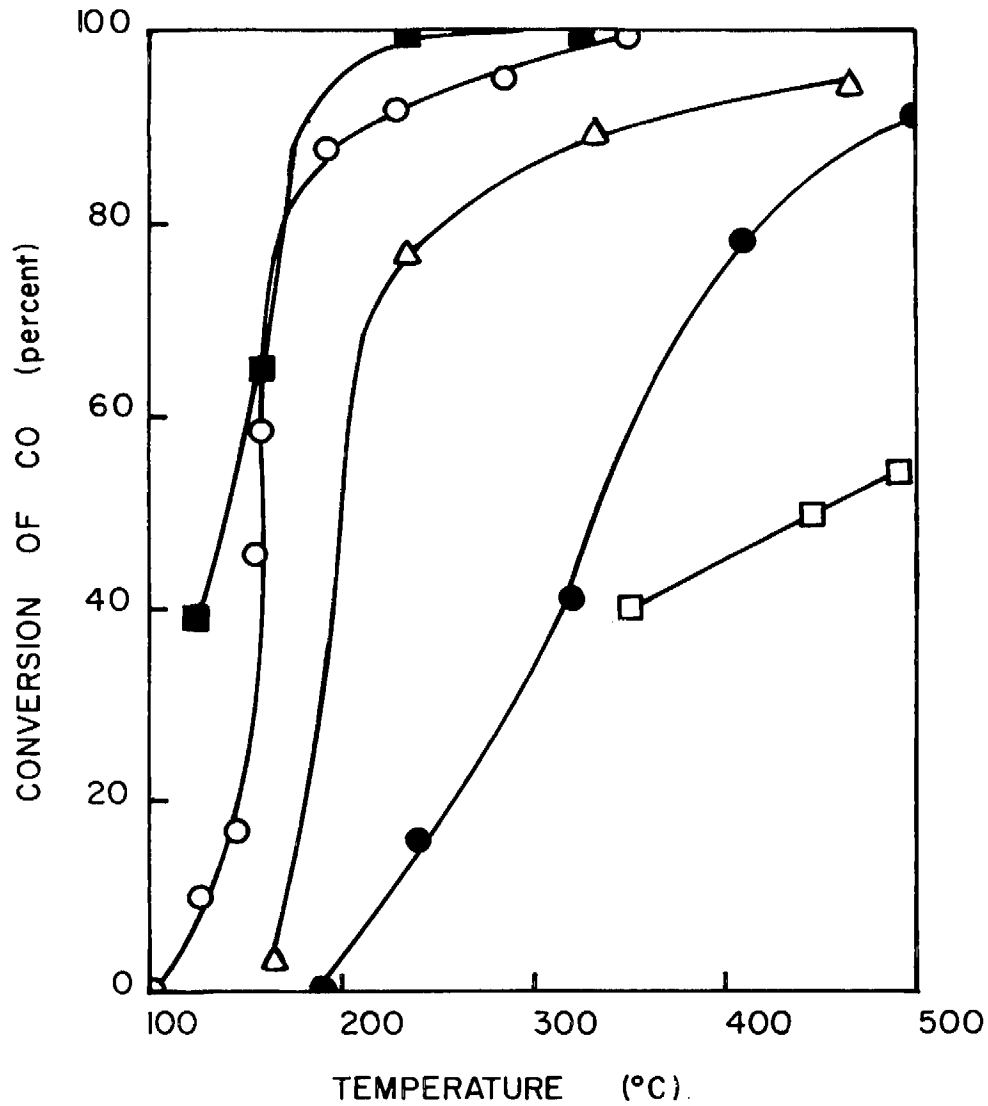
Figure 4-12 shows data for the nickel-chromium spinel series of catalysts. Oxidation activity for the four non-doped spinels is in the following order:



Thus, as in the studies of NO reduction with CO, excess NiO leads to improved activity. In addition, doping the 1:2 Ni:Cr catalyst with Li_2O improved the activity, but not to the level of the 3:2 Ni:Cr catalyst.

4.1.3 Catalytic NO Reduction with H_2 .

Table 4-5 summarizes the results of the activity tests of NO reduction with H_2 . Included in the table (last column) are the yields of NH_3 calculated as percentages of the converted NO. Tables 4-6 and 4-7 are summaries of the data for catalysts which had high activity for NO conversion (90% or higher) and which produced either high or low levels of NH_3 , respectively.



Catalysts Calcined At 1000°C

- AlSiMag Monolith
- △ Cercor Monolith
- Cercor-Al₂O₃ Monolith
- β-Spodumene Pellets

Catalysts Calcined at 500°C

- β-Spodumene Pellets

Figure 4-10 Oxidation of CO on Impregnated Rare Earth Cobalt Oxide Supported on Various Carriers.

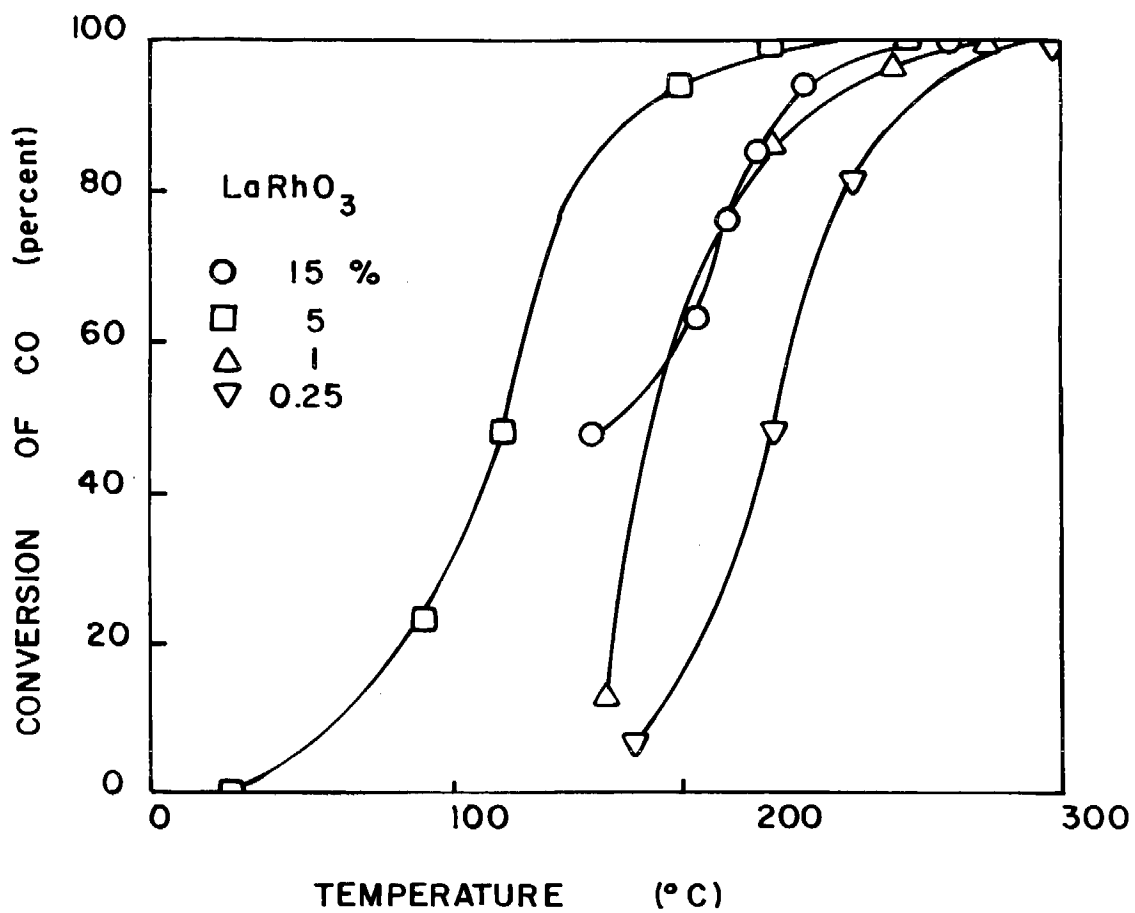


Figure 4-11 Oxidation of CO on LaRhO₃ Catalysts.

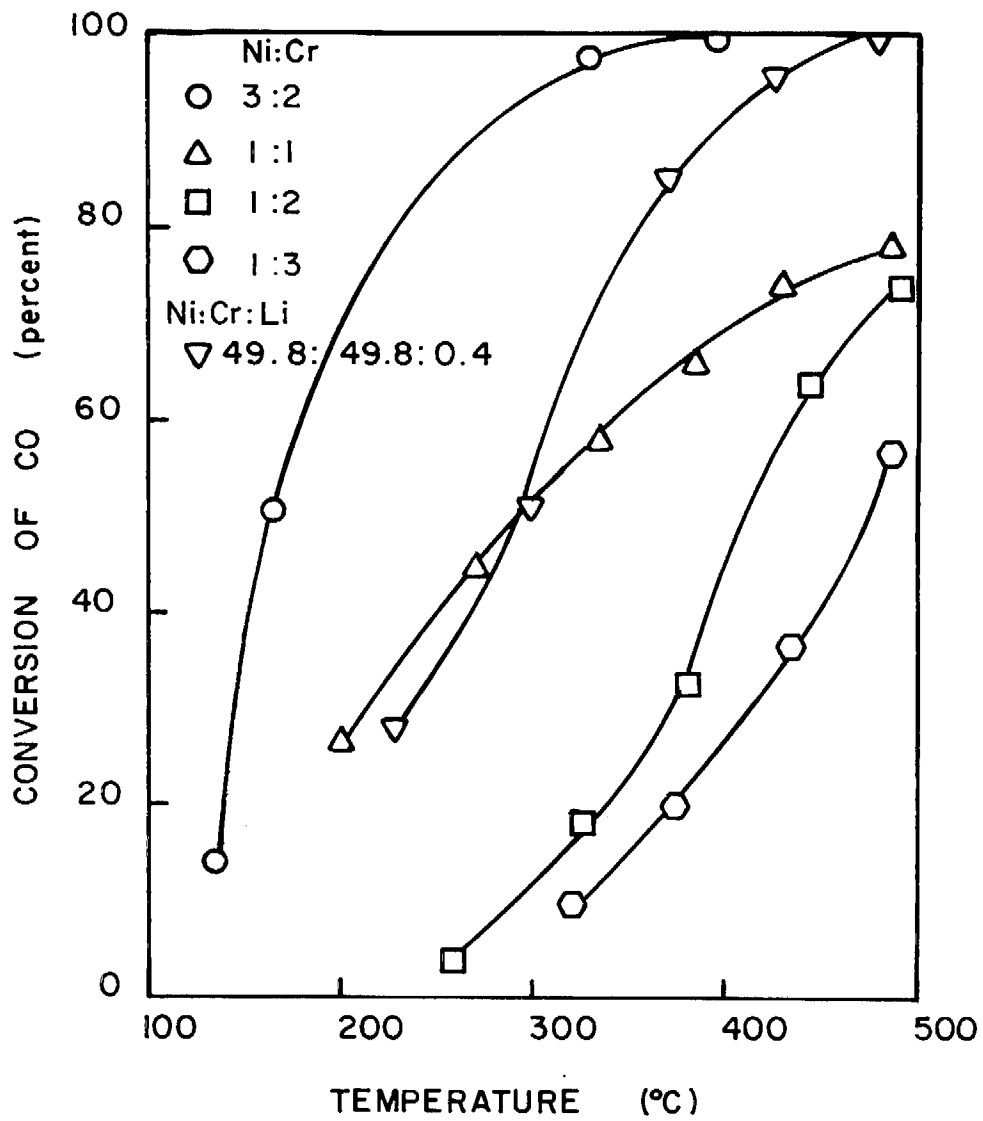


Figure 4-12 Oxidation of CO on NiO·Cr₂O₃ Catalysts.

Table 4-5. Summary of Activity Tests of NO Reduction
with H₂.

Catalyst	Temperature (°C)	Conv. of NO (%)	Conc. of NH ₃ (ppm)	Yield (% of NO Reacted converted to NH ₃)
<u>Cobalt Based Catalysts</u>				
22	260	12	12	19
	335	14	13	18
	420	30	30	19
	463	54	80	28
	480	66	88	26
24B	385	20	0	0
	431	31	33	20
	476	51	73	28
<u>Rare Earth Oxide Catalysts</u>				
111	465	9	N. A.	N. A.
	506	22	N. A.	N. A.
<u>Chromium Based Catalysts</u>				
56	475	0	0	--
	500	36	112	60
131	300	10	0	0
	375	13	0	0
	450	20	5	5
	500	36	15	8
	580	91	135	29
<u>Nickel-Chromium Catalysts</u>				
84	325	17	10	11
	380	31	35	22
	440	93	92	19
	500	100	107	21

Table 4-5. (cont.)

Catalyst	Temperature (°C)	Conv. of NO (%)	Conc. of NH ₃ (ppm)	Yield (% of NO Reacted converted to NH ₃)
86	315	12	25	40
	385	63	43	13
	432	95	68	14
	495	99	58	11
61	300	19	0	0
	335	31	0	0
	365	43	17	8
	380	83	32	7
	395	94	92	19
	425	100	71	14
	480	100	65	12
85	260	30	--	--
	320	44	55	24
	380	83	100	23
	440	100	140	27
	485	100	105	20
98	350	4	0	0
	435	10	15	29
	500	21	20	18
	555	40	35	17
97	370	17	65	74
	445	68	155	44
	505	89	175	38
	528	97	170	34
	550	99	135	26
91	150	17	--	--
	185	35	65	36
	230	100	270	52
	270	100	345	66
	425	100	400	77
	400	100	160	31
83A	490	100	25	5
	345	22	16	14
	386	67	32	9
	435	87	61	13
	490	100	86	16

Table 4-5. (cont.)

Catalyst	Temperature (°C)	Conv. of NO (%)	Conc. of NH ₃ (ppm)	Yield (% of NO Reacted converted to NH ₃)
127	182	25	0	0
	244	38	70	35
	291	96	213	43
	343	100	249	48
	404	100	268	52
	450	100	272	52
128	101	12	0	0
	150	24	0	0
	200	35	26	14
	256	58	124	41
	306	97	243	48
	398	100	386	74
	463	100	380	73
<u>Other Nickel-Based Catalysts</u>				
35	200	7	0	0
	250	24	12	10
	285	80	--	--
	350	97	75	15
	415	100	185	36
	440	100	155	30
	495	100	130	25
50	290	27	5	4
	355	62	35	11
	425	92	90	19
	475	98	156	31
68	310	56	0	0
	410	75	115	29
	510	84	95	21
47	200	2	0	--
	275	17	18	20
	305	77	107	27
	360	90	218	47
	410	96	235	47
	435	98	272	53
49	105	7	0	--
	145	63	38	12
	200	100	520	100
	260	100	365	70
	390	100	325	62

Table 4-5. (cont.)

Catalyst	Temperature (°C)	Conv. of NO (%)	Conc. of NH ₃ (ppm)	Yield (% of NO Reacted converted to NH ₃)
89	275	14	22	30
	332	47	100	41
	365	67	105	30
	412	92	105	22
	495	100	52	10
73	265	37	5	3
	320	91	53	11
	270	96	120	24
	285	99	142	28
	310	100	135	26
	390	100	135	26
57	330	33	5	3
	400	97	160	32
	450	99	160	31
	500	100	150	29
46	140	32	0	--
	215	81	92	22
	313	98	196	38
	385	99	257	50
	435	100	260	50
129	180	56	40	14
	200	93	125	26
	230	100	170	33
	285	100	290	56
	325	100	330	63
	387	100	390	75
	437	100	360	69
	485	100	150	29
58 U	225	9	0	0
	295	13	37	55
	345	99	225	44
	415	100	295	57
	520	100	115	22
58	230	15	50	6
	280	49	105	41
	400	100	335	64
	500	100	180	35

Table 4-5. (cont.)

Catalyst	Temperature (°C)	Conv. of NO (%)	Conc. of NH ₃ (ppm)	Yield (% of NO Reacted converted to NH ₃)
<u>Copper-Nickel Catalysts</u>				
54	315	15	7	9
	350	40	68	33
	400	62	143	44
	480	88	246	54
123	200	16	19	23
	270	35	160	89
	335	62	340	105
	400	88	456	100
	460	96	468	94
124	165	18	8	9
	240	43	69	31
	290	69	287	70
	320	98	369	72
	400	100	391	75
	480	100	369	71
125	165	20	15	14
	220	46	146	61
	290	90	421	90
	400	98	497	98
126	170	18	0	0
	200	36	44	24
	245	99	201	39
	310	100	374	72
	400	100	387	84
	480	100	392	75
52u	220	26	0	0
	320	100	390	75
	370	100	460	88
	455	100	515	99
	510	100	115	22
<u>Other Copper-Based Catalysts</u>				
62	372	8	--	--
	415	19	100	100
	460	39	155	76
	495	59	310	100
44	320	12	15	24
	365	83	112	26
	424	98	195	38
	465	100	175	34

Table 4-5. (cont.)

Catalyst	Temperature (°C)	Conv. of NO (%)	Conc. of NH ₃ (ppm)	Yield (% of NO Reacted converted to NH ₃)
64	330	16	65	83
	420	81	470	111
	455	96	460	92
	500	99	415	81
66	290	16	0	0
	375	41	213	100
	410	66	325	95
	470	84	490	112
<u>Other Non-Noble Metal Catalysts</u>				
51	300	0	0	--
	390	18	14	15
	443	41	98	46
	500	88	325	71
115*	140	12	0	0
	230	80	270	53
	330	96	540	88
	405	98	570	91
	505	100	550	96
103	250	6	8	19
	325	9	9	19
	375	13	9	13
	435	17	19	21
	475	18	19	20
104	325	2	5	48
	375	3	6	38
	425	5	7	27
	490	12	9	14
<u>Noble Metal-Based Catalysts</u>				
119	25	38	0	0
	35	97	10	2
	100	100	90	18
	215	100	520	100
	280	100	520	100
	320	100	520	100
	410	100	520	100
	485	100	520	100
	515	100	440	85

Table 4-5. (cont.)

Catalyst	Temperature (°C)	Conv. of NO (%)	Conc. of NH ₃ (ppm)	Yield (% of NO Reacted converted to NH ₃)
120	170	14	10	14
	170	21	25	16
	175	10	35	67
	180	29	70	46
	195	43	90	40
	205	35	105	58
	215	41	95	45
	220	72	95	25
	225	46	35	15
	230	69	65	18
	247	74	25	6
	255	75	20	5
	255	75	15	4
	275	100	40	8
	280	100	35	7
	285	100	20	4
	305	100	60	12
	312	100	65	11
	360	100	20	4
	380	100	12	2
395	100	12	2	
445	100	10	2	
121	25	18	0	0
	60	96	250	50
	125	100	370	71
	220	100	470	90
	275	100	520	100
	320	100	460	88
	440	100	440	85
	505	100	400	77
122	110	13	0	0
	135	55	15	5
	185	100	350	67
	275	100	510	98
	330	100	460	88
	400	100	220	42
	485	100	30	6

Table 4-5. (cont.)

Catalyst	Temperature (°C)	Conv. of NO (%)	Conc. of NH ₃ (ppm)	Yield (% of NO Reacted converted to NH ₃)
78	235	23	10	3
	300	95	55	11
	380	100	63	12
	420	100	65	12
	490	100	54	10
82	342	30	0	0
	385	44	0	0
	427	70	5	1
	480	75	15	4
	495	81	17	4
90	322	17	4	5
	355	33	3	2
	377	49	2	1
	388	81	11	3
	400	95	12	2
	443	97	17	3
	470	100	15	3
	500	98	11	2
96	310	12	0	0
	350	45	0	0
	400	71	0	0
	440	77	0	0
	470	82	26	6
	500	90	5	1
76	150	0	--	--
	183	87	145	32
	225	97	265	53
	275	100	400	79
	315	100	295	57
	415	100	127	24
77	185	33	--	--
	215	100	160	31
	260	100	250	48
	300	100	220	42
	340	100	220	42
	385	100	245	47
	410	100	310	60
	445	100	320	62
	485	100	260	50
495	100	240	46	

Table 4-5. (cont.)

Catalyst	Temperature (°C)	Conv. of NO (%)	Conc. of NH ₃ (ppm)	Yield (% of NO Reacted converted to NH ₃)
79	200	0	0	--
	265	93	195	40
	300	96	328	66
	315	97	345	68
	365	100	432	83
	470	91	190	40
	505	91	220	42
80	180	11	25	44
	225	81	170	40
	270	100	320	62
	280	100	335	64
	335	96	340	68
	355	92	290	61
	375	88	270	59
	435	75	195	50
	485	71	135	37
114	200	29	45	30
	245	69	90	25
	295	88	170	37
	327	93	230	48
	368	95	245	50
	400	97	255	51
	432	98	225	50
	475	99	210	41
	522	100	185	36

* 638 ppm NO inlet, all others 520 ppm.

Table 4-6. Summary of Results with Catalysts Producing High Yields of NH₃ and Higher than 90% Conversion of NO.

Catalyst		Temperature	Maximum NH ₃
Number	Type	90% Conversion of NO (°C)	output (ppm)
119	Pd (0.5%)	30	520
121	Pt (0.5%)	70	520
122	Rh (0.5%)	150	510
49	R. E. Fe Ni Oxide*	160	520
129	NiO	185	390
76	LaRhO ₃	190	400
91	NiO·Cr ₂ O ₃ +NiO, Li-doped	200	400
126	Cu Oxide-Ni Oxide (1:99)**	240	392
79	LaRhO ₃ (1%)	250	432
125	Cu Oxide-Ni Oxide (1:3)**	290	497
52	Monel	290	515
124	Cu Oxide-Ni Oxide (1:1)**	305	391
123	Cu Oxide-Ni Oxide (3:1)**	410	468
64	V-Cu Oxide	430	470

All catalysts pressed 15% with Al₂O₃ unless noted

* Impregnated on AlSiMag Monolith.

** Impregnated on Al₂O₃ Pellets.

Table 4-7. Summary of Results with Catalysts Producing Low Yields of NH_3 and Higher than 90% Conversion of NO.

Catalyst		Temperature for 90% Conversion of NO	Maximum NH_3 output
Number	Type	(°C)	(ppm)
120	Ruthenium (0.5%)	267	105@ 35% conv.; 65@ 100% conv.
82	SrRuO_3 (0.25%)	287	65
35	LaNiO_3	300	185
57	R. E. NiCo Oxide	375	160
44	CuMo Oxide	383	195
50	R. E. Ni Oxide	390	156
90	$\text{SrY}_{0.5}\text{Ru}_{0.5}\text{O}_{2.75}$	390	17
85	$\text{NiO} \cdot \text{Cr}_2\text{O}_3 + 2 \text{NiO}$	393	140
61	$\text{NiO} \cdot \text{Cr}_2\text{O}_3 + \text{NiO}$	415	92
86	$\text{NiO} \cdot \text{Cr}_2\text{O}_3$	416	68
84	$\text{NiO} \cdot \text{Cr}_2\text{O}_3 + 1/2 \text{Cr}_2\text{O}_3$	430	107
83A	R. E. -Ni-Cr Oxide	443	86
96	$\text{LaNi}_{0.5}\text{Ru}_{0.5}\text{O}_3$	495	26
97	$\text{NiO} \cdot \text{Cr}_2\text{O}_3$ (3% on monolith)	500	175

It is interesting to note that many of the catalysts listed in Table 4-7 contain nickel. Meguerian et al (1972) discussed the use of nickel oxide promoted with one or more other metal oxides and reported good activity at low temperatures and minimal NH_3 production. Klimish and Taylor (1973) reported similar results.

Catalysts 84 through 87 were made with varying ratios of nickel to chromium. Figure 4-13 shows data of NO conversion and ammonia formation for the four catalysts. The 1:1 and 1:2 Ni-Cr catalysts showed approximately equivalent activity at lower temperatures; the 3:2 Ni-Cr catalyst appeared somewhat superior to both. Above 370°C the 1:1 and 3:2 catalysts were equally active. The 1:3 catalyst had the lowest activity of the four catalysts over the entire temperature range. The 1:2 catalyst produced the lowest amount of ammonia. The 3:2 catalyst produced the largest amount of ammonia, but above 440°C , NH_3 output decreased rapidly, indicating that the higher nickel content results in accelerated NH_3 decomposition.

The 1:2 Ni-Cr catalyst, which produced the lowest amount of ammonia, is the spinel, $\text{Cr}_2\text{O}_3 \cdot \text{NiO}$. Compositions with excess NiO were somewhat more active for total NO conversion while excess Cr_2O_3 leads to decreased activity.

Performance of the pressed catalysts shown in Figure 4-13 can be compared with the nickel-chromium catalysts prepared by impregnation methods; these latter results are summarized in Figure 4-14. With the impregnated catalysts, activity for 1:1 NiO + Cr_2O_3 and 3:1 NiO + Cr_2O_3 samples were approximately equivalent throughout the entire temperature range. Again, the catalyst containing higher Ni content produced the larger amount of NH_3 . The rapid decrease in NH_3 above 440°C observed with the pressed 3:2 Ni-Cr catalyst was not observed with the impregnated catalyst. A composition analogous to the $\text{Cr}_2\text{O}_3 \cdot \text{NiO}$ spinel (i. e., 1:2 Ni-Cr) was not prepared by impregnation methods.

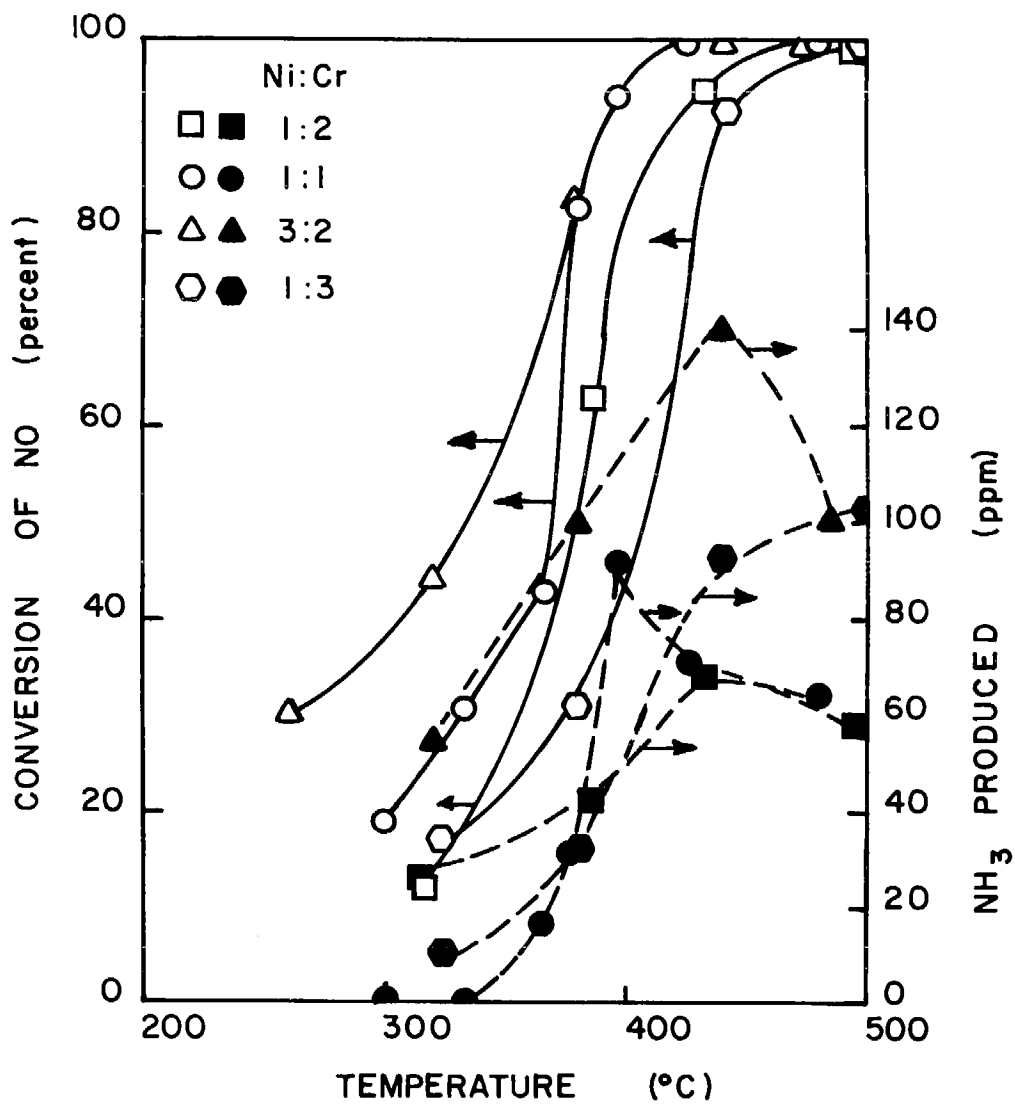


Figure 4-13 Reduction of NO with H₂ and Production of NH₃ on Pressed Nickel-Chromium Spinel Catalysts.

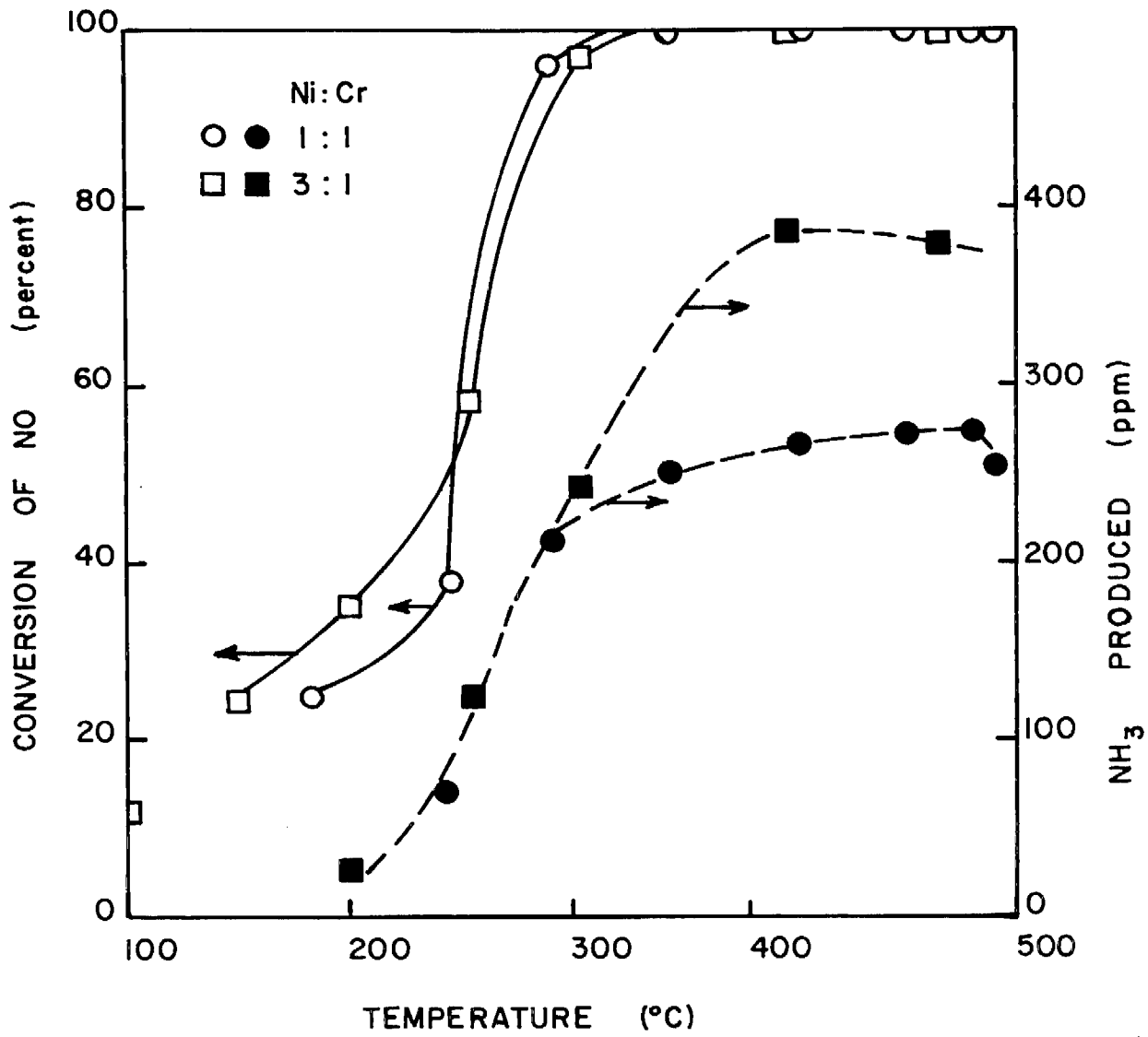


Figure 4-14 Reduction of NO with H₂ and Production of NH₃ on Impregnated Nickel-Chromium Catalysts.

The impregnated nickel-chromium catalysts produced higher overall levels of NH_3 than the pressed catalysts; in addition, activity for NO conversion was significantly higher than with the pressed catalysts (e. g., 90% conversion was attained with the 1:1 $\text{NiO} + \text{Cr}_2\text{O}_3$ catalyst at 289°C while the pressed 1:1 catalyst showed that conversion at 390°C). The higher activity of the impregnated catalysts may be attributed to better dispersion and higher surface area of the active material.

Shelef and Gandhi (1972) showed that the decomposition of NH_3 is favored thermodynamically as temperature is increased. Klimish and Barnes (1971) presented evidence that the decomposition of NH_3 may account for the decrease in NH_3 levels at high temperatures.

The higher level of NH_3 production with the more active impregnated catalysts may be due to the lower temperatures required to attain complete conversion of NO. At the lower temperatures employed to attain high conversion of NO on the more active catalysts, the rate of NH_3 decomposition is low. On the other hand, it seems reasonable to expect that the more active catalyst should also promote decomposition of NH_3 above 440°C , but such a study was not made.

Figure 4-15 summarizes results of tests with impregnated nickel-copper catalysts. The activity of these catalysts appeared to follow a definite trend. At 90% conversion the activities followed the order,

$$(99:1 \text{ Ni/Cu}) > (3:1 \text{ Ni/Cu}) \approx (1:1 \text{ Ni/Cu}) > (1:3 \text{ Ni/Cu})$$

Activity thus increased with nickel content for the impregnated nickel/copper catalysts. Ammonia production was not a strong function of nickel content. With these catalysts, unlike the nickel/chromium series, the highest nickel content did not produce the largest amount of NH_3 , and an extensive decrease in NH_3 at elevated temperatures was not seen.

The results with the impregnated Ni/Cu catalysts can be compared with Catalyst 54 (1:1 Ni-Cu) prepared by the dry pressing method. Approximately ninety-percent conversion with the latter catalyst was reached at 480°C with a maximum NH_3 production of 246 ppm. The 1:1

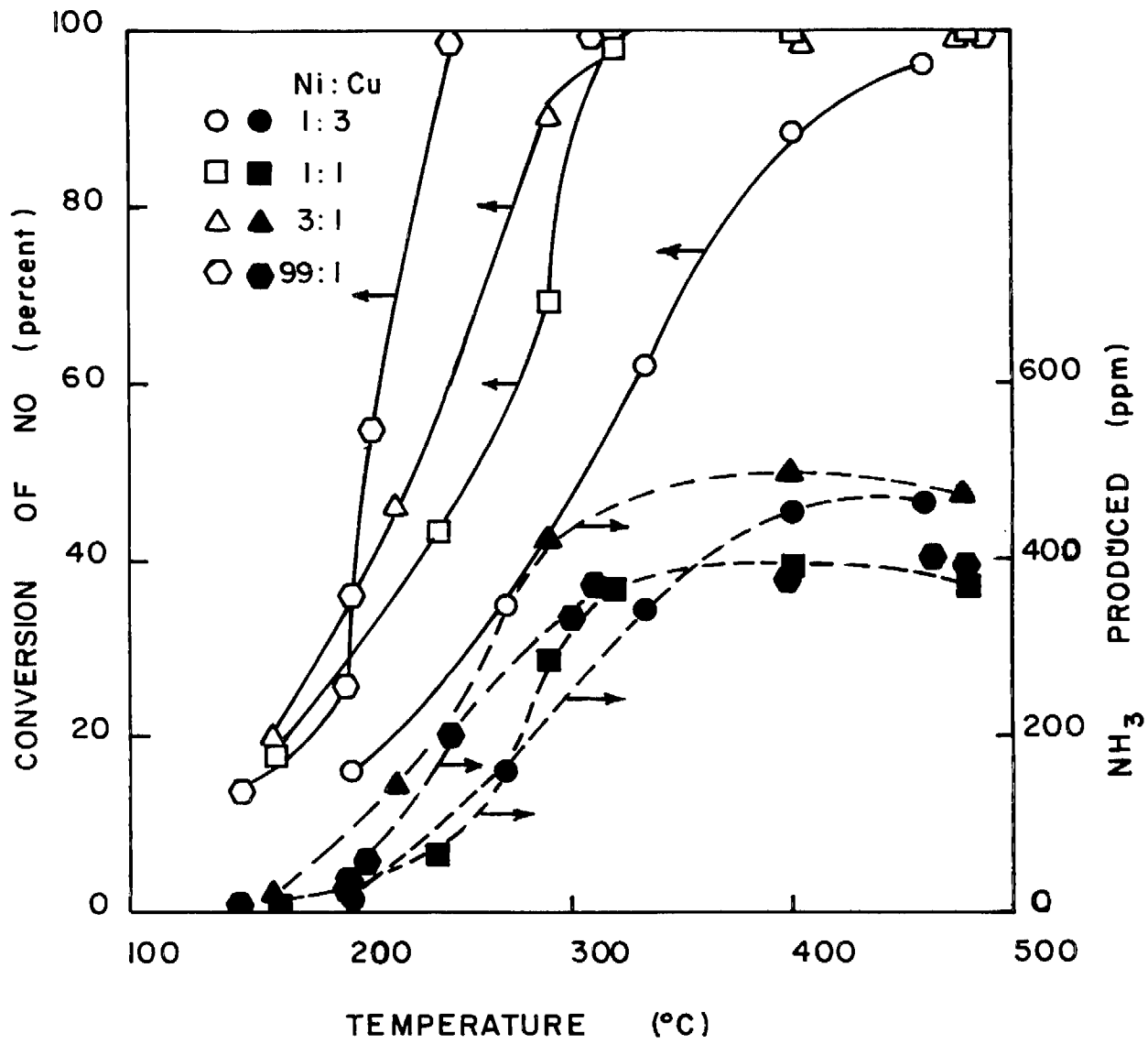


Figure 4-15 Reduction of NO with H₂ and Production of NH₃ on Impregnated Nickel-Copper Catalysts.

Ni/Cu catalyst prepared by impregnation techniques showed similar conversion levels at 310°C. It is interesting also to note that monel metal (nominally 2:1 Ni/Cu) showed 90% conversion at about 300°C. As mentioned earlier, monel appeared to sharply accelerate NH₃ decomposition above 440°C.

Catalyst 76, lanthanum rhodium oxide, was another catalyst that showed a sharp decrease in NH₃ with increasing temperature above the temperature at the maximum NH₃ level. For instance, at 275°C, 400 ppm NH₃ was produced. At 415°C, the NH₃ level dropped to only 127 ppm. Catalysts 77, 79, and 80 were made by successive dilution of catalyst 76 with Al₂O₃ (with subsequent regrinding in a mortar and reforming in the pellet press). Figure 4-16 summarizes the activity for NO reduction and NH₃ formation of this series.

Low temperature activity was relatively unaffected by the concentration of LaRhO₃. Above 300°C, conversion of NO decreased with increasing temperature for the 1% and 0.25% LaRhO₃ Catalysts. The decrease was more pronounced at the lower concentration.

Above 350°C, the lowest production of NH₃ was observed with the 15% LaRhO₃ catalyst. Although the double maximum in NH₃ output with the 5% catalyst was verified in replicate testing, no explanation for this observation is evident at this time. With the other catalysts the general observation was that NH₃ output peaked at approximately the temperature at which 100% conversion occurred.

Conversion of NO and production of NH₃ on the noble metals are shown in Figure 4-17. Platinum and palladium showed extremely high activity for NO conversion. However, both of these catalysts promoted nearly stoichiometric conversion of NO to NH₃ in the temperature range from 200°C to 500°C. Rhodium produced a stoichiometric amount of NH₃ at about 280°C with a sharp drop-off in production at higher temperatures. Although ruthenium was the least active of the noble metals tested, NH₃ production was very low over the entire temperature range. An important feature with ruthenium catalyst was the existence of the apparent double peak in NH₃ production at the 50% conversion level and at the

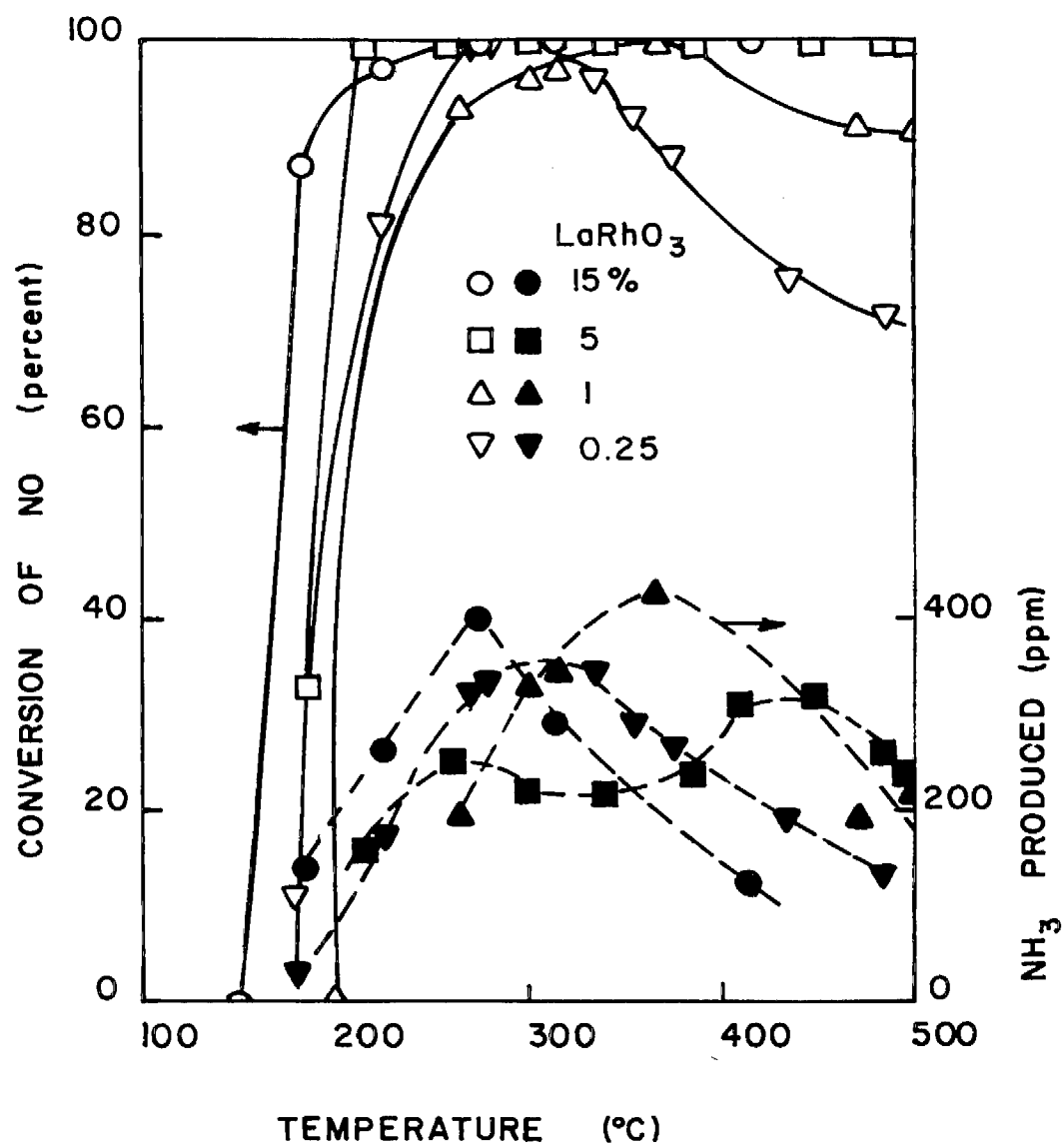


Figure 4-16 Reduction of NO with H₂ and Production of NH₃ on LaRhO₃ catalysts.

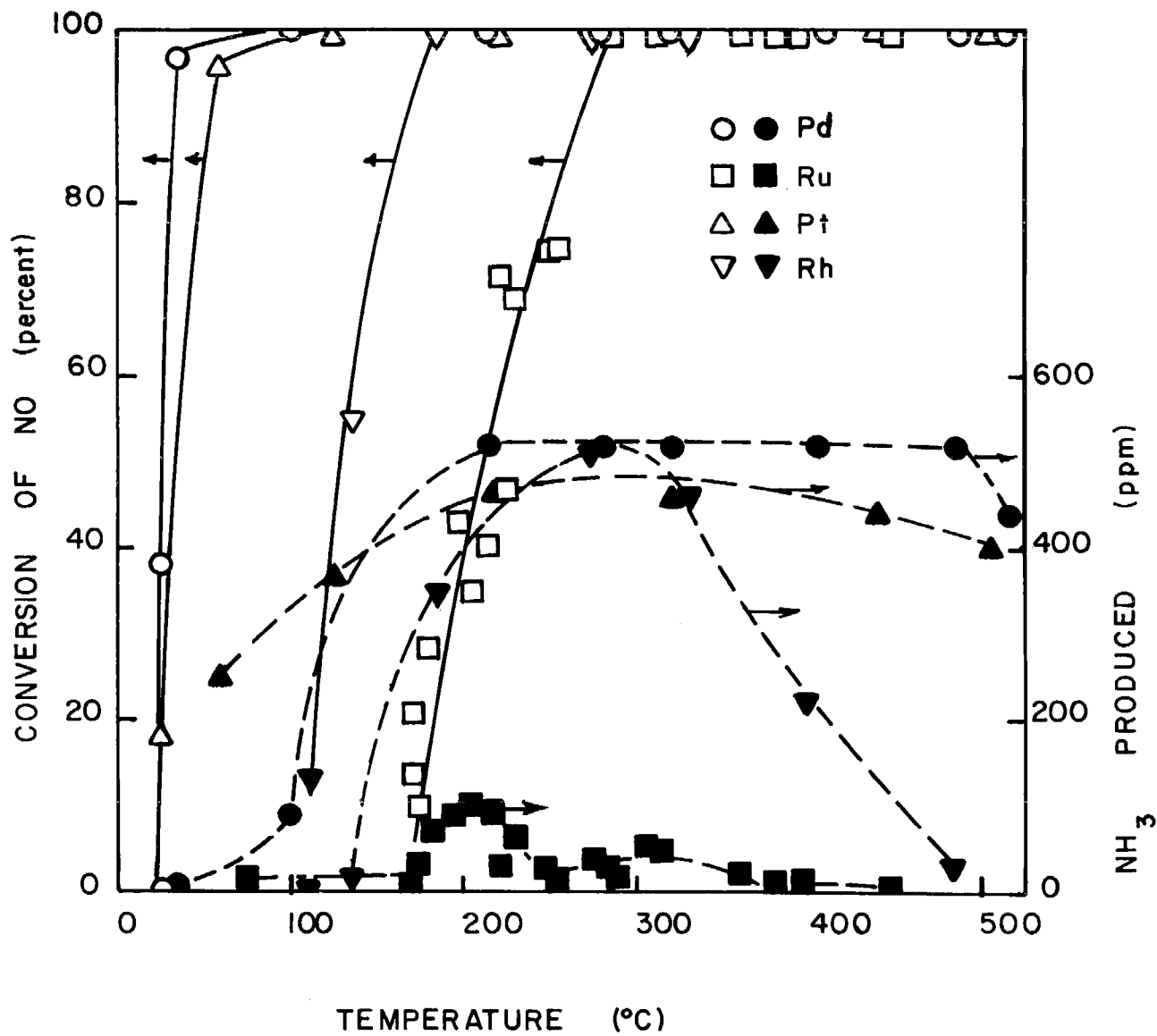


Figure 4-17 Reduction of NO with H₂ and Production of NH₃ on Noble Metal Catalysts.

100% conversion level.

Figure 4-18 shows data for NO conversion and ammonia production for catalysts 78, 82, and 90 - 5% strontium ruthenium oxide (SrRuO_3), 0.25% strontium ruthenium oxide and 15% strontium yttrium ruthenium oxide ($\text{SrY}_{0.5}\text{Ru}_{0.5}\text{O}_{2.75}$), respectively. Dilution of SrRuO_3 from 5% to 0.25% caused a considerable decrease in activity. Ammonia production with 5% catalyst was comparatively low. Addition of yttrium (replacing half of the ruthenium) lowered activity and decreased the maximum NH_3 production to less than 20 ppm.

As mentioned, a number of catalysts containing nickel were effective for promoting high conversion of NO with low yields of NH_3 . Figure 4-19 shows NO conversion and NH_3 production data for Catalyst 129, 15% NiO on Al_2O_3 . Few of the mixed oxide catalysts containing nickel had the high NO conversion activity exhibited by NiO; however, NH_3 production was relatively high with NiO compared to much lower yields for several of the mixed oxides (e. g., the pressed Ni-Cr spinel series). Although maximum NH_3 production with NiO was very high at 385°C , the NH_3 yield dropped to less than 40% of the maximum value at higher temperatures (485°C).

The two nickel metal catalysts 58U and 58 (the latter calcined at 1000°C) showed very similar activity and NH_3 production, as seen in Table 4-5. Maximum NH_3 production was observed at 400°C with both catalysts, which was very close to the point of maximum NH_3 production with the NiO catalysts, described above.

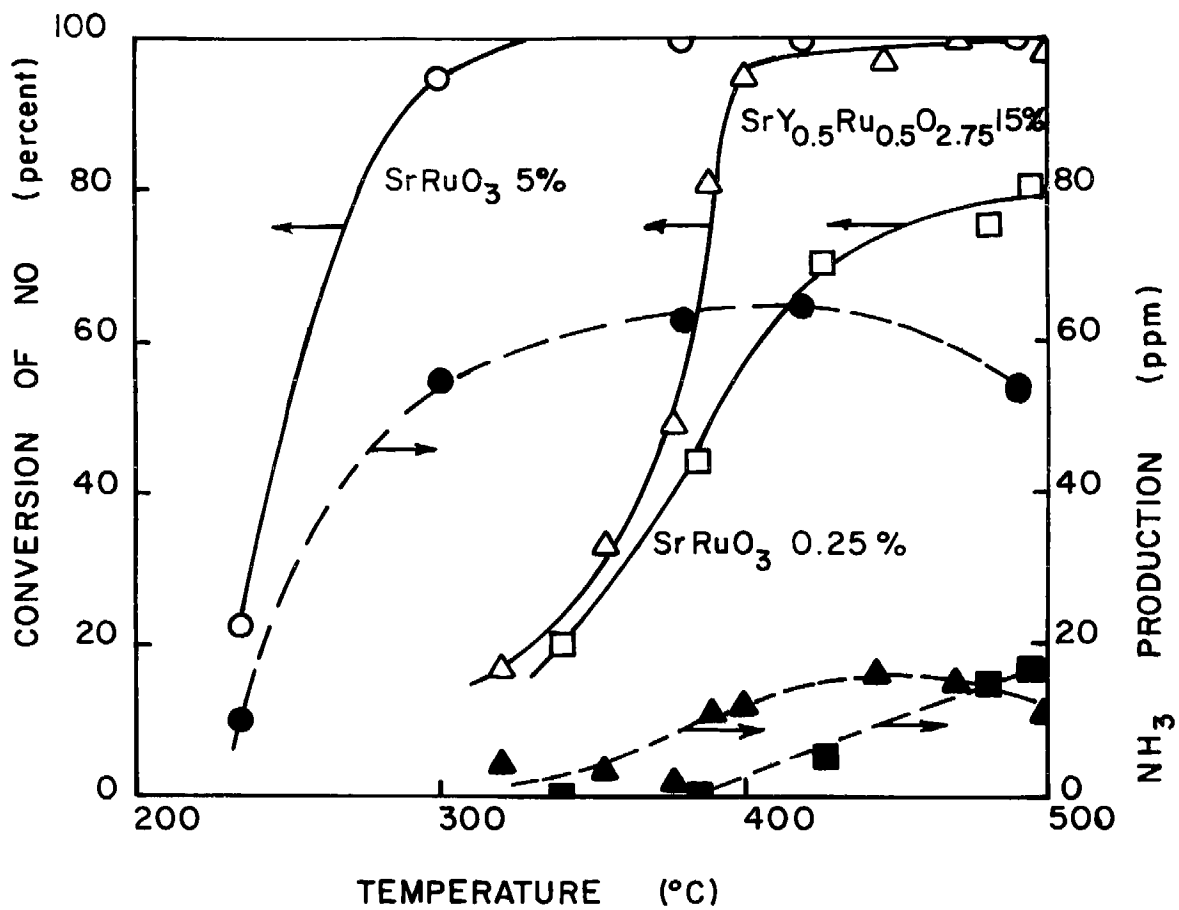


Figure 4-18 Reduction of NO with H₂ and Production of NH₃ on Ruthenium-Based Catalysts.

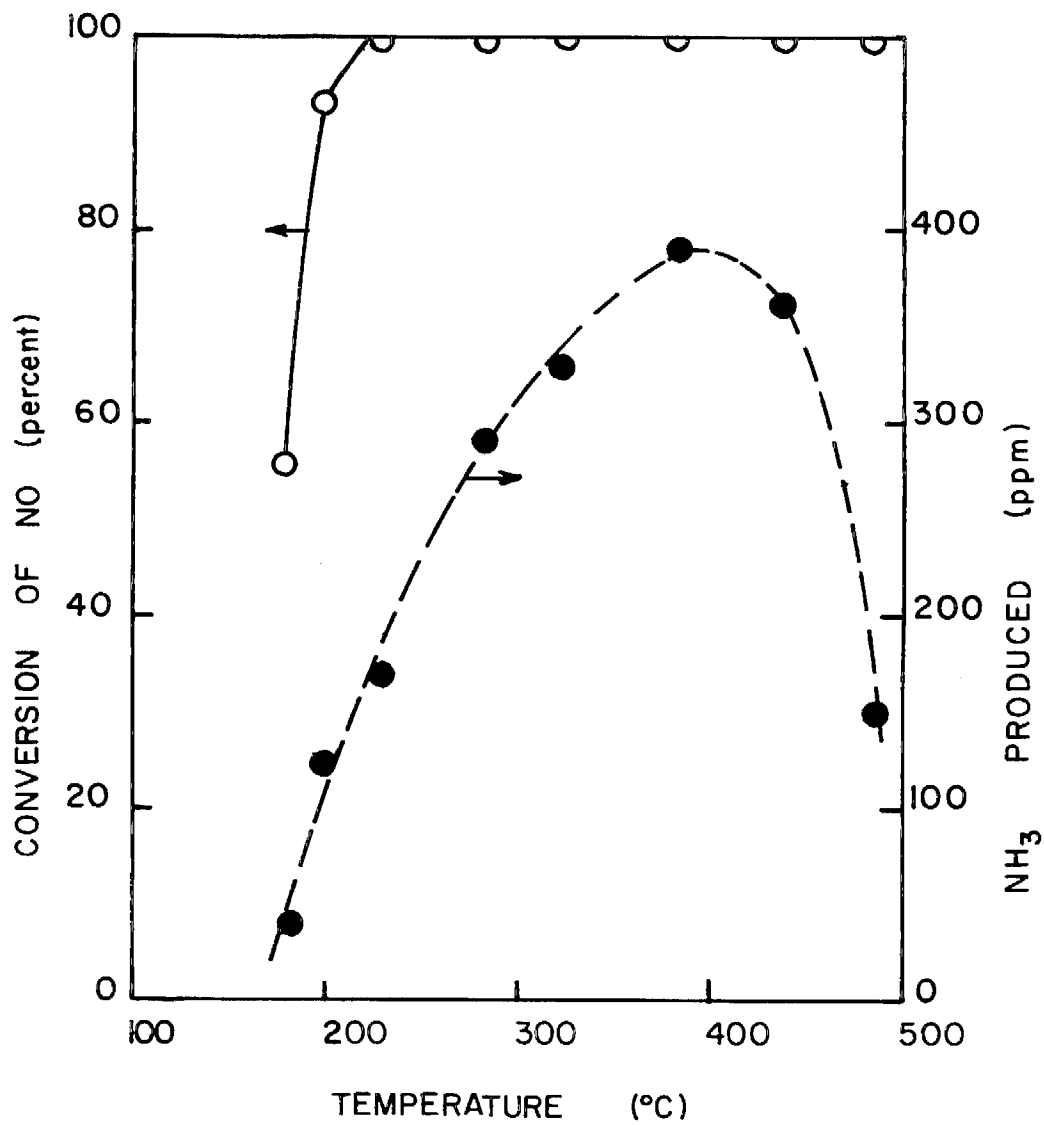


Figure 4-19 Reduction of NO with H₂ and Production of NH₃ on NiO Catalyst.

4.2 Automotive Exhaust Tests.

Based on the screening studies, several of the more promising catalysts were tested with actual auto exhaust. For NO reduction, catalysts were selected on the basis of reasonable activity for reduction with either CO or H₂, as well as demonstrated low production of ammonia with the latter reductant.

The exhaust tests were conducted in three phases which overlapped during the course of the project. Early in the project several existing catalysts were obtained and some other promising catalysts were prepared for test as either reductive or oxidative catalysts in the large cylindrical reactor. This approach proved to be uneconomical in view of the large quantities of materials required.

The small reactor was designed and constructed as a logical and economical extension of the screening studies; in many cases the same batch of catalysts used in the screening studies were employed.

A second large scale converter was designed and constructed for full two-stage capability.

Results of the automotive exhaust tests follow.

4.2.1 Auto Exhaust Tests with a Small Reactor.

Results of the screening studies and preliminary experience with the prototype converter generated an extensive list of catalysts that were of sufficient promise to merit further study with the small auto exhaust reactor. A few catalysts not studied in the screening tests were tested in the small reactor

The reactor was operated under either reducing or oxidizing conditions. The engine was operated under idle or low-load conditions without the manifold air pump in operation. Thus, the exhaust was fuel rich (See Table 3-3). In order to provide sufficient flow for the analyzers, the reactor was operated at slightly below atmospheric pressure by withdrawing the reactor exhaust through a pump. To provide an oxidizing atmosphere, air was admitted by opening a valve near the inlet to the reactor. To simulate high-load conditions in a reducing atmo-

sphere, NO was mixed with N₂ in a manifold and injected into the reactor feed. The NO levels shown in Table 3-3 are somewhat high for typical, fuel-rich operation; however, the level selected was felt to provide an adequate test for each catalyst.

Since either reducing or oxidizing conditions could be readily obtained most of the catalysts selected for study were tested in both modes.

In figures to follow data for the more pertinent catalysts will be shown, enabling comparison of activities for CO oxidation and NO reduction, as well as for production of NH₃. Table 4-8 lists these catalysts and shows the symbols used for presentation of data in the graphs. Tables 4-9a and 4-9b are tabulations of data for small-reactor tests with other catalysts (considered to be of somewhat less importance than those shown in the graphs).

Oxidation of CO. Figure 4-20 shows data for oxidation of CO. All of the more active catalysts contain noble metals. The activity of platinum and LaRhO₃ were very similar and were the most active catalysts tested.

As in the screening studies, it can be seen that addition of yttrium to SrRuO₃ caused a sharp decrease in activity. Both rare earth cobalt oxide (Fig. 4-20) and bastnasite nickel oxide (Table 4-9a) were not active. The former catalyst was particularly promising in the screening studies.

The curve representing conversion of CO with the empty reactor is shown at the right in Figure 4-20. It can be seen that conversion with catalysts of low activity became coincident with the empty-reactor data. The coincidence of conversion levels at high temperatures, along with the sharp vertical rise of the curve probably is an indication of the onset of thermal reaction.

It is evident that considerable further research is required to develop non-noble catalysts comparable to Pt and LaRhO₃.

Reduction of NO. Figures 4-21 and 4-22 show typical performance of the catalysts for NO reduction and ammonia production, respectively. The mixed oxides containing noble metals were quite active for NO reduction. The three catalysts, LaRhO₃, SrRuO₃ and SrY_{0.5}Ru_{0.5}O_{2.75}, as well as ruthenium, all had "light-off" temperatures for NO reduction at about 225°C, and the conversion increased sharply between 300 and 400°C.

Table 4-8. List of Catalysts Tested in Small Exhaust Reactor.

Catalyst Screening Number	Symbol	Catalyst	Description*
121	○	Platinum	
77	●	Lanthanum Rhodium Oxide	
120	◇	Ruthenium	
78	◆	Strontium Ruthenium Oxide	
90	◈	Strontium Yttrium Ruthenium Oxide	
87	□	Nickel Chromium Oxide Spinel	
	■	Stainless Steel	4.8 mm x 4.8 mm hollow, perforated semi-cylinders
129	△	Nickel Oxide	
52	▲	Monel	
54	▲	Copper Nickel Oxide	
24	▽	Rare Earth Cobalt Oxide	
	▼	Empty Reactor (cleaned)	

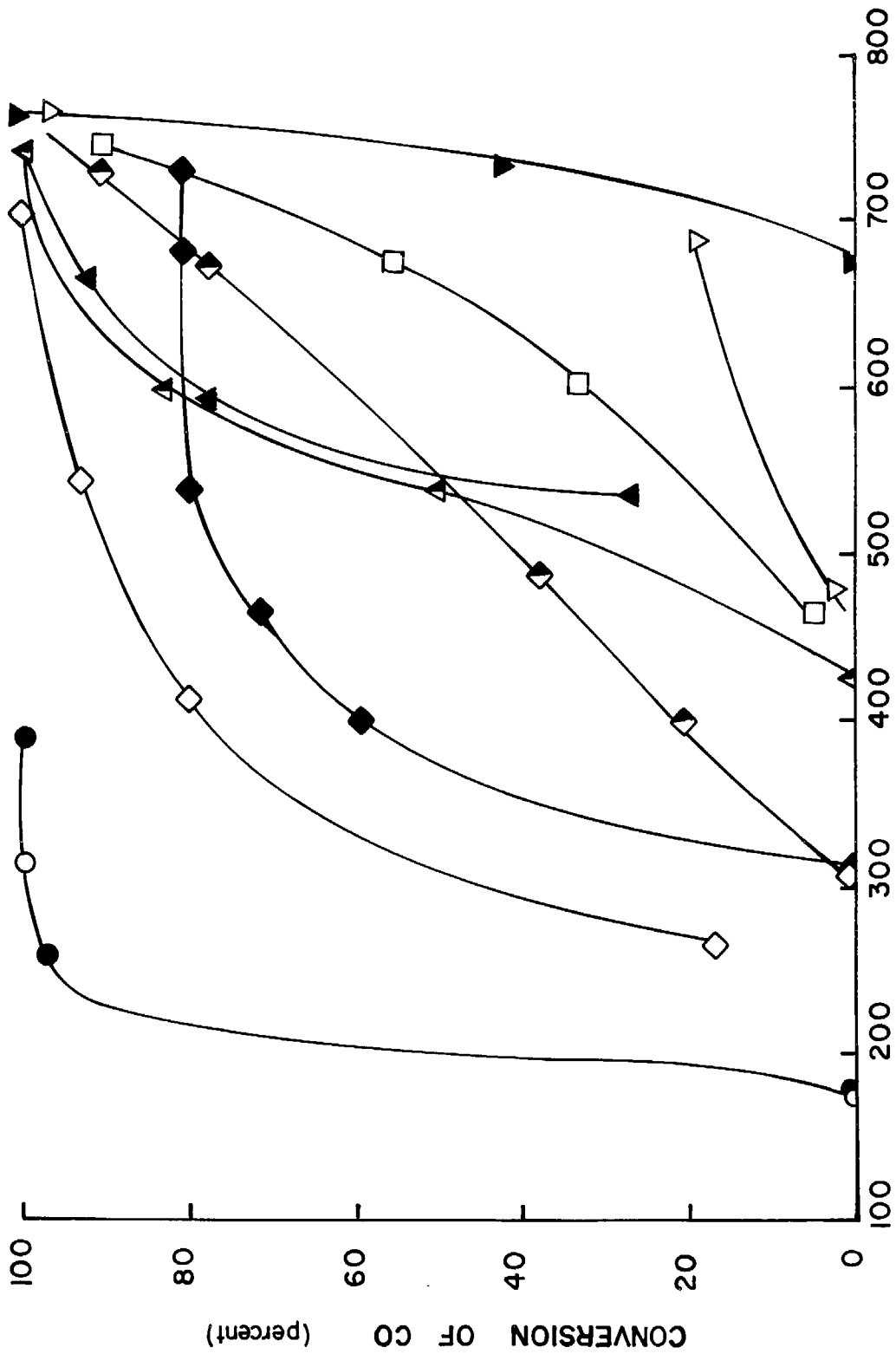
* Descriptions are given in Table 3-1 for those catalysts which were also screened in the laboratory tests.

Table 4-9a. Catalytic Oxidation of Auto Exhaust
in the Small Reactor.

<u>Catalyst</u>	<u>Temperature (°C)</u>	<u>Conv. of CO (%)</u>
Lanthanum Nickel Ruthenium Oxide	260	6
	445	22
	580	51
	645	61
	745	71
Bastnasite Nickel Oxide	450	0
	620	11
	700	12
	720	93

Table 4-9b. Catalytic Reduction of Auto Exhaust
in the Small Reactor.

<u>Catalyst</u>	<u>Temperature (°C)</u>	<u>Conv. of NO (%)</u>	<u>Conc. of NH₃ (ppm)</u>
R. E. Nickel Oxide	485	8	
	600	40	20
	650	48	35
	750	66	35
Lanthanum R. E. Nickel Oxide	585	12	30
	695	76	70
	800	90	100
Nickel Oxide (Reagent NiO)	515	10	0
	575	28	10
	620	39	100
	690	50	268
	760	58	149
Nickel Metal	460	0	--
	555	88	--
	570	100	--
Iron Oxide	500	49	330
	590	79	670
	690	90	780
	750	90	810
	785	90	830
Lanthanum Ruthenium Oxide	405	12	--
	465	60	--
	585	93	50
	655	94	100
	775	100	110
Bastnasite Nickel Oxide	435	0	0
	515	38	0
	645	62	85
	770	90	150



TEMPERATURE (°C)

Figure 4-20 Oxidation of CO in Auto Exhaust Using Small Reactor.
 (See Table 4-8 for List of Symbols)

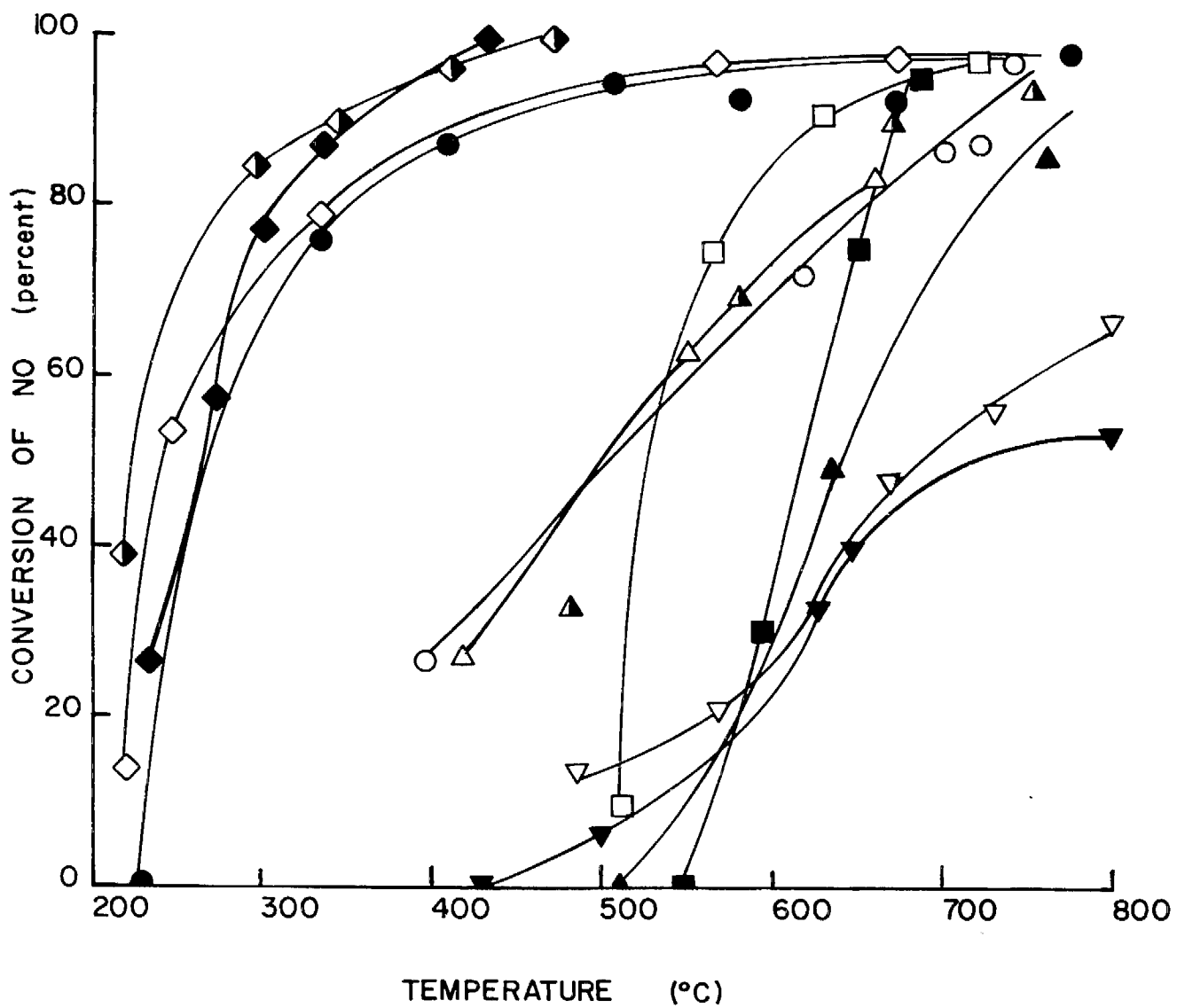


Figure 4-21 Reduction of NO in Auto Exhaust Using Small Reactor.
 (See Table 4-8 for List of Symbols)

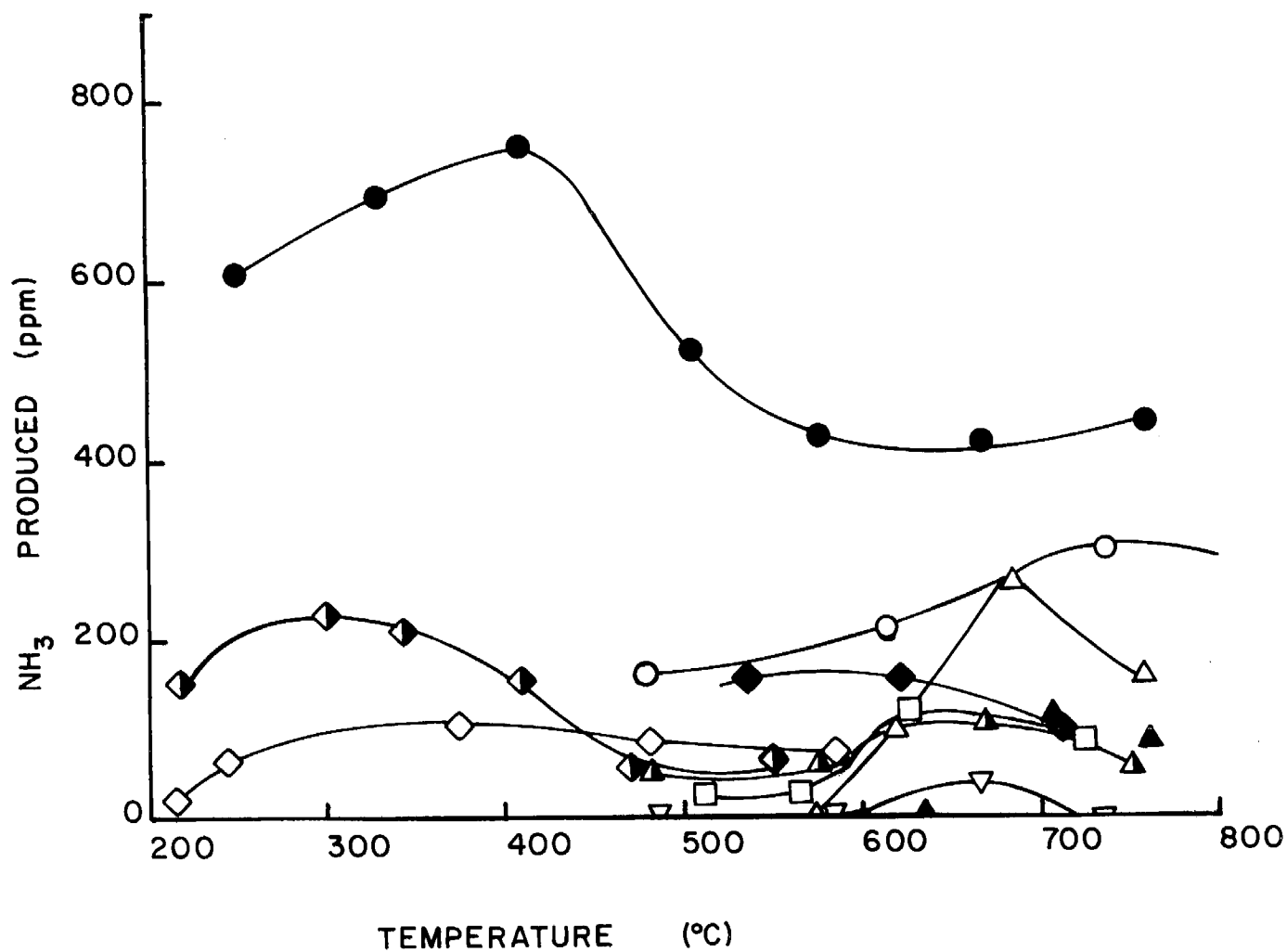


Figure 4-22 Production of NH_3 During Reduction of NO in Small Reactor.
 (See Table 4-8 for List of Symbols)

Platinum was in a catalyst group exhibiting only moderate activity. The earlier laboratory tests indicated that platinum was very active for the H_2 -NO reaction. The inhibiting effect of CO on the reduction of NO by H_2 (Shelef and Gandhi, 1972) on Pt may be responsible for this decrease in activity.

In the laboratory studies, 90% of the NO was reduced on $SrRuO_3$ at $287^\circ C$ and at $390^\circ C$ on $SrY_{0.5}Ru_{0.5}O_{2.75}$. In engine exhaust with both catalysts 90% reduction was attained at $400^\circ C$ suggesting that the addition of yttrium stabilized the catalyst toward inhibitive effects of exhaust constituents.

Of the catalysts initially tested in the laboratory and selected for study in the auto exhaust tests, only $LaRhO_3$ produced large amounts of NH_3 . Even platinum which promoted stoichiometric production of NH_3 up to $500^\circ C$ in the laboratory tests converted less than 20% of the inlet NO to NH_3 in the auto exhaust tests. The presence of CO has been shown to cause a decrease in NH_3 production on Pt catalyst (Shelef and Gandhi, 1972).

Figure 4-23 shows NO reduction in the empty reactor with the quartz-chip preheater and post-reaction sections in place (the reactor was sandblasted and the chips thoroughly cleaned in solvent before the tests). The observed activity of the empty reactor was not surprising in view of the high nickel and chromium content of the stainless steel reactor shell.

During the extended tests of $SrRuO_3$, one of the catalysts producing very low amounts of NH_3 , it was noticed that NH_3 production became abnormally high at high temperatures. The catalyst was removed and the empty reactor was tested. Ammonia production remained at the high levels, as shown in Figure 4-23 (curve for the empty, dirty reactor); in addition, the activity was substantially higher than that observed with the cleaned reactor. The higher activity originally was considered to be due to catalyst particles blown from the main reactor section and retained by the post-reactor, quartz-chip section. The high output of NH_3 was surprising since it occurred at reactor tem-

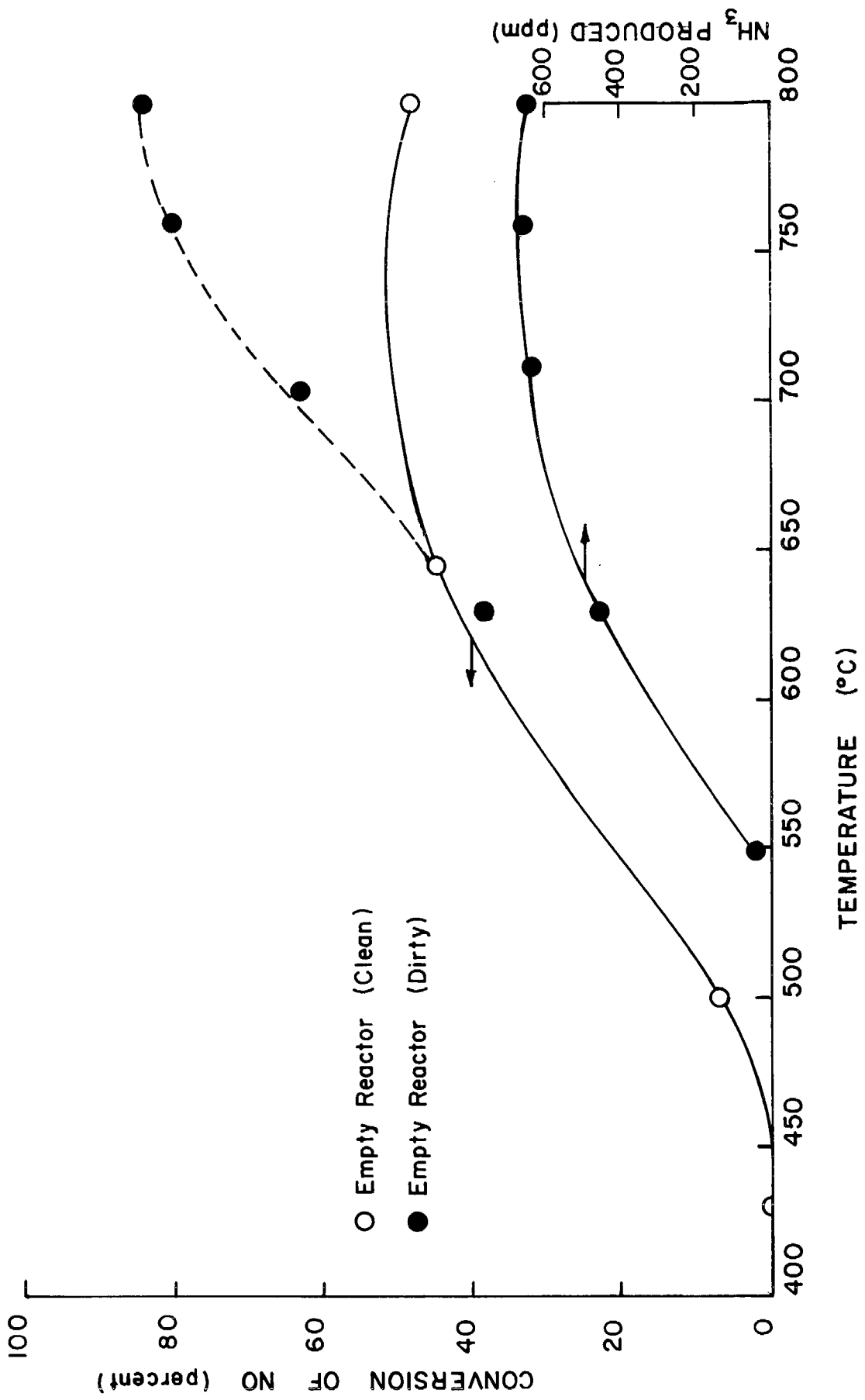


Figure 4-23. NO Reduction and NH₃ Production in Auto Exhaust Using Small Empty Reactor.

peratures favoring NH_3 decomposition. This phenomenon was not observed with catalysts previously tested. Temperatures shown on the abscissa of Figure 4-23 refer to the reaction zone; thus, it appears that the reduction of NO to NH_3 may have occurred in the post-reaction zone at somewhat lower temperatures which were less favorable for NH_3 decomposition. Since no catalyst showed such NH_3 levels during normal testing at these lower temperatures (except for LaRhO_3) the retained catalyst particles in the post-reaction zone may have had much lower selectivity for reduction of NO to N_2 than the pelletized catalysts. Another plausible explanation of the high NH_3 levels in the dirty, empty reactor is the presence of iron oxide formed on the stainless steel reactor surface. Since iron-containing catalysts were not particularly promising due to high NH_3 production in the screening studies, they were not originally included in the exhaust tests. It should be recalled that the catalysts tested were routinely cycled between reducing and oxidizing environments. During the oxidation periods, reactor surface oxidation occurred. In order to determine temperature levels for NH_3 formation on iron oxide, $\text{Fe}_2\text{O}_3\text{-Al}_2\text{O}_3$ catalyst was prepared and tested. Table 4-9b shows the activity and NH_3 production for this catalyst. It can be seen that very high NH_3 production occurred over the same temperature range that was observed with the empty, dirty reactor. If the iron oxide formed in the exhaust system is responsible for the high NH_3 levels, due consideration must be made for this problem in the design of two-stage, automotive converters.

The nickel oxide catalyst made by calcination of nickel carbonate was significantly more active than that made with reagent-grade NiO. No explanation for the difference in activity can be given at this time.

Several catalysts showed no significant improvement in activity over that of the empty reactor. These catalysts were reagent NiO, rare earth cobalt oxide and rare earth nickel oxide. The more active non-noble metal catalysts included nickel metal, iron oxide (which produced high levels of NH_3), nickel oxide, nickel chromium oxide spinel, and copper nickel oxide. Bastnasite nickel oxide was slightly more active than rare earth nickel oxide. Of the three metallic catalysts nickel metal appeared to be the most active.

An interesting feature of Figure 4-21 is that all the catalysts can be classified by activity into two general groups (with the possible exception of the moderately-active $\text{LaNi}_{0.5}\text{Ru}_{0.5}\text{O}_2$). All the members of the more active group contained ruthenium or rhodium. All of the base metal catalysts were in the group exhibiting lower activity. If cost is the primary criterion for selection of catalysts for full-scale converters, it is apparent that operation above 600°C is required. At these temperatures the base-metal catalysts produced the same, general levels of ammonia (Figure 4-22 and Table 4-9b). Consequently, final selection would be based primarily on durability and mechanical properties and in this regard, metallic catalysts appear to be particularly promising.

The very high activity of SrRuO_3 and its very low level of NH_3 production may outweigh the high cost of this material; additional study of SrRuO_3 under full-scale conditions is considered to be important.

One conclusion that can be made from both the laboratory and auto exhaust tests is that the very active catalysts (promote extensive reduction of NO at low temperatures) may lead to high NH_3 production unless (a) selectivity for NO reduction to N_2 rather than to NH_3 is exhibited or (b) the catalyst is extremely active for NH_3 decomposition as well as for NO reduction. The LaRhO_3 catalyst appears to exhibit neither quality while the ruthenium-containing catalysts promote either one or both mechanisms. Catalysts which only promote NO reduction at elevated temperatures may not produce large quantities of NH_3 because of the favorable thermodynamics for NH_3 decomposition.

4.2.2 Prototype Full-Scale Converter.

Initial tests began with the establishment of base-line conditions (uncontrolled emissions) over the complete range of speeds and load conditions. The test engine (1967 Ford six-cylinder, 170 CID) was equipped with a manifold air injection reactor system and an anti-backfire valve.

The engine was run with and without the air pump in operation to determine its efficiency for reducing hydrocarbons and carbon monoxide emissions.

The fact that the engine was equipped with the air pump was fortunate for two reasons. First, it was anticipated that the engine would have to be operated fuel-rich in later two-stage converter tests. The air pump could be used later as the secondary air injection source. Second, should first-stage temperatures be too low, the manifold reaction system could be used to elevate the exhaust temperature by reacting CO and hydrocarbons with air. In the latter case manifold air flow would be at a sufficiently low rate to minimize excess O₂. A series of test conditions over the entire operational range was selected to permit comparison of catalytic reactors and included a simulated idle, street driving, cruise and full throttle, maximum power modes. Table 4 10 gives typical emissions for these modes with and without the air pump.

Material balances on the carbon monoxide, carbon dioxide and oxygen constituents across the manifold reactor for the four modes show the following conditions:

(1) Air added as percent of primary exhaust flow:

Idle	65%
Street	52%
Cruise	36%
Power	2%

(2) Percent conversion of CO in manifold reactor assuming negligible hydrocarbon conversion:

Idle	59%
Street	26%
Cruise	0%
Power	12.5%

Dilution of the exhaust caused a decrease in concentration. For the cruise and power modes, the dilution effects based on NO concentration were in close accord with the amounts of added air given above.

In order to establish a reference to compare potential oxidation catalysts, initial tests were made with an Engelhard PTX converter. Figure 4-24 shows the PTX converter used and a typical monolith. Table 4-11 shows the test results with and without secondary air.

Table 4-10. Baseline Emission Levels for 170 CID,
Six-Cylinder Engine.

Emissions Without Pumped Manifold Air Added

	Speed (rpm)	Power (bhp)	NO (ppm)	CO (vol%)	CO ₂ (vol%)	O ₂ (vol%)	HC (ppm FIA)	HC (ppm NDIR)
Idle	615	0	330	3.75	9.8	0.2	880	330
Street	1508	20	530	3.75	8.2	0.2	700	280
Cruise	2614	36	3100	0.15	13.7	1.6	280	90
Power	3000	60	1300	3.45	10.9	0.2	380	135

Emissions with Pumped Manifold Air Added

Idle	579	0	100	1.35	8.2	8.6	300	130
Street	1484	20	290	2.08	7.0	7.8	250	115
Cruise	2615	36	2400	0.10	9.3	6.0	200	80
Power	3007	66	1280	2.62	9.8	0.5	100	50

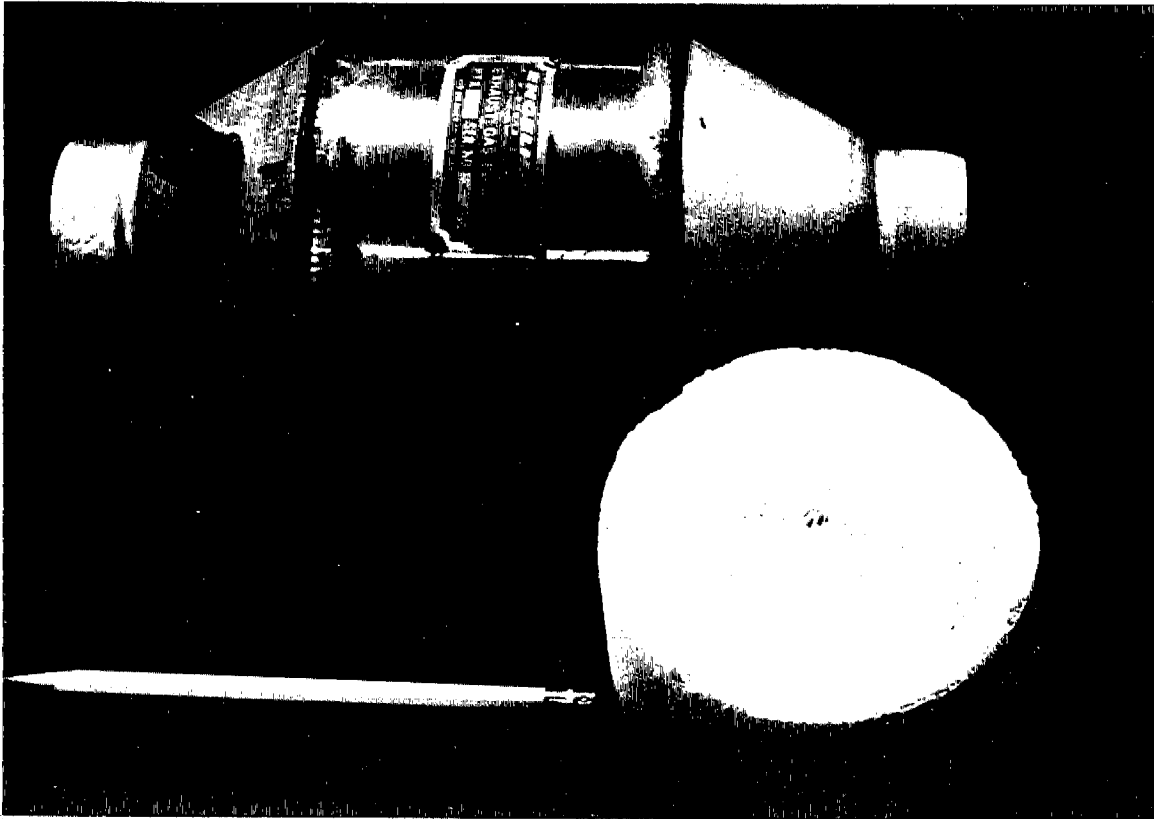


Figure 4-24. Engelhard PTX Converter and a Monolithic Structure as Typically Incorporated.

Table 4-11. Performance of Platinum Oxidation Converter
(Engelhard PTX Converter)

Emissions Without Secondary Air

	NO (ppm)	CO (vol%)	CO ₂ (vol%)	O ₂ (vol%)	HC (ppm FIA)	HC (ppm NDIR)
Idle In	295	3.50	10.6	0.0	1480	667
Out	260	3.50	10.1	0.0	1420	612
Street In	460	4.63	11.0	0.2	690	248
Out	460	4.75	11.8	0.0	650	248
Cruise In	3460	0.38	12.1	1.0	420	140
Out	3080	0.10	12.3	0.6	110	0.0

Emissions With Secondary Air

Idle In	50	1.77	9.2	8.6	200	65
Out	20	0.0	9.8	7.9	12	0
Street In	310	2.40	8.8	7.2	210	105
Out	275	0.15	11.6	5.4	50	32
Cruise In	2400	0.19	10.6	5.5	250	100
Out	220	0.0	11.2	5.4	31	20
Power In	1400	2.08	12.8	0.5	80	15
Out	650	1.61	12.8	0.0	27	10

In general, dilution effects were again significant. Since the air pump injection point was at the manifold, some oxidation occurred in the exhaust manifold and the line leading to the converter. The platinum reactor performs quite well over all modes except the full load, full-throttle mode (due to the low secondary air rate at full throttle). In all modes, some conversion of NO occurred, which was most evident at full power, possibly due to the combination of a high CO level, low O₂ level and high temperature. In the power mode, the exhaust line to the converter as well as the converter itself were observed to glow bright red. Upon quick engine shut-down from a high load condition the converter attained an even more incandescent glow, due to sudden release of unburned hydrocarbons and, possibly, raw gasoline. Several intense backfires occurred at the converter.

Disassembly of the exhaust system showed that there was significant damage to the entrance section of the monolith in the PTX converter. Figure 4-25 shows the incipient melting or burn-out of the monolith. Consultation with representatives of American Lava Co. revealed that such damage was common with monoliths made with spiral-wound ceramic-impregnated, corrugated paper (the paper is calcined from the finished assembly leaving the hard, solid ceramic). They indicated that later production methods involving straight-layered corrugated paper were significantly more stable (such an assembly is considerably more expensive since the cylindrical monoliths must be cored from large blocks while the spiral-wound versions are simply wrapped in successive layers until the desired diameter is reached).

Full-scale converters tested in the cylindrical, prototype reactor were:

- A. Rare earth cobalt oxide 9%, two 1-lb monoliths in series.
- B. Rare earth cobalt oxide 16%, five 1-lb monoliths in series.
- C. Rare earth nickel oxide 15%, four 1-lb monoliths in series.
- D. Girdler G-22 barium-promoted copper chromite, unsupported pellets, 4.5 lb.
- E. Girdler G-43, 3% Ni-0.1% Pt, on Al₂O₃ pellets, 7 lb.
- F. Rare earth cobalt oxide, 15% on Al₂O₃ pellets, calcined at 500°C, 6.7 lb.

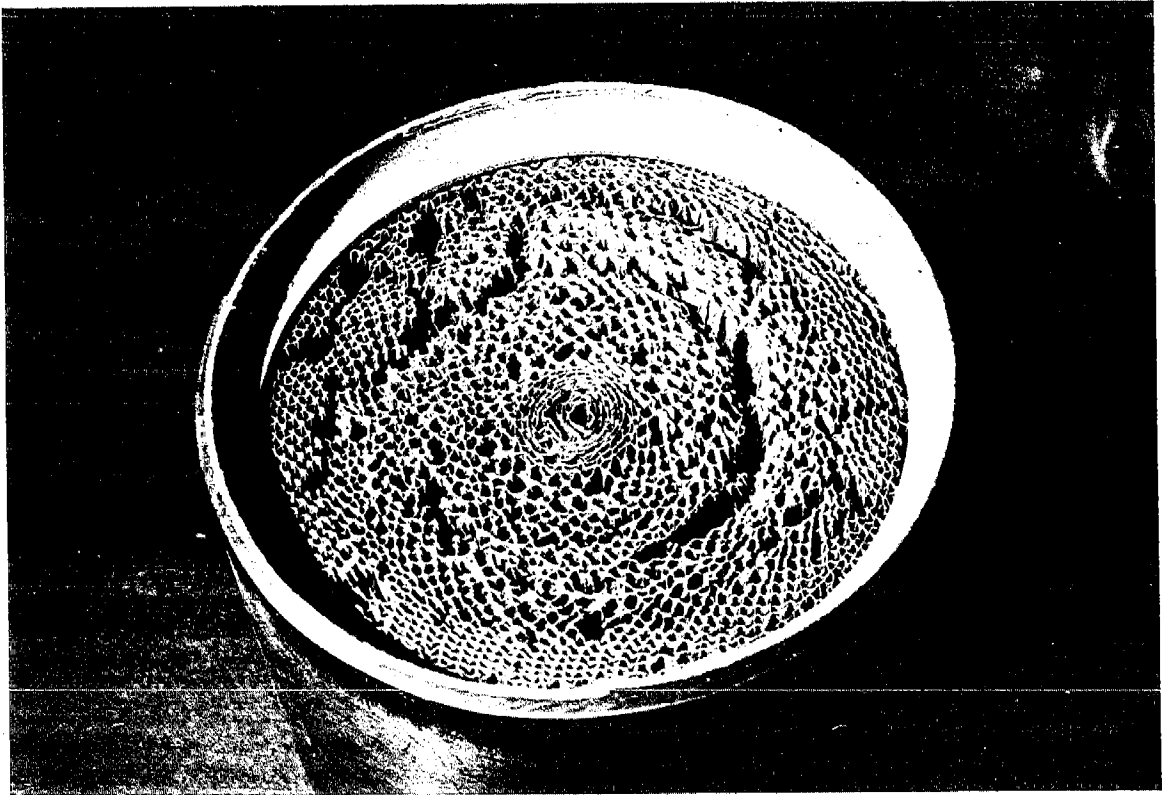


Figure 4-25. Incipient Burnout of PTX After Less than 10 Hours Operation.

The catalysts prepared in the laboratory were all made by impregnation methods.

Converters A, B, and C were selected on the basis of promising laboratory results. Initial tests were performed on converters A, B, and D with the converters placed in a normal muffler position (about 5 feet from the manifold). Practically no activity was observed for converters A and B for either hydrocarbon and CO oxidation or NO reduction. In the power mode, NO reduction capability should have been evident due to low O₂ levels. Converter D, copper chromite, showed about 30% conversion of CO in the street driving mode compared with typical conversions of 94% under similar conditions with the PTX converter. Copper chromite tests for NO_x removal in the power mode were not made due to excessive back pressure built up across the pelletized catalyst.

The very low conversions with the monolithic catalyst were somewhat surprising; laboratory tests for air oxidation of CO with a small rare-earth cobalt oxide monolith showed a temperature for complete conversion of CO only 135°C above that of platinum pellets.

It is evident that hydrocarbons, water or CO₂ inhibit the oxidation of CO on the rare earth cobalt oxide catalyst. Inhibitive effects due to water on cobalt catalysts are well known; however, it was not known that mixed cobalt oxides were water-poisoned.

A brief series of laboratory experiments was conducted to investigate inhibitive effects. The monolith, Catalyst 38 (essentially a small version of Converter B) was re-installed in a screening reactor and water vapor was included with the 2000 ppm CO in air. The gas stream was saturated with water vapor by bubbling it through water at 26°C and 58°C in two separate series of tests. In a third series of tests, 850 ppm propylene was added to the dry reactant stream. Table 4-12 shows the results of these tests.

At low temperatures, both water and propylene inhibited the oxidation of CO. In the latter case, inhibition may be due to water formed by oxidation of propylene. Oxygen was in considerable excess so that its concentration was essentially maintained constant.

Table 4-12. Inhibition Effects on CO Oxidation over Rare Earth
Cobalt Oxide on Cordierite Monolith Carrier

Reactant and Inhibitant/Temp (°C)	Conversion (Percent)			
	100	200	300	400
CO (2000 ppm) + Air	0	90	97	100
CO (2000 ppm) + H ₂ O (3%) + Air	0	6	88	96
CO (2000 ppm) + H ₂ O (15%) + Air	0	6	85	95
CO (2000 ppm) + C ₃ H ₆ (850 ppm) + Air	0	35	92	97

In a typical run, conversion of CO in the presence of 850 ppm C_3H_6 was 77% at 230°C. When the propylene was turned off conversion immediately rose to 92%, exactly the value determined for that temperature with a propylene-free reactant mixture.

It was felt that operation of the rare earth cobalt oxide monolith at elevated temperatures may not be sensitive to inhibitive effects in view of similar conversion levels at 400°C for the cases with and without H_2O and/or C_3H_6 (Table 4-12). The small monolith was then placed in the steel reactor to be described more fully in a later section and evaluated with auto exhaust.

Table 4-13 shows typical performance of the small rare earth cobalt oxide monolith. Onset of significant oxidation of CO and hydrocarbons appeared to occur at about 650°C with an O_2 concentration of about 2.5%. It was shown earlier (Figure 4-20) that this temperature is very close to the thermal reaction "light-off" temperature for CO oxidation. Nevertheless, at the time it was felt that a re-evaluation of the full-scale rare-earth cobalt oxide monolith (B) was warranted. This catalyst and the remainder of those described earlier were tested in the next series of tests.

Converters E and F were tested at the standard muffler position while Converters B and C were evaluated at both the muffler position and a position close to the manifold (i. e., about 6 inches from the manifold). Table 4-14 shows typical data for the pelletized nickel-platinum and rare earth cobalt oxide converters (E and F).

It was determined earlier that the belt-driven pump used to provide the secondary air did not deliver sufficient air at high engine speeds. This air deficiency is reflected in low O_2 concentrations and, consequently, low CO conversion in the power mode with the G-43 and rare earth oxide-alumina converters. Interestingly, because of the low O_2 level, NO conversion was substantial in the power mode with both converters. In the other modes, in which O_2 supply was adequate, CO and HC conversion was high with the G-43 converter.

Activity of the mixed oxide converter was not as high as the nickel-platinum converter. The inlet temperature of each converter in the

Table 4-13. Performance of Rare Earth-Cobalt Oxide Monolithic Converter (small scale).

Average Temp. (°C)	O ₂ Conc. (%)	Percent Removal		
		CO	NO	HC
304	0	0	0	20
440	0	0	0	0
538	0	9	12	0
649	0	5	35	13
388	2.5	2	0	10
571	2.3	13	5	30
627	2.8	17	15	41
704	2.3	88	26	85

Flow Rate: 8 SCFH (8000 hr⁻¹ vol. space velocity).

CO inlet composition: 2.2-3.0 vol. %

NO inlet composition: 170-350 ppm

HC inlet composition: 275-720 ppm

Table 4-14. Performance of Pelletized Ni-Pt-Al₂O₃ and Pelletized Rare Earth Cobalt Oxide-Al₂O₃ Converters.

Catalyst	Driving Mode	NO (ppm)	CO (vol%)	O ₂ (vol%)	HC (ppm FIA)	HC (ppm NDIR)	Mid-Bed Temp. (°C)
E	Street IN	156	2.24	5.6	200	90	710
	OUT	187	0.0	4.0	35	40	
E	Cruise IN	2358	0.25	2.4	220	85	650
	OUT	2163	0.0	2.2	20	40	
E	Power IN	918	3.87	1.1	250	65	760
	OUT	451	3.74	0.0	250	65	
F	Street IN	130	2.23	5.8	212	92	470
	OUT	170	2.03	5.6	160	79	
F	Cruise IN	2280	0.14	1.8	195	70	620
	OUT	2040	0.14	1.7	110	50	
F	Power IN	760	3.28	0.1	240	70	790
	OUT	178	2.82	0.0	212	65	

street mode was about 427°C. It can be seen that about a 280°C increase in temperature occurred with the G-43 converter due to the "bootstrapping" effect caused by the heat of reaction. However, since some conversion did occur with the mixed oxide converter at 427°C, it was expected that the "light-off" temperature could be attained by placing the converters closer to the exhaust manifold.

The G-43 catalyst was approximately as active as the Engelhard PTX platinum converter. Both converters contained approximately the same quantity of platinum.

A major drawback in the use of the pelletized system, as compared with the monolithic system, is the higher pressure drop across the converter (in axial flow). For example, in the power mode, the pressure at the bed entrance was 15.8 in. HG. gauge for the G-43 converter, but only 1.8 in. Hg gauge for the PTX converter.

To provide more flexibility in the air injection system, the belt-driven pump was removed and a manually-operated flow system using laboratory air was installed. Measurement of the effect of oxygen concentration at any driving condition was then possible. Previously with the pump, the air flow was governed by the engine speed and the exhaust back-pressure acting on a relief valve. In Table 4-14, for example, O₂ concentrations in the cruise mode were 2.4% and 1.8%, for the pelletized G-43 and pelletized rare earth cobalt oxide catalysts, respectively. Table 4-15 shows performance data for the G-43 converter using the variable secondary air system. Air was injected directly into the converter entrance in these tests rather than into the manifold. The street mode was used in most of these runs to provide relatively high CO levels and to emphasize the oxidation performance of the converters.

With the G-43 converter it can be seen that CO removal increased with added air flow, and was essentially complete when stoichiometric O₂ levels (for CO and H₂ oxidation) were exceeded. It should be also noted that air addition above 5.6 SCFM caused cooling of the converter.

In an effort to improve the performance of the B and C catalysts for NO reduction, the converter was relocated from an initial position which was approximately five feet from the exhaust manifold exit to a position approximately six inches from the manifold exit. It was anticipated that closer proximity to the engine would increase the catalyst bed temperature and improve the performance of the catalyst.

Table 4-15. Performance of Pelletized Ni-Pt-At₂O₃ (G-43) Converter.
Emissions with Variable Secondary Air Flow.

Catalyst (mode)	Air Flow (SCFM)		NO (ppm)	CO (vol%)	O ₂ (vol%)	HC (ppm FIA)	Hc (ppm NDIR)	Mid-Bed Temp (°C)
E(G-43) (Street)	0	IN	170	5.80	0.2	250	211	400
		OUT	120	5.15	0.2	250	198	
"	1.5	IN	60	6.55	2.0	250	172	690
		OUT	50	4.32	0.3	--	135	
"	3.8	IN	80	5.28	3.1	232	130	850
		OUT	0	1.66	0.1	90	90	
"	5.6	IN	80	4.91	4.2	210	120	930
		OUT	0	0.10	0.6	20	20	
"	7.5	IN	25	4.60	5.2	175	100	870
		OUT	0	0.00	2.4	15	10	

Table 4-16 shows typical data with the B and C converters at the different locations. Monolithic catalyst C was tested at the muffler location using secondary air injected either into the manifold by the air pump or into the reactor from the laboratory compressed air line. The rare earth cobalt oxide monolith (B) reactor was tested at the muffler position using manifold-injected, pumped air only. For both catalysts at the manifold position, compressed air was injected into the manifold.

The street driving mode without secondary air provided typical CO concentrations of about 5% and entrance temperatures of about 370°C and 540°C at the muffler and manifold position, respectively (Tests 3 and 15). With pumped secondary air added at the manifold, the O₂ concentration was about 7% and CO concentration decreased to about 2% (Tests 1 and 13). The decrease in CO concentration was due principally to dilution; however, the entrance temperature (about 410°C) indicates that some oxidation of CO occurred in the manifold as well.

At the manifold position, entrance temperatures increased sharply with addition of air. For example, with Converter C, entrance temperature increased from 470°C to 820°C as air injection was greater than the stoichiometric amount for CO oxidation (Tests 8, 9, 10). "Light off" temperature for Converter C appears to be relatively low for CO oxidation in excess air; however, complete oxidation was not attained even at 820°C.

In the cruise mode, relatively little temperature variation with air addition was observed at the muffler location due to the inherently low CO concentration. Temperatures at the muffler-position were typically about 590°C. In the cruise mode entrance temperatures at the manifold location were about 700°C with O₂ levels up to 2.7%.

Table 4-16. Performance of Large-Scale Catalytic Converters.

Converter	Test	Driving Mode	NO (ppm)	CO (vol%)	O ₂ (vol%)	HC (ppm FIA)	HC (ppm NDIR)	Entrance Temp. (°C)
C (Muffler position- Air pumped into mani- fold)	1	Street in	153	2.13	6.5	265	120	420
		out	235	2.02	6.5	250	115	
	2	Cruise in	2310	0.14	4.5	280	118	570
		out	2310	0.07	4.5	265	113	
C (Muffler position- Air added through regulator into reactor)	3	Street in	160	4.80	0.0	680	290	370
		out	150	4.60	0.0	690	300	
	4	Street in	100	4.04	1.6	655	289	350
		out	90	3.76	1.6	650	289	
	5	Street in	100	1.98	4.4	565	258	310
		out	100	1.78	4.5	325	250	
	6	Cruise in	3100	0.61	0.6	450	176	540
		out	3100	0.57	0.5	430	169	
	7	Cruise in	570	0.63	2.1	390	162	550
		out	570	0.50	2.0	390	162	
C (Manifold position- Air pumped into mani- fold)	8	Street in	256	4.70	0.2	750	320	470
		out	252	4.90	0.2	720	300	
	9	Street in	49	4.50	1.5	600	210	480
		out	0	4.20	0.0	500	210	
	10	Street in	102	0.45	2.5	0	0	820
		out	75	0.15	1.7	0	0	
	11	Cruise in	828	0.10	2.5	0	0	790
		out	882	0.05	2.0	0	0	
	12	Cruise in	2496	0.77	1.0	440	160	715
		out	1420	0.62	0.2	330	150	
B (Muffler position Air pumped into mani- fold)	13	Street in	240	1.85	7.0	230	100	405
		out	255	2.00	6.9	227	100	
	14	Cruise in	650	0.11	4.8	257	--	570
		out	690	0.11	4.8	256	--	

Table 4-16. (cont.)

Converter	Test	Driving Mode	NO (ppm)	CO (vol%)	O ₂ (vol%)	HC (ppm FIA)	HC (ppm NDIR)	Entrance Temp. (°C)
B (Manifold position-Air added through regulator into manifold)	15	Street in	186	5.3	0.0	700	190	<540
		out	166	5.3	0.0	670	180	
	16	Street in	42	1.7	4.0	100	40	732
		out	88	1.9	4.0	100	40	
	17	Cruise in	1758	1.47	0.5	390	150	671
		out	1678	1.50	0.5	400	170	
	18	Cruise in	1772	1.08	2.7	380	130	671
		out	1757	1.17	2.7	380	130	

Based on the final O₂ concentration as an indication of a reducing or oxidizing atmosphere, it can be seen that NO reduction with Converter C was significant only in reducing atmospheres. Similarly, with the B converter, NO reduction occurred only under reducing conditions (Test 17). "Light off" temperatures for NO reduction with both catalysts appears to be about 650°C.

As seen in Table 4-15, some improvement in performance with converters B and C was observed over earlier tests; however, the close proximity of the converter to the engine resulted in dangerously high temperatures in the converter, especially during high power runs. In fact, the tests were suspended at one point due to the failure of an overheated thermowell joint on the catalyst housing. After repairing the well, additional tests were conducted in which the converter was covered with a two inch high-temperature ceramic blanket insulator. In this case, with the monolithic converter, it was observed that the addition of insulating material on the outside of the catalyst made no observable difference on the mid-bed temperature. This observation is in accord with theoretical studies performed earlier which showed that for all practical purposes uninsulated automotive exhaust converters operate essentially adiabatically over normal driving modes (Bauerle and Nobe, 1973).

Further tests with the axial-flow converter were not conducted for two reasons. First, several of the promising catalysts developed in the laboratory could only be made in pelletized form with the equipment available; the axial flow converter using pelletized catalysts presented excessive back pressure in the exhaust manifold. Second, it was desirable to develop a more rapid and economical screening method using auto exhaust. Thus, advanced design two-stage converter and small-scale exhaust converters were constructed. Before progressing to the sections presenting the results of these converters, the results of actual automotive tests of the PTX converters will be described.

4.2.3 Automotive Tests of a Two-Stage Platinum Converter.

Instantaneous emission levels during actual driving of an automobile equipped with PTX Engelhard converters were determined. Engelhard Industries donated to UCLA several of the platinum converters for these tests.

Vehicle and Modification* Emission tests were performed on a Chevrolet Chevelle with a 350 cubic inch displacement V-8 engine. The vehicle was modified with bolt-on equipment to improve performance. No internal modifications were made to the engine. Stock vehicle emissions under CVS testing were HC 1.1 gm/mi, CO 8.65 gm/mi and NO_x 2.1 gm/mi. The engine was dyno-tuned by a speed shop. The carburetor was adjusted based on final A/F ratio, rather than manifold levels resulting in somewhat richer operation than required for NO conversion. Under such adjustment, CVS emissions were: HC 2.24 gm/mi, CO 59.6 gm/mi, and NO_x 1.02 gm/mi. Readjustment of the carburetor to a more desirable A/F ratio gave: HC 1.01 gm/mi, CO 19.6 gm/mi and NO_x 0.43 gm/mi. It is of interest to note that the leaner setting resulted in lower NO_x emissions.

To improve the vehicle's acceleration, the original factory carburetor, inlet manifold, and distributor were replaced with high performance equipment which consisted on an Offenhauser dual port high-rise inlet manifold, a 700 cfm Holly carburetor with a vacuum-operated secondary throttle, and an ACCel dual point, centrifugal-advance distributor.

Exhaust System Modifications. Four Engelhard PTX platinum exhaust gas purifiers were installed on the exhaust system and arranged to provide a two-stage catalytic converter. The engine was set to run fuel rich. Air from the engine-driven air pump was injected between the exhaust reactors.

* The vehicle was entered by two UCLA students in a University of California (Davis) Reduced Emissions Rally (From the Davis campus to UCLA).

Test Procedure. The vehicle was mounted on the UCLA chassis dynamometer. Only the FTS 7-mode driving cycle was capable of being simulated at this facility. The exhaust was analyzed for its carbon dioxide, carbon monoxide, hydrocarbon, nitric oxide, and oxygen content. Unleaded fuel was used in all tests. The leaner carburetor settings were used in the tests.

Results

a) Modified carburetion and two-stage PTX reactors. The CO, NO, and HC exhaust concentrations for the first configuration using the high performance equipment and the two-stage converters are shown in Figure 4-26. Measurements were made at the engine exhaust manifold and at the car exhaust. Typical emissions during late (hot) cycles are shown. The emissions curves were traced from actual recorder charts (discounting noise). Concentration scales were added to the ordinates; in some cases nonlinearity of the analyzer curves is apparent.

The sample taken at the engine exhaust manifold showed that the carbon monoxide concentration varied from around 6% at idle and cruise modes to about 1% near the end of the acceleration modes. The hydrocarbon concentration was 200 ppm during the acceleration mode and greater than 1000 ppm during most other modes.

The concentrations measured at the vehicle exhaust showed that the HC concentration decreased by at least 85% in all modes. Typical concentrations varied from 15 to 130 ppm, when measured during a hot cycle after the engine had warmed up. The CO concentration decreased about 70% and the nitric oxide showed a decrease of 50 to 100%.

The overall air/fuel ratio at the vehicle exhaust, as determined from the vehicle exhaust gas analysis, was about 14:1 while the engine air/fuel ratio was about 12:1. Insufficient air was injected into the second reactor since the overall air/fuel ratio should have been greater than stoichiometric or about 16:1 to carry out the CO and HC oxidation to completion. Thus, the second reactor operated in a net reducing atmosphere, and some nitric oxide reduction occurred in the second reactor. Since

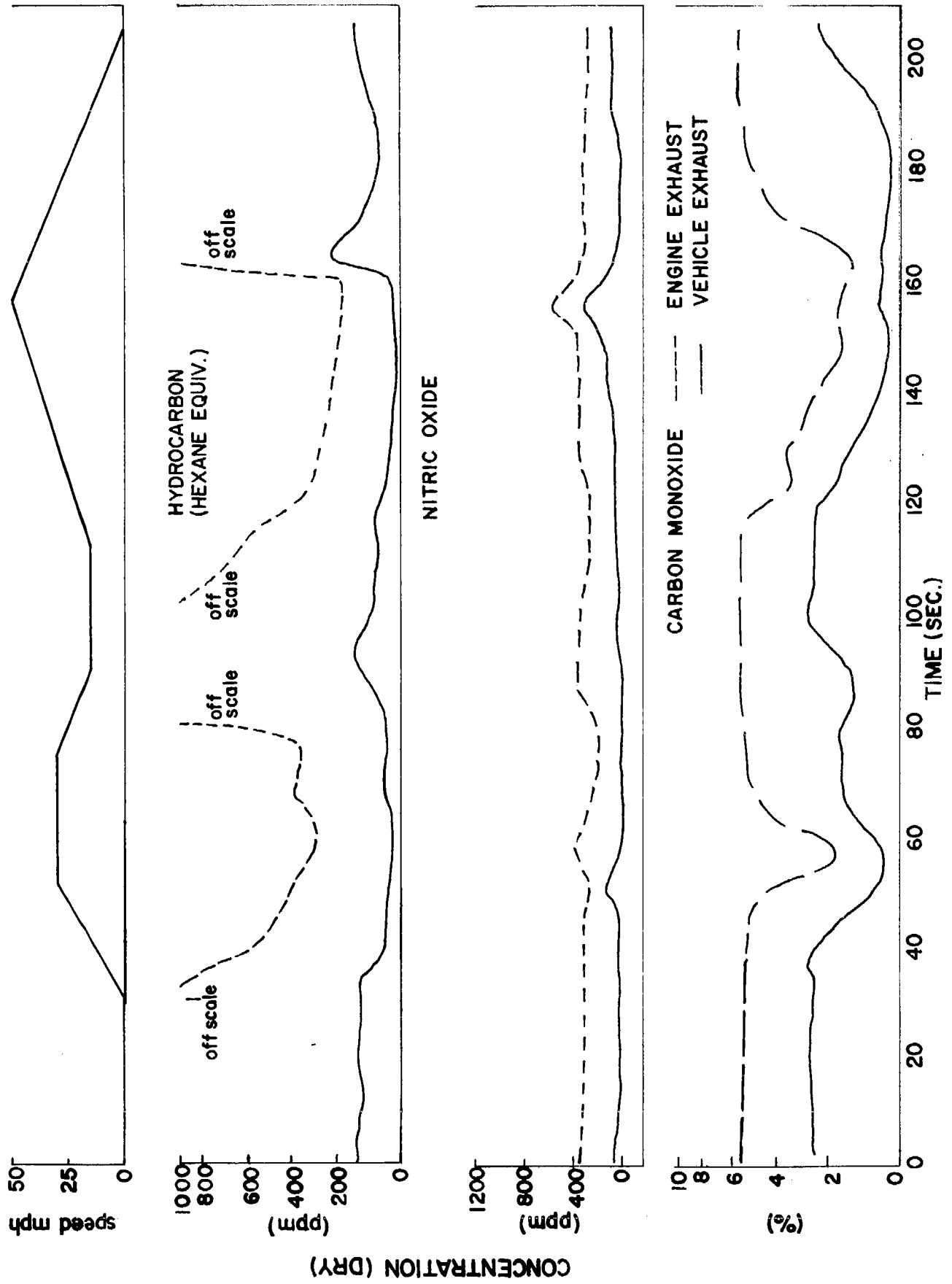


Figure 4-26 Exhaust Gas Concentration over FTP Cycle (Timex1.5) with Two-Stage PTX Converter and High-Performance Carburetion and Ignition Systems.

platinum is known to promote the formation of ammonia from the NO-H₂ reaction, a considerable amount of the NO reduction may have resulted in the formation of ammonia. However, this was not confirmed since ammonia measurements were not made in these tests. A maladjustment in the vehicle speed recorder caused the duration of the test cycle to be 50% higher than the correct duration. NO emissions were lower, as result of this error, than in subsequent tests of other configurations with the correct cycle duration.

Examination of Figure 4-26 shows the behavior of the modified carburetion system. The CO concentration indicates that the carburetor delivered a fairly uniform air/fuel ratio of 12:1 during most modes except during acceleration when the ratio changed to about 14:1. Thus, during these periods, the carburetor venturi did not draw enough fuel to provide a maximum acceleration rate which would occur with an air/fuel ratio of about 12:1. This carburetor behavior in extreme cases results in complete fuel starvation and is the typical source of driver complaints about flat spots in a car's response.

The results of the test with the modified system are summarized in Table 4-17. The concentrations are those existing at the end of the particular mode except for hydrocarbons during the deceleration mode; peak values are listed in the latter case.

It is seen that hydrocarbons were oxidized effectively in all modes. The oxidation of carbon monoxide was less than that desired in some modes and was most likely the result of an excessively rich setting of the carburetor and insufficient air injection into the second stage reactor. The NO reduction was high corroborating the CVS tests but may have been accompanied by considerable ammonia production.

Standard carburetion with two-stage PTX converters. After the tests with the modified carburetion and ignition system were completed, the original carburetor and distributor were reinstalled. The tests were repeated using the seven-mode driving cycle and the two-stage platinum exhaust reactors.

Figure 4-27 and Table 4-18 show the results for this configuration. The stock carburetor produced a much leaner air/fuel ratio of about 13.5:1 (determined from the exhaust composition) at idle and about

Table 4-17. Exhaust Concentrations During Various Driving Modes with Modified Carburetion and Ignition System and Two-Stage Platinum Exhaust Reactor.

Mode	Engine Exhaust		Vehicle Exhaust		% Reduction	
	CO(%)	HC(ppm) NO(ppm)	CO(%)	HC(ppm) NO(ppm)	CO	HC NO
Idle	5.2	1000 300	2.5	130 40	52	87 86
Accel. 0-30 mph	1.5	300 350	0.2	30 120	87	90 66
Cruise 30 mph	5.2	350 300	0.8	50 0	85	86 100
Decel. 30-15 mph	5.2	>1000 350	1.4	150 0	73	>85 100
Cruise 15 mph	6.0	510 300	2.5	70 40	58	84 86
Accel. 15-50 mph	1.0	200 500	0.2	20 260	80	90 48
Decel. 50-0 mph	5.2	>1000 350	2.5	200 0	52	>80 100

Table 4-18. Exhaust Concentrations During Various Driving Modes with Stock Carburetor and Ignition Systems and Two-Stage Platinum Exhaust Reactor.

Mode	Engine Exhaust		Vehicle Exhaust		% Reduction	
	CO(%)	HC(ppm) NO(ppm)	CO(%)	HC(ppm) NO(ppm)	CO	HC NO
Idle 0-30 mph	2.7	70 90	0	0 100	100	100 0
Accel. 0-30 mph	0.25	30 920	0	0 890	100	100 0
Cruise 30 mph	0.75	30 90	0.4	0 100	47	100 0
Decel. 30-15 mph	2.5	70 90	0	0 100	100	100 0
Cruise 15 mph	1.2	30 90	0	0 100	100	100 0
Accel. 15-50 mph	0.25	30 1100	0	0 1100	100	100 0
Decel. 50-0 mph	4.5	1000 90	1.4	500 100	69	50 0

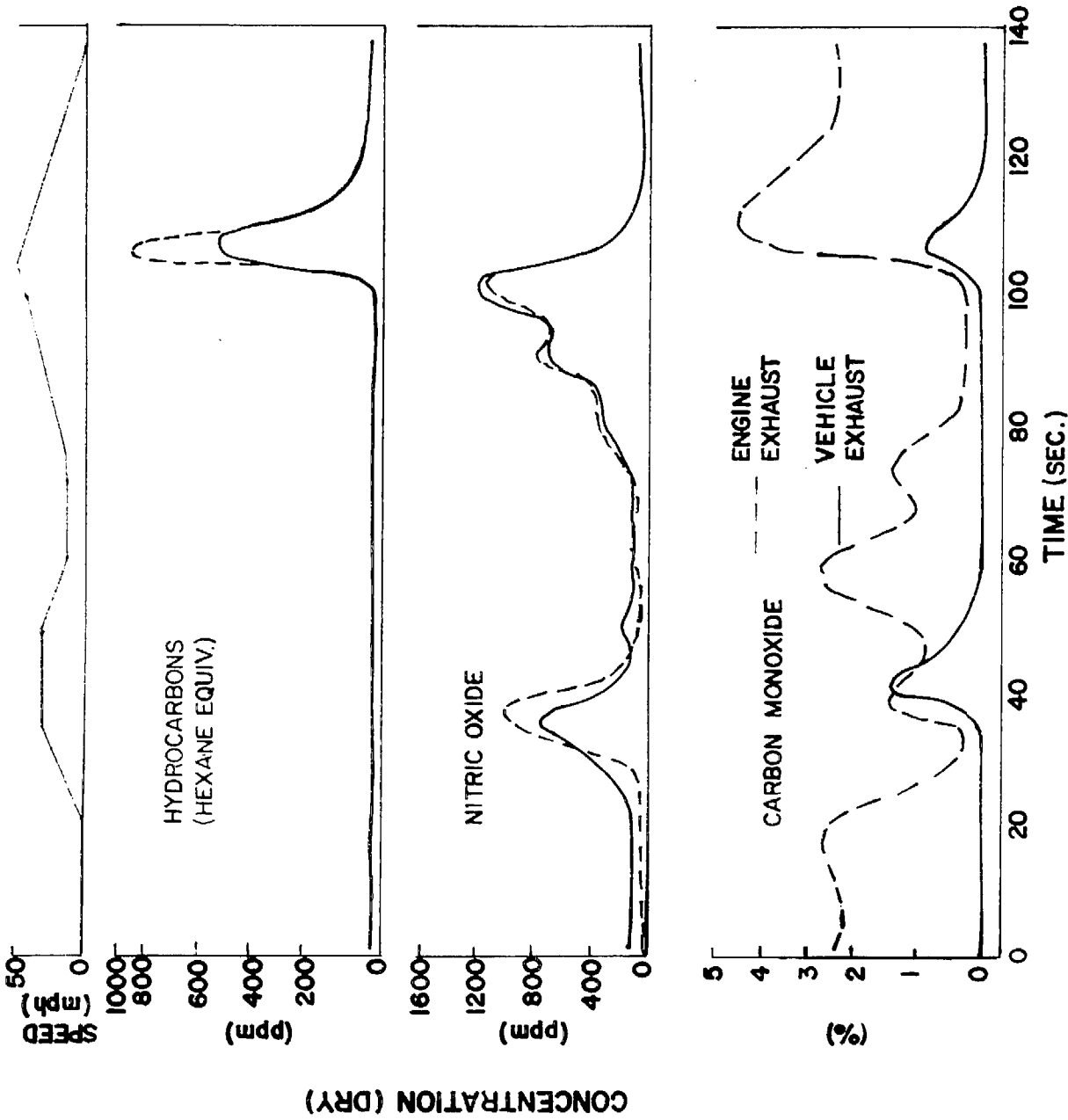


Figure 4-27 Exhaust Gas Concentration over FTP Cycle with Two-Stage PTX Converter and Standard Carburetion and Timing.

15:1 during cruise and acceleration. This leaner mixture resulted in the injection of an adequate amount of air into the second stage reactor. In this case, oxidation of the CO and HC was complete except during the 30 mph cruise and the last deceleration mode. During these modes, sharp spikes occurred in the trace of the CO and HC concentrations at the vehicle exhaust.

As mentioned earlier, the tabulated values are indicative of concentrations at the end of each mode. The spike at about 40 seconds in the CO curves of Figure 4-27 (during the cruise mode) was actually caused by the sudden cessation of acceleration at the end of the previous mode. CO output due to this speed change was still significant at the end of this short cruise mode. Conversion of CO during this period, as well as during the last deceleration mode, was incomplete due to a lack of secondary air.

The NO concentration was not significantly affected by the converters. This undoubtedly results from lower CO and HC concentrations available in the first stage reactor for reduction with NO and by complete lack of reductants in the second stage for reduction after oxygen depletion, as observed with the high-performance carburetor.

Standard Carburetor and Exhaust System. After these tests were completed, the platinum converters were removed and the original exhaust system and thermal exhaust manifold reactor re-installed. The vehicle was again tested using the seven-mode test. The results are shown in Figure 4-28. The data obtained with the platinum reactors are also shown for comparison.

As expected, there is little difference in the NO concentration with the standard exhaust system with and without the catalytic converters. A substantial decrease in the CO concentration was obtained with the catalyst as compared to the standard system, but HC oxidation with either the catalyst or the stock thermal reactor was equally effective.

The tests confirmed that platinum is an extremely good oxidation catalyst for CO and HC in the vehicle exhaust. When used with excess air, the hydrocarbon and carbon monoxide conversion is 100% under most vehicle operating modes. With very fuel rich operation, platinum promotes the reduction of NO, as well.

The tests did not permit determination of the life expectancy of the converters. It was noted, however, that even for the short mileage

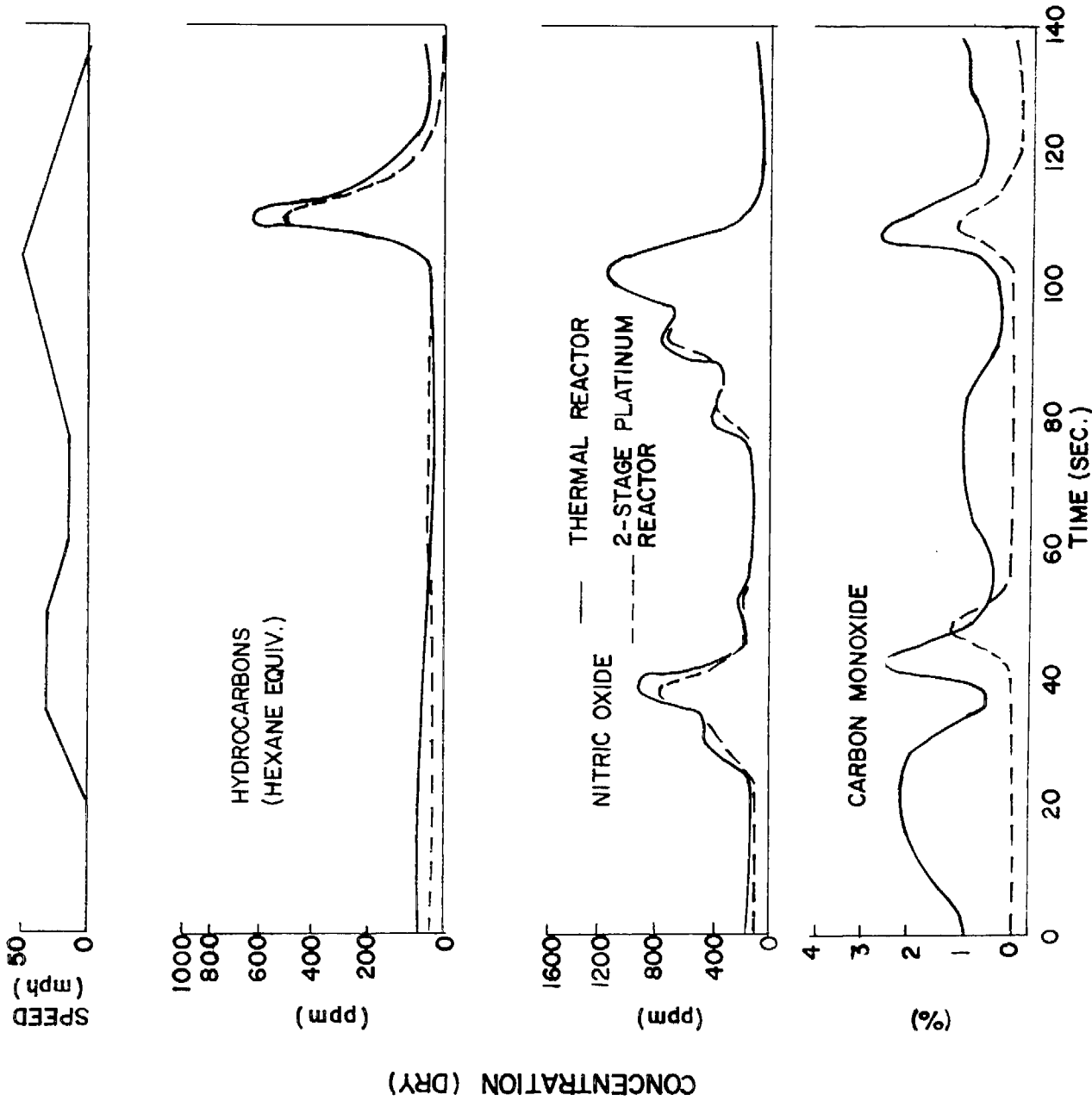


Figure 4-28 Comparison of Exhaust Gas Concentration over FTP Cycle with Exhaust Thermal Reactor and Two-Stage P-TX Converter.

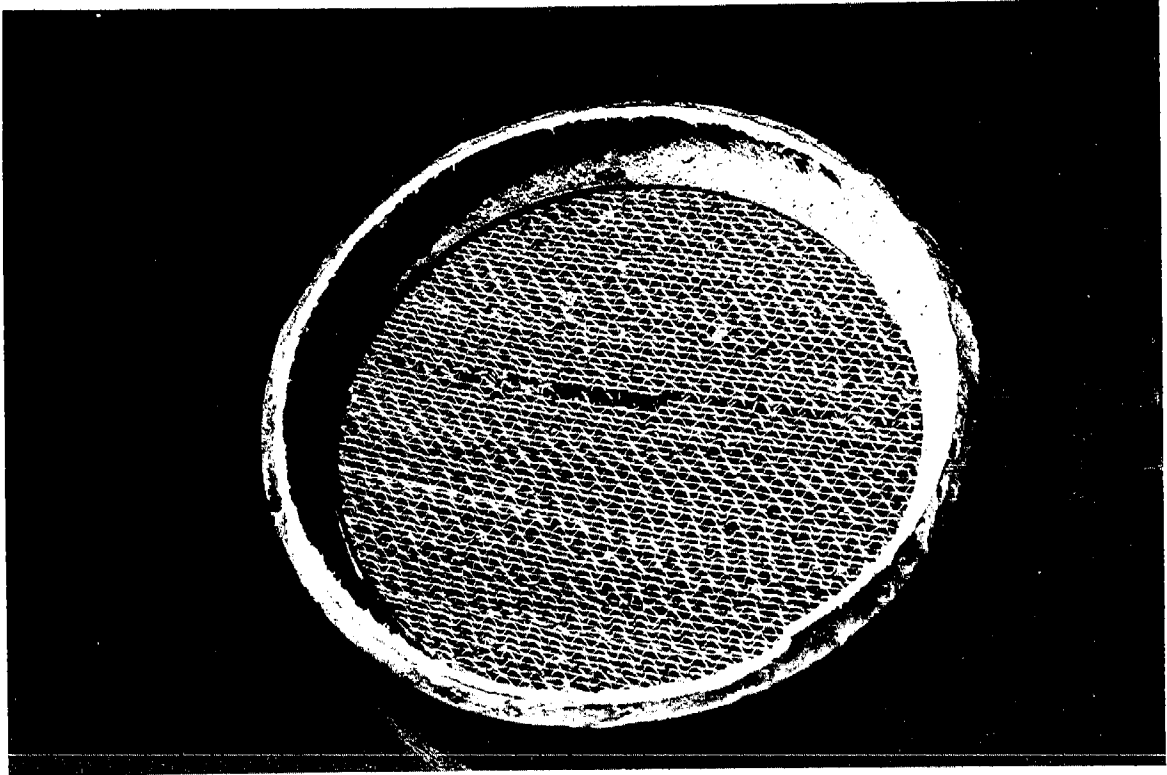


Figure 4-29. Damage to PTX Converter after Less than 2000 Miles Operation.

involved in the Rally and these tests some physical deterioration of the catalyst support was observed. Figure 4-29 shows the deterioration at one of the converter inlet faces.

4.2.4 Auto Exhaust Tests with Full-Scale Two-Stage Converter.

The screening tests showed several catalysts with sufficient promise to justify full-scale auto emissions tests. The steady state and transient start-up performance of four catalysts for nitric oxide reduction was investigated using a full-scale two-stage converter attached to an auto engine mounted on a dynamometer. The four catalysts tested in the first stage were:

- a. copper chromite (Girdler G-22)
- b. type 304 stainless steel lathe turnings
- c. monel chips
- d. strontium yttrium ruthenium oxide

In the second stage, Girdler G-43 catalyst (0.1% Pt, 3% Ni) was used to oxidize CO and hydrocarbons during the entire test series. The two-stage converter, the engine-dynamometer and the gas analysis equipment have been described in Section 3.

Seven pounds of 304 stainless chips and nine pounds of monel chips were used. Approximately 7 pounds of copper chromite were used. The stainless and monel were pre-oxidized by heating to 1000°C overnight in a moist air stream and then conditioned in situ in the first stage by passing through auto exhaust containing 3 to 5 percent CO at a temperature of 750°C for two hours.

The mixed ruthenium oxide catalyst was monolithic. Aqueous nitrate solutions of yttrium, strontium and ruthenium were impregnated on 2-in. x 2-in. x 3-in. AlSiMag (3M Co) monoliths. The monoliths were calcined at 800°C prior to use. Concentration of active material was about 0.7% $\text{SrY}_{0.5}\text{Ru}_{0.5}\text{O}_{2.75}$ (about 3 gm ruthenium).

Although ruthenium is moderately expensive, the high level of performance observed with Sr-Y-Ru oxide in preliminary tests justified extended study. Bernstein et al., (1971) calculated that the cost of a catalytic material is only a fraction of the total catalytic control package cost.

The earlier tests with the prototype exhaust converter indicated that proper converter performance is dependent on two major operational considerations. First, inlet exhaust gas temperature must be sufficiently high so that both stages of a two-stage catalytic converter are operating soon after startup. Second, sufficient quantity of reductants must be present in the exhaust to ensure adequate NO removal in the first stage.

Temperatures were varied by altering the spark advance and/or by injecting some secondary air into the exhaust manifold to promote partial afterburning of CO and hydrocarbons. Hancock et al., (1971) showed that "light-off" time of a CO/HC converter (FTP test) could be decreased from 75 to 40 seconds after startup using a spark retard system which would revert to normal advance characteristics when the coolant temperature reached 180°F.

Bernhardt and Hoffman (1972) discussed the advantages of diverting air into an in line thermal reactor at startup and then back into the second stage after catalyst bed warmup. They also showed that a rich engine A/F ratio decreases the time required to reach operational temperatures.

It is beyond the scope of this project to develop operational devices and logic systems to control either spark advance or programmed air injection. The dynamometer-mounted, engine-converter system was limited to tests involving fixed spark-advance and secondary air injection characteristics (variable only from test to test). The variable A/F carburetor was described in Section 3. This device enabled variation of reductant concentration in the exhaust. Standard steady state test conditions (2000 rpm, 27 BHP and 10.5 in. Hg manifold vacuum) were used to compare the catalysts. Such operation provided a first stage inlet temperature representative of the average temperature during latter stages of a CVS test as shown by others (e. g., Meguerian et al., 1972).

After the catalysts were in place, the engine was started and operated until steady state temperatures were achieved in both stages. The composition of the exhaust gas was sampled at the engine manifold, at

the interstage plenum, and at the reactor outlet. Ammonia was determined by the method described in Chapter 3. Very little or no ammonia was detected.

The effect of air/fuel ratio was studied with load and speed readjusted to maintain standard conditions. Secondary air flow was maintained at 20 to 25 percent of the total exhaust flow, providing good CO and HC oxidation over the range of air/fuel ratios studied.

Concentrations of various components of the exhaust gases at the reactor outlet were continuously recorded during transient startup operation (the engine was started cold after setting overnight).

In the first stage, there was considerable channeling of exhaust gas at the end of the inlet plenum farthest from the exhaust inlet. This was caused by high static pressure due to an abrupt 90 degree change in flow direction. These flow problems were corrected by the development of a staged exhaust injection tube. Figure 4-30 is a schematic of the tube in the inlet plenum of the converter. The density of holes drilled in the tube decreased from the inlet; in addition, turning vanes were employed at the inlet end to provide a more uniform pressure profile in the plenum. Figure 4-31 shows overall pressure drop with the four NO_x catalysts (G-43 was in the second stage for all tests).

Figures 4-32 through 4-36 show inlet NO concentrations, conversions and midbed temperatures (first stage) for the copper chromite, stainless steel, monel, and Sr-Y-Ru monolith, respectively. Total secondary air flow was maintained at 25% of the primary air flow. This flow rate was necessary for total CO conversion over the full concentration range. The relative inactivity of the stainless steel led to first-stage bed temperatures below 550°C over the entire CO concentration range. Higher conversion of NO resulted in somewhat higher temperatures with copper chromite.

Figures 4-32 through 4-36 show that with the spark retarded NO concentration in the manifold varies from 2000 ppm with a CO concentration of about 0.2% to about 400 ppm with a CO concentration of 7% and with normal spark advance from about 2700 ppm to 600 ppm over the same range of CO concentrations.

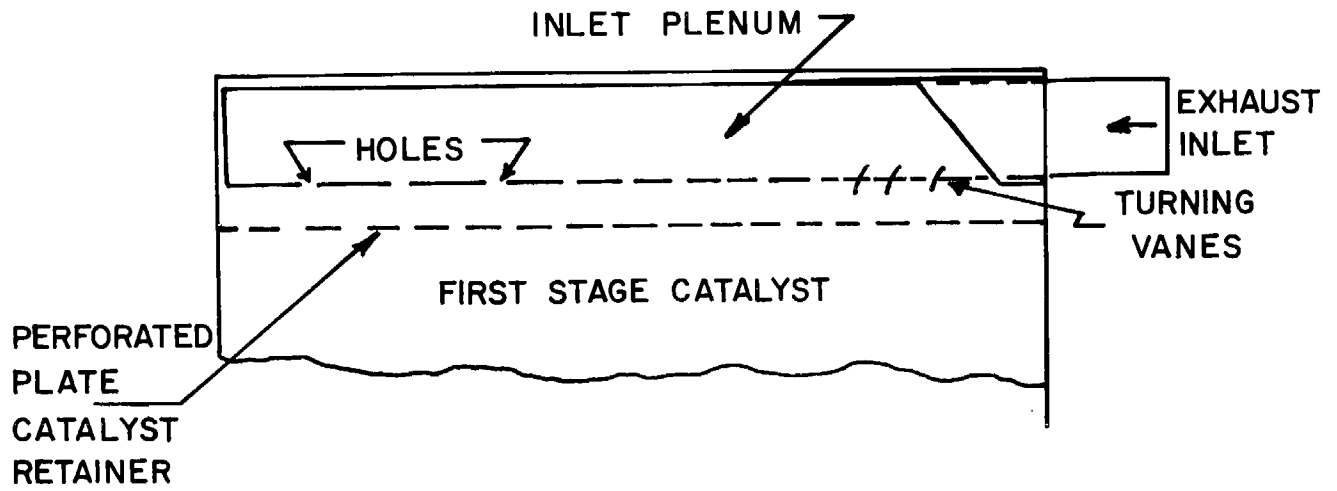


Figure 4-30 Flow Diverting Tube Installed in Inlet Plenum Chamber.

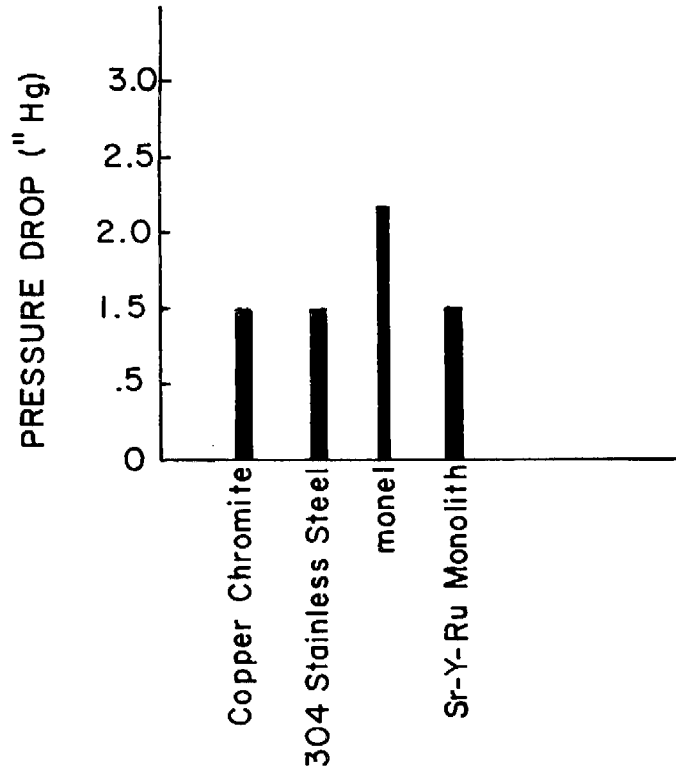


Figure 4-31 Pressure Drop through Two-Stage Converter. Girdler G-43 Used as Second Stage.

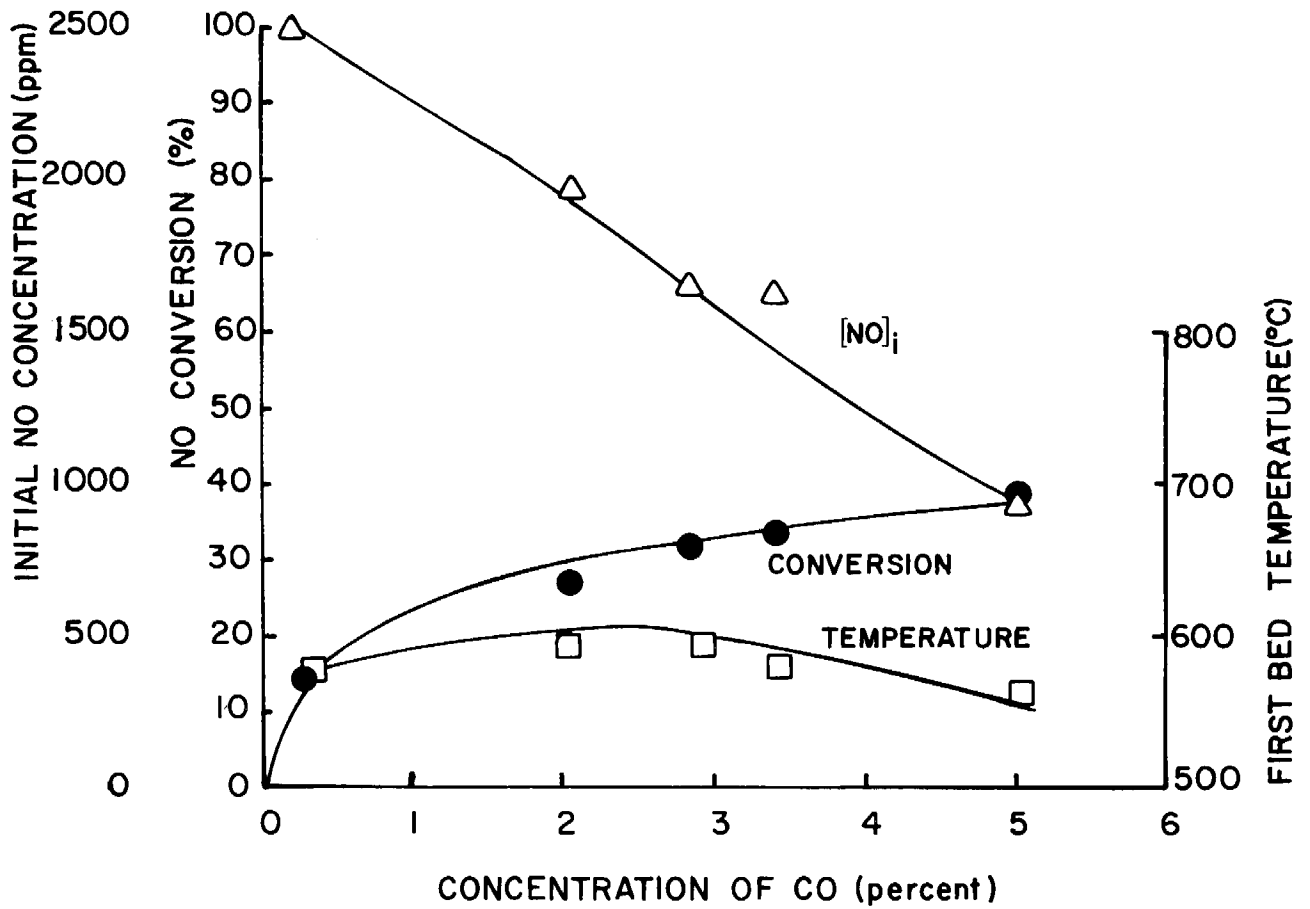


Figure 4-32 Effect of initial CO Concentration on NO Conversion with Copper Chromite Catalyst. Normal Spark Advance.

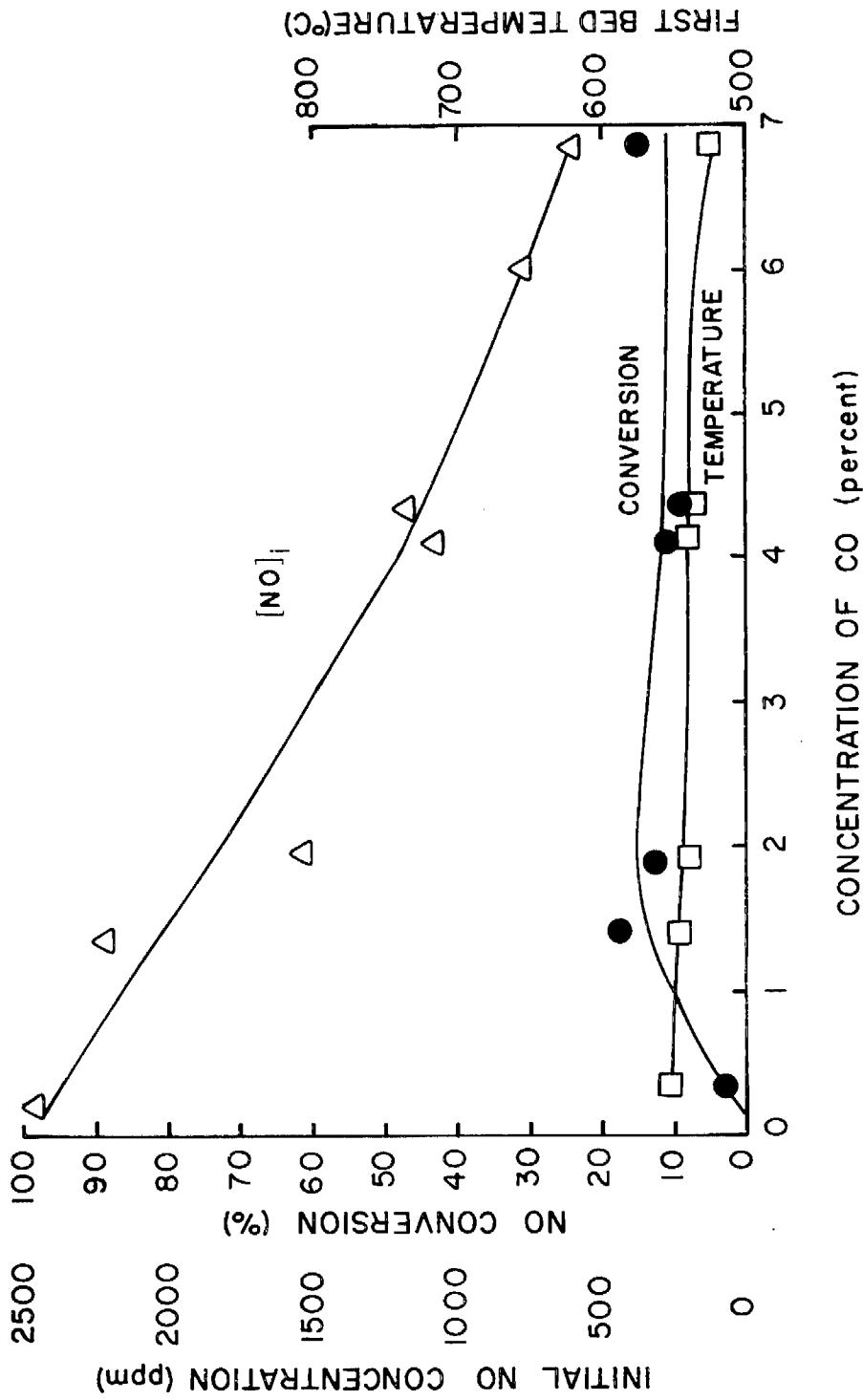


Figure 4-33 Effect of Initial CO Concentration on NO Conversion with 304 Stainless Steel Catalyst. Normal Spark Advance.

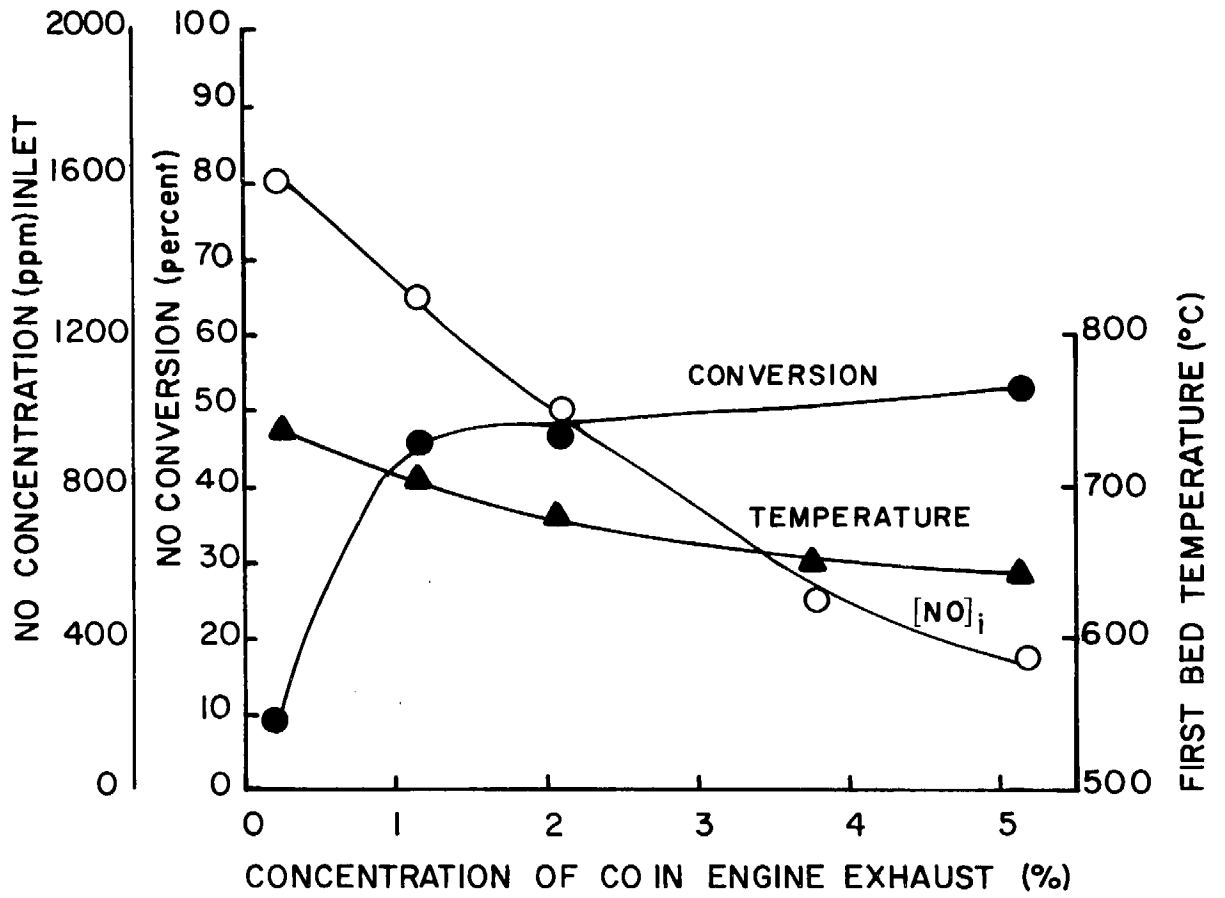


Figure 4-34 Effect of Initial CO Concentration on Conversion of NO using Monel Chips. Tests run with retarded Spark

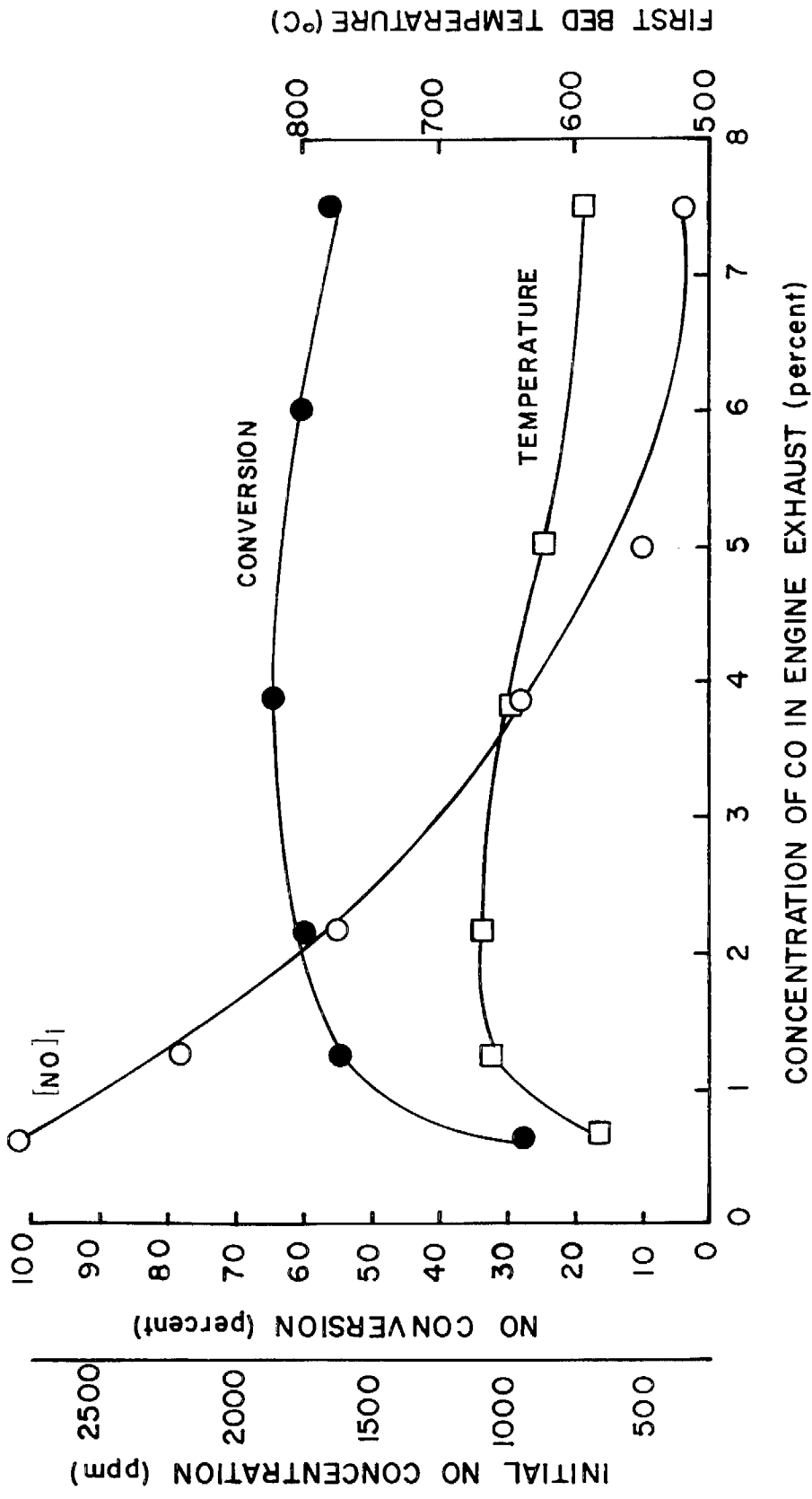


Figure 4-35 Effect of CO Concentration of Conversion of NO using Sr-Y-Ru monolith, Standard Spark Advance.

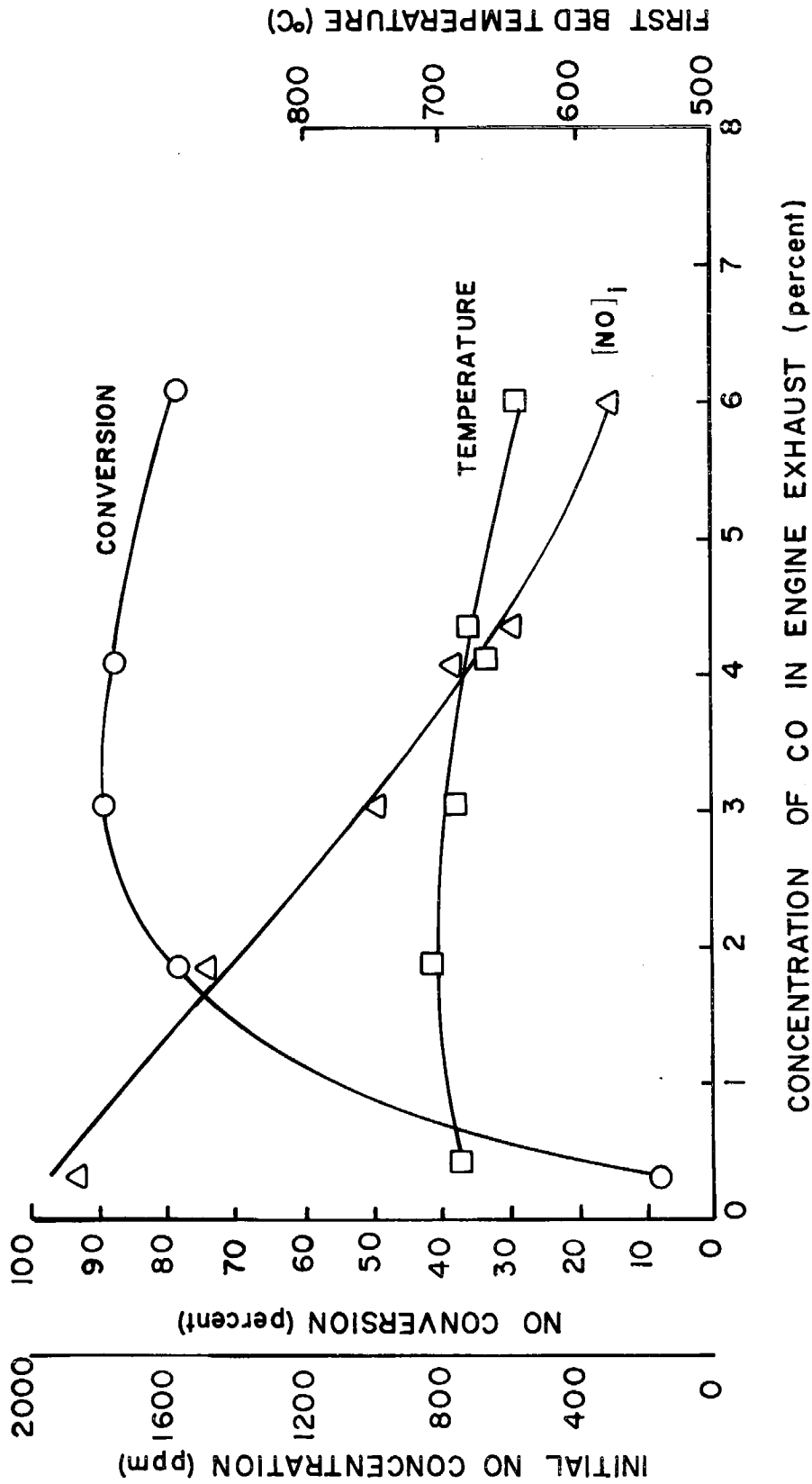


Figure 4-36 Effect of CO Initial Concentration on NO Conversion on Sr-Y-Ru Monolith. Tests Run with Spark Retarded.

The relative flatness of first stage temperature curves can be explained as follows: The exhaust gas temperature decreased uniformly with increasing CO content due to reduced combustion temperatures in the engine. First stage reactions, on the other hand, tend to increase with increasing CO exhaust content. Thus the combined effect produced a relatively unchanging first stage temperature.

Retarding the spark 8 degrees from a normal advance of 36 degrees (the vacuum advance was disconnected) caused an increase of approximately 40^oC (Figures 4-35 and 4-36) in the same first stage temperature. Figure 4-37 shows that this increase in exhaust temperature resulted in a substantial increase in NO conversion (conversions for Sr-Y-Ru and monel with retarded and normal spark advance are shown).

Figure 4-37 shows that maximum NO conversion occurred at about 3 to 4 percent CO. At greater CO concentrations, NO conversion decreased slightly. This resulted from the decreased exhaust gas temperature which caused the first stage temperature to also decrease. Figure 4-38 shows that three or four percent CO resulted in a 3 percent loss in fuel economy with advanced spark or 11 percent with a retarded spark. Since temperature is so important in the operation of the first stage, utilization of the sensible heat of the final exhaust to heat the first stage would improve performance and fuel economy.

Bernstein et al., (1971) estimated that the NO concentration would have to be below 100 ppm based on the 1976 Federal CVS test for a 4000 pound vehicle. For the test conditions of this study that level could be achieved with the Sr-Y-Ru catalyst and a retarded spark, As previously stated this would result in an 11 percent fuel penalty. Exhaust gas recirculation was not used in any of these tests. This technique might be employed to provide additional reduction of NO and perhaps decrease the fuel penalty.

Although time did not permit long term studies of the NO catalysts, no physical damage or increase in back pressure was observed except for copper chromite (the only pelletized first-stage catalyst studied). After only a few hours operation considerable powdering and fracturing of the catalyst pellets occurred (about 10% weight loss).

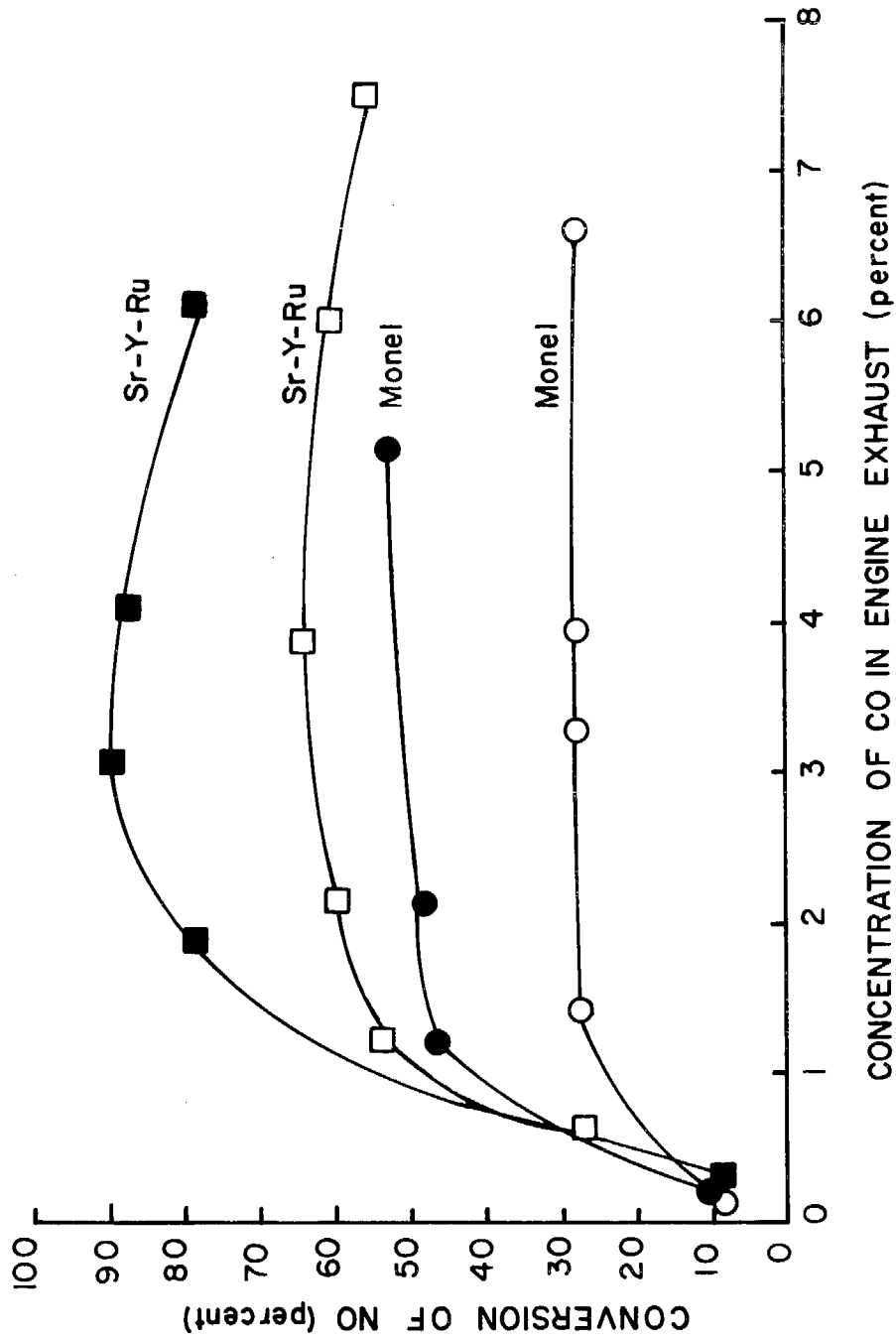


Figure 4-37 Comparison of Sr-Y-Ru Monolith and Monel Catalysts with Two Different Spark Settings. Open Symbols: data taken with spark advance; Closed Symbols: with spark retard.

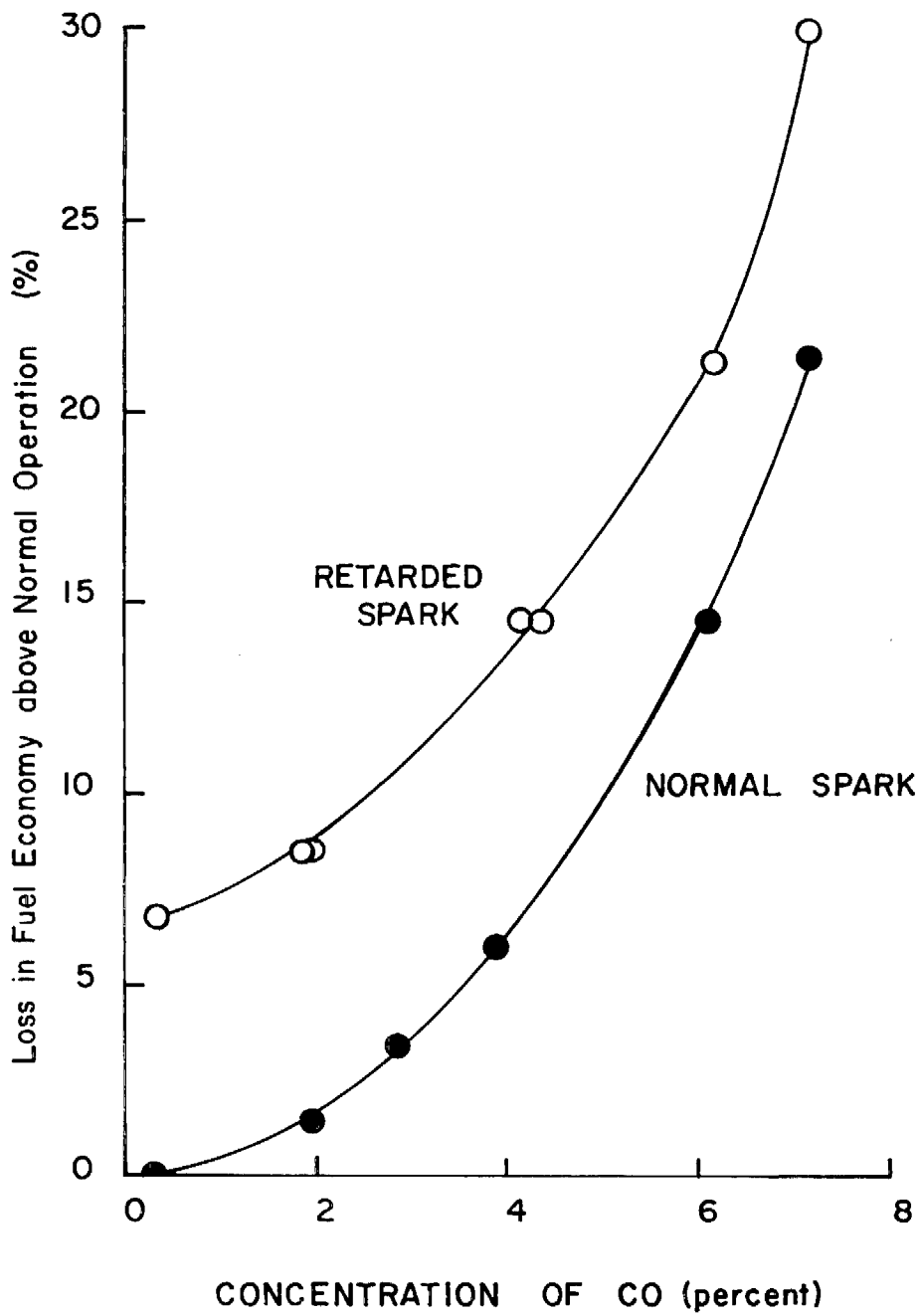


Figure 4-38 Effect of Spark Advance and CO Concentration on Fuel Economy.

Figure 4-39 shows how the performance of the converter is affected by the amount of air injected to the thermal reactor. Initiation of significant CO conversion in the manifold occurs at a manifold/second stage air ratio of 1:3. Conversion of NO starts to decrease indicating the approach to an oxidizing atmosphere in the first stage at that ratio. The dotted part of the CO curve in Figure 4-39 is the theoretical amount of CO after air dilution in the manifold. It can be seen that CO was not significantly oxidized in the manifold until 25% of the total secondary air was added at that location.

Reduction of NO ceased when 45% of the injected air was added to the manifold. Forty percent of the CO was removed in the manifold at that air ratio. The remaining CO (about 4.2% concentration based on manifold conditions) was then completely consumed in the converter. Total CO conversion was stable at 80% until CO oxidation was initiated in the manifold. Since total added air was constant, the increase in CO conversion from 80 to 100% was due to thermal oxidation in the manifold and, perhaps, some catalytic reaction in the first stage. The net amount of CO oxidized in the second stage decreased due to depletion of CO.

Figure 4-40 shows how the converter temperatures are affected by the manifold/second stage air ratio. Up to 25% air ratio there was only a moderate influence of the air flow on the first stage temperature. However, the increase in temperature did lead to the improvement in NO conversion up to that air ratio, as was seen in Figure 4-39. Above 25% manifold air, the manifold temperature increased more sharply indicating CO oxidation in the manifold. First stage bed temperatures roughly paralleled the manifold temperature, indicating that most of the CO oxidation occurred in the manifold rather than in the first stage.

The second stage temperature increased with increased manifold air but not to as great an extent as in the first stage. The drop in final exhaust temperature reflects non-adiabatic operation of the converter, coupled with a decrease in the net CO oxidation in the second stage.

Figure 4-36 and 4-39 show that there is little advantage in employing both CO oxidation in the manifold and increasing CO content from 3 to 7% to reduce NO concentration. Figure 4-38 shows a 28%

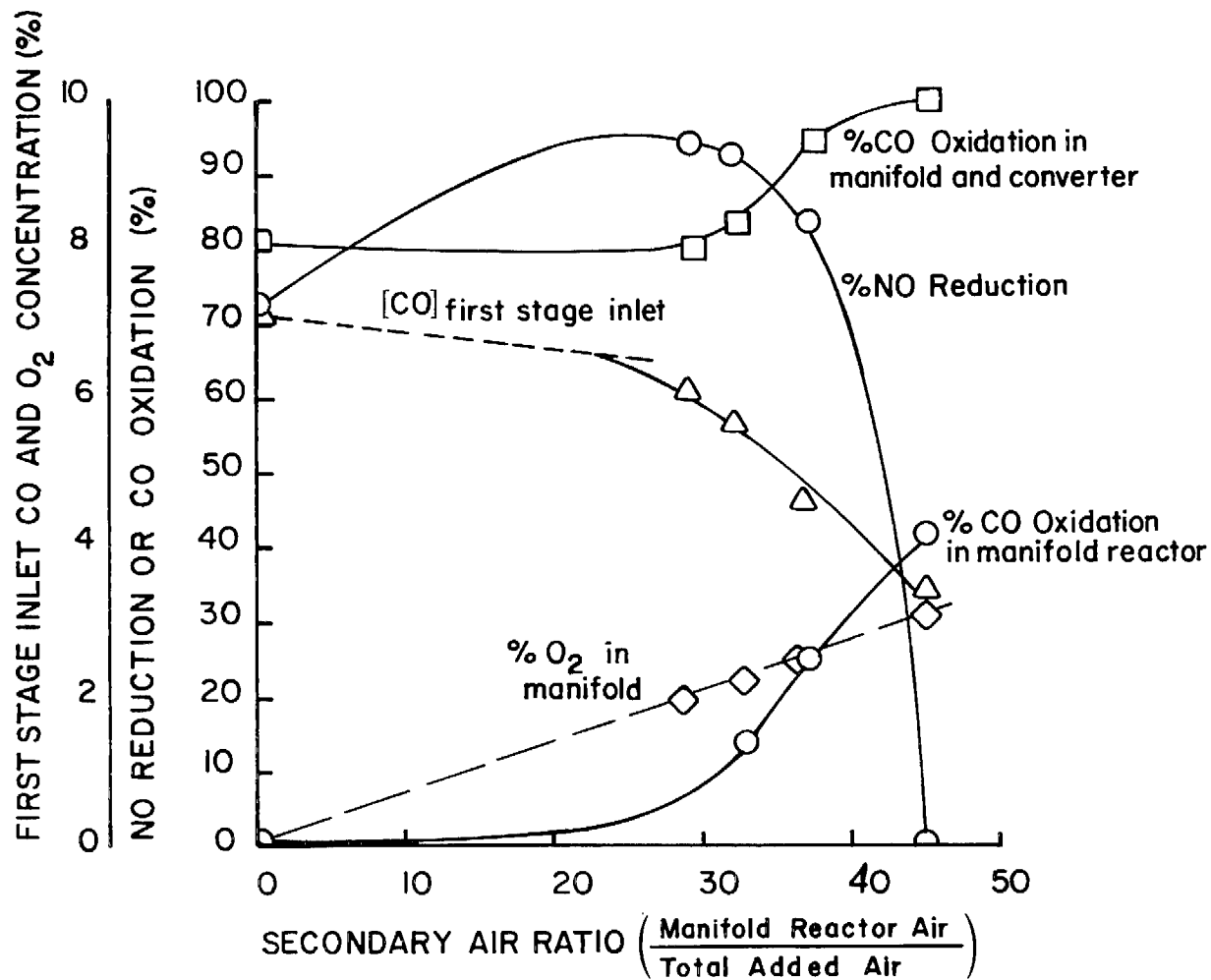


Figure 4-39 Effect of Manifold Afterburning on NO Reduction on Sr-Y-Ru Monolithic Catalyst. Spark Retarded.

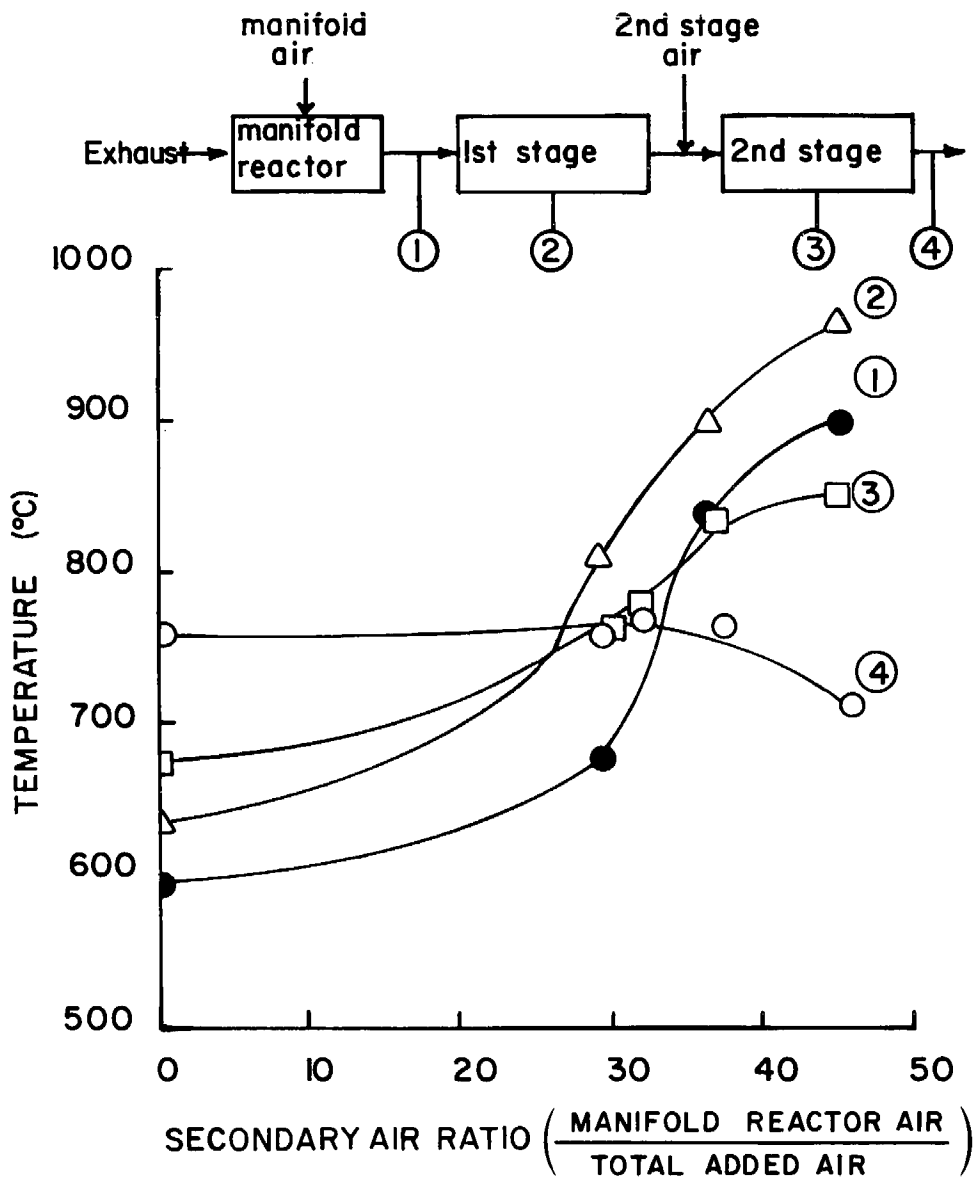


Figure 4-40 Effect of Manifold Afterburning on Reactor Temperatures.

fuel loss for 7% CO compared to 11% for the optimum 3% CO. The decreased air/fuel ratio caused a decrease in inlet NO concentration of 800 ppm; the 20% improvement in NO conversion (Figure 4-39) would amount to additional NO removal of only about 30 ppm. The influence of manifold reactions with air/fuel ratios and spark advance was not studied. However, there was little improvement at lower CO concentrations due to difficulty of initiating and sustaining homogeneous manifold reactions with lower CO content.

Warmup characteristics of the converter upon startup of the dynamometer-mounted engine was investigated. The engine was started cold and manually adjusted continuously to maintain the rpm, power and manifold vacuum conditions listed earlier until steady operation was achieved.

Figures 4-41 and 4-42 show exhaust concentrations (corrected to manifold conditions) of the converter for Sr-Y-Ru first stage and G-43 second stage with normal advance and spark retarded, respectively. Since the air/fuel ratio was slightly different for the two tests, steady-state inlet concentrations were somewhat different. However, both cases show the same transient characteristics. A sharp peak in hydrocarbons is observed in the first 10 seconds as a result of the unburned air and fuel mixture drawn through the cylinders upon start-up. The CO concentration peaks between one and two minutes. After 200 seconds, CO concentration decreased sharply. A peak in NO occurs in the first 10 seconds and is much more pronounced for the spark retarded case. The high NO results from a lean air/fuel ratio during the first 20 seconds of startup. Before the engine comes up to speed the venturi vacuum in the carburetor is too low to draw in much fuel. Thus, a lean mixture results, and high NO is observed.

The first stage reached "light-off" temperatures after 80 seconds with the spark retarded and after 120 seconds with the spark advanced. In both cases the second stage reached light-off temperatures after 200 seconds indicating the spark setting has very little influence on the initiation of oxidation in the second stage. However, the spark setting did affect the time for the second stage to reach steady state operation. With the spark retarded, steady state CO conversion was reached after

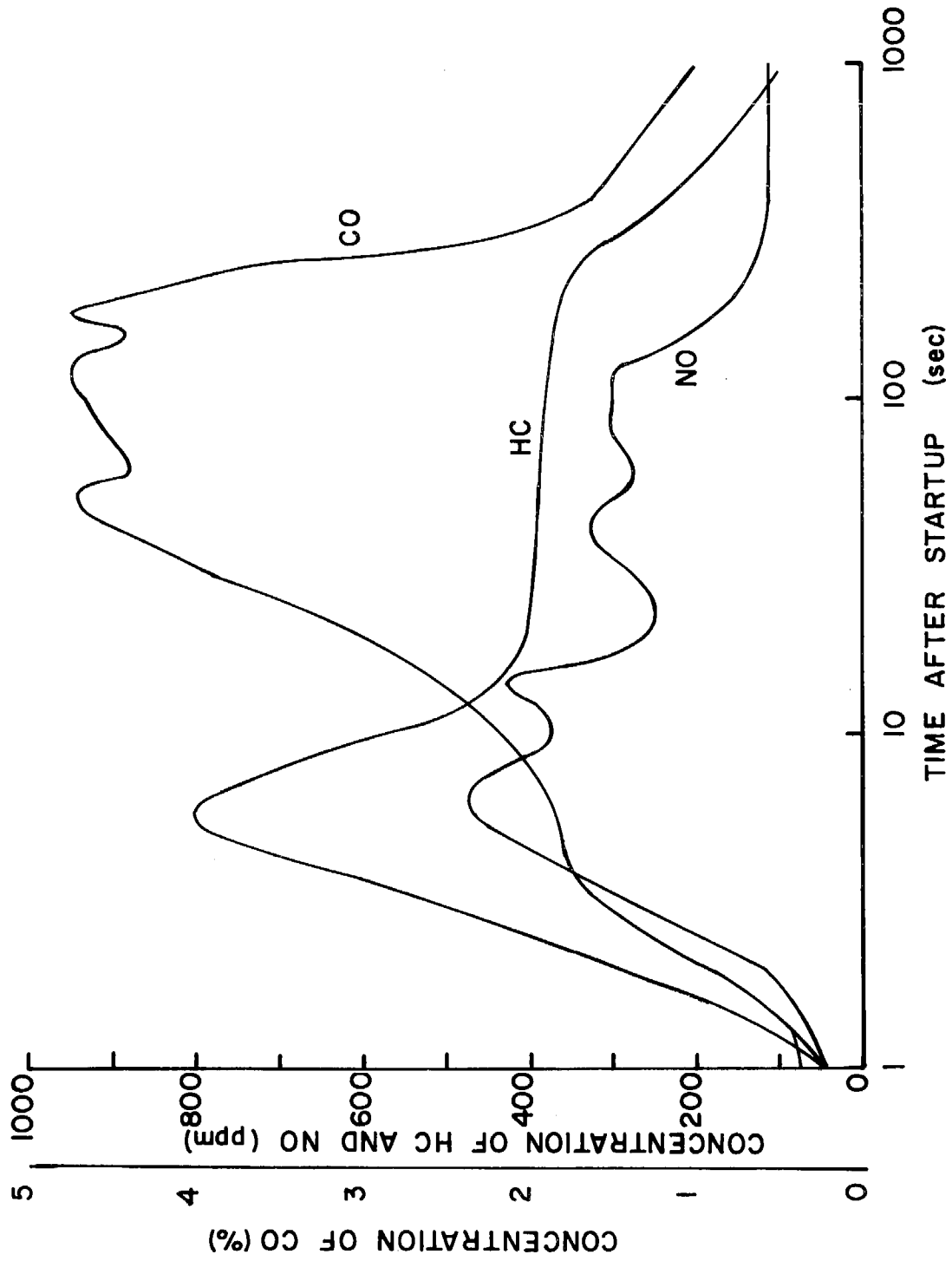


Figure 4-41 Transient Operation of Two-Stage Converter, Sr-Y-Ru Monolith in First Stage, G-43 in Second Stage. Normal Spark Advance, 25% Secondary Air.

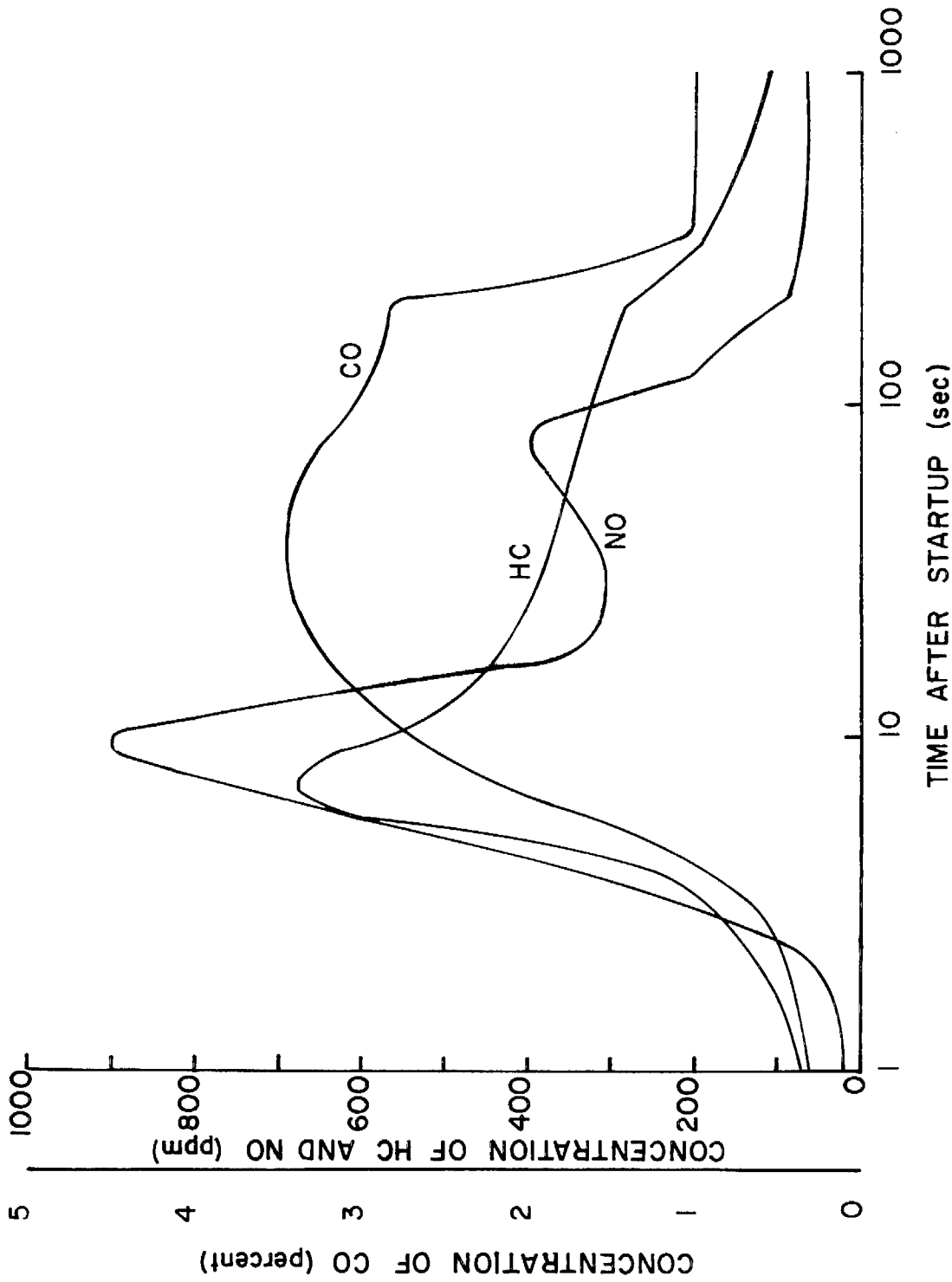


Figure 4-42 Transient Operation of Two-Stage Converter. Sr-Y-Ru Monolith in First Stage, G-43 in Second Stage. Spark Retarded, 25% Secondary Air.

360 seconds while 1000 seconds were required with the spark advanced. The higher exhaust gas temperatures with the spark retarded caused the above effect.

Figure 4-43 shows similar data using monel as the first-stage catalyst. The NO conversion with monel was less than with the Sr-Y-Ru catalyst. In general, the test engine was relatively easy to start, usually requiring only a single startup of about 4 seconds. In the test shown in Figure 4-43 the engine required a second start. For this hard start hydrocarbon concentrations were extremely high (off scale). Such a hard start under automotive test during a certifying driving cycle could result in complete failure of the tests.

Figure 4-43 shows a sharp peak in the CO concentration at about 10 seconds. This peak was not present in the two previous graphs indicating some afterburning in the exhaust manifold. The "light-off" temperatures of the second stage occurred at about 200 seconds, as in the previous tests. The monel first stage did not show the sharp "light-off" temperatures as did the Sr-Y-Ru.

As mentioned previously, no ammonia was detected in the inter-stage plenum. During all tests the Girdler G-43 catalyst was the second-stage catalyst. Conversion levels of CO and hydrocarbons were frequently checked and the conversion and accumulated operating time was recorded. Figure 4-44 shows CO conversion as a function of time for standard test conditions of 3% CO and 25% total secondary air. Figure 4-45 shows the influence of CO concentration in the engine exhaust on CO conversion for early tests and after 191 hours of operation.

This particular batch of G-43 had been used in earlier studies with the prototype converter as well as in a previous program conducted at this laboratory. The continuous lines in Figure 4-44 show the running time for the two-stage converter tests. Conversion of hydrocarbons was relatively constant at about 70% up to the cessation of the tests while CO conversion fell off significantly at about 150 hours. By assuming a 50 mph equivalent speed, CO conversion was stable for 7500 simulated miles. Examination of the catalyst showed no physical deterioration or weight loss.

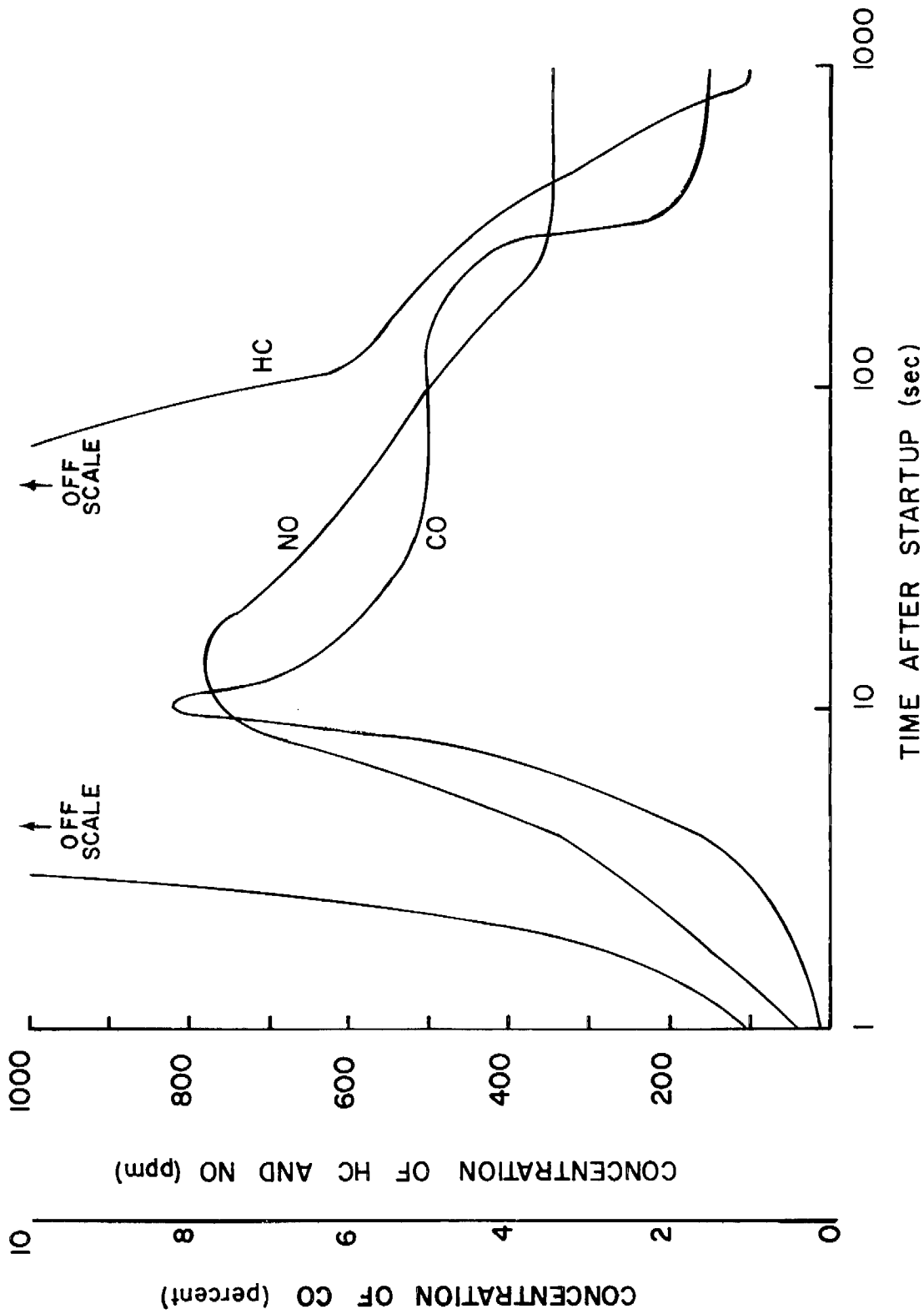


Figure 4-43 Transient Operation of Two-Stage Converter. Monel in First Stage, G-43 in Second Stage, 25% Secondary Air.

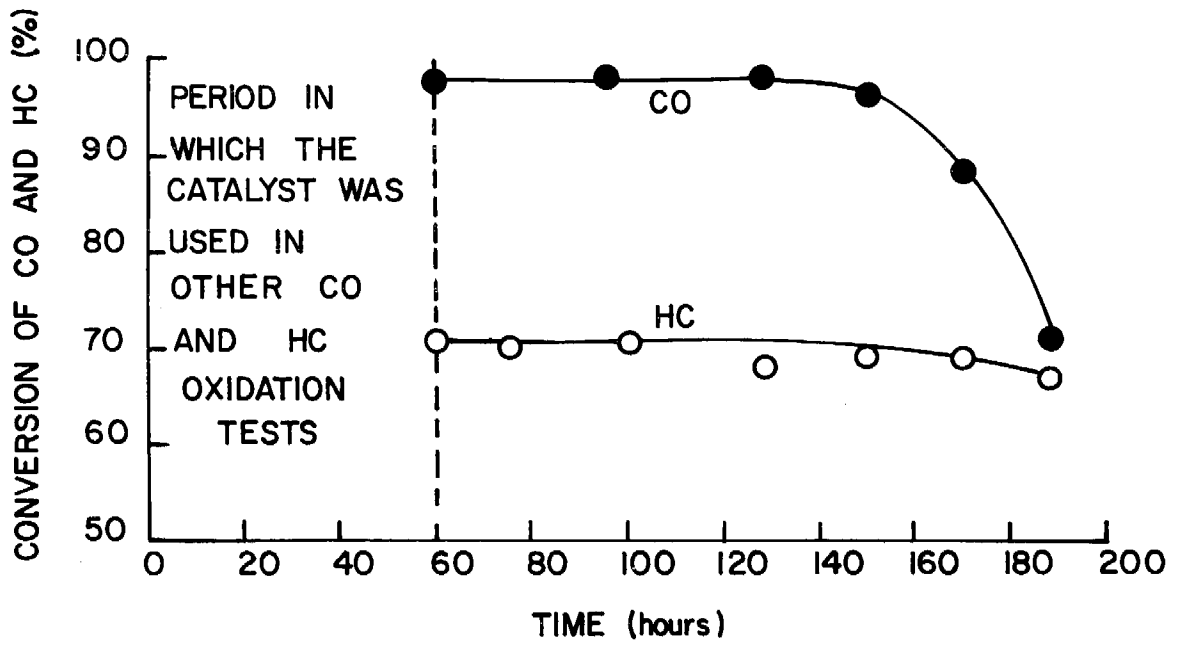


Figure 4-44 Effect of Running Time on CO and Hydrocarbon Conversion.

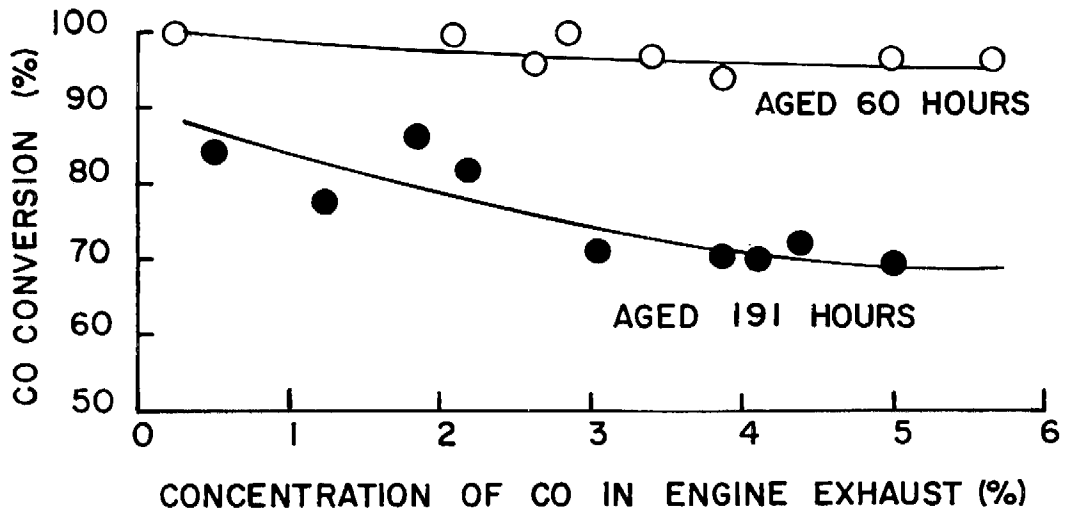


Figure 4-45 Influence of CO Concentration on CO Conversion for Platinum Catalyst at Start and End of Two-Stage Tests.

Unleaded Chevron gasoline was used throughout this program. However, after about 120 hours of operation (60 hours of the two-stage converter tests) the unleaded gasoline supply purchased from the Chevron district distributor was depleted and a new supply had to be obtained. Since there was a gasoline shortage at the time, the Chevron district distributor would not sell UCLA the required unleaded gasoline to complete the converter tests. Therefore, the second batch of unleaded gasoline was purchased from a neighborhood Chevron dealer who stated that his supply was relatively old. The subsequent decline in the catalyst activity for CO oxidation at about 150 hours as shown in Figure 4-44 suggests lead contamination of the second batch of unleaded gasoline. It should be noted that there was a period of 30 hours from the time the new gasoline supply was used to the time at which CO conversion decreased significantly.

A dithizone test (Feigl, 1960) gave a positive indication of lead in the fuel and on the G-43 platinum catalyst. Since the original supply of unleaded gasoline was delivered in new barrels the observed lead contamination must have come from the storage tanks of the neighborhood Chevron dealer.

This experience indicates that lead contamination of unleaded gasoline may be a serious problem. As quantities of unleaded fuel are used the contamination will decrease with time. However, if the motorist is unlucky enough to purchase the first batch of unleaded fuel which has been stored in a contaminated tank serious loss of converter performance may result.

Conclusions and recommendations from the motor studies are:

(1) Mixed ruthenium oxide catalysts were the most active found for removal of NO. Further work under test conditions as well as additional catalyst stability studies are desirable.

(2) Lead contamination of the unleaded fuel appears to be responsible for a 25% loss of activity of the Pt oxidation catalyst.

REFERENCES

- Andersen, R.B., Stein, K.C., Feenan, J.J. and Hofer, L.J., Ind. Eng. Chem., 53, 809 (1961).
- Ayen, R.F. and Ng, Y.S., Int. J. Air Water Poll. (Pergammon Press), 10, 1(1966).
- Baker, K.A. and Doerr, R.C., Air Poll. Con. Assn. J., 14, 409 (1964).
- Bartok, W., Crawford, A.R., Hall, H.J., Manny, E.H. and Skopp, A., Systems Study of Nitrogen Oxide Control Methods for Stationary Sources, Interim Status Dept., No GR-1-NOS-9, Esso Res./Engr. Co. (1969).
- Bauerle, G.L. and Nobe K., "Catalytic Afterburner Design Studies- Part II Transient Operation" Air Pollution Control by Catalysis, Report UCLA-ENG-7103, University of California, Los Angeles, Jan (1971).
- Bauerle, G.L., Service, G.R., and Nobe, K., Ind. Eng. Chem. Prod. Res. Develop., 11, 54, (1972).
- Bauerle, G.L., Sorensen, L.L.C., and Nobe, K., UCLA Report, UCLA-ENG-7309, pp. 1-20, Jan. 1973.
- Bernhardt, W.E. and Hoffman, E., SAE National Auto. Eng. Meeting, SAE Paper 720481, Detroit, Mich. May (1972).
- Bernstein, L.S., Raman, A.K.S., and Wigg, E.E., Presentation to Technical Session, "Engines and Emissions," Central States Section, The Combustion Institute, Ann Arbor, Mich., (1971).
- Broyde, B., J. Catalysis, 10, 13 (1968).
- Cannon, W.A., and Welling C.E., Ind. Eng. Chem. Prod. Res. Develop., 1, 152 (1962).
- Feigl, F. Spot Tests in Organic Analysis, Elsevier Pub. Co., Amsterdam, Neth., (1960).
- Hancock, E.E., Campau, R.M., and Connoly, R., SAE Auto. Eng. Congress, SAE Paper 710291, Detroit, Mich., Jan (1971).
- Klimish, R.L. and Barnes, G.J., Environ. Sci and Tech., 6, 541 (1973).
- Libby, W.F., Science, 171, 499 (1971).
- Lunt, R.S., Bernstein, L.S., Hansel, J.G., and Holt, E.L., SAE Paper 720209, (1972).
- Meadowcroft, D.B., Nature, 226, 847 (1970).
- Meguerian, G.H., and Lang, C.R., SAE Paper 710291, (1971).

Meguerian, G.H., Rakowsky, F.W., Hirschberg, E.H., Lang, C.R. and Schock, D.N., SAE Natl. Auto. Engr. Meeting. SAE Paper 720480, Detroit, Mich., May (1972).

Roth, J.F., Ind. Eng. Chem. Prod. Res. Develop., 10, 381 (1971).

Shelef, M. and Gandhi, H., Ind. Eng. Chem. Prod. Res. Develop., 11, 393 (1972).

Shelef, M. and Kummer J. T. "The Behavior of Nitric Oxide in Heterogeneous Catalytic Reactions" Important Chemical Reactions in Air Pollution Control, Part II, 138, Symposium, AIChE, 62nd Annual Meeting, Washington, D. C., Nov. (1969).

Shelef, M. and Otto, K., J. Catalysis, 10, 413 (1968).

Shelef, M., Otto, K., and Gandhi, H., Atm. Environ., 3, 107 (1969).

Sourirajan, S. and Accomazzo, M.A., Can. J. Chem. Eng., 39, 88 (1961).

Sourirajan, S. and Blumenthal, J.L., Int. J. Air Water Poll. (Oxford), 5, 24 (1961).

Taylor, F.R., "Elimination of Oxides of Nitrogen from Automobile Exhaust," Air Poll. Found. Report No. 28 (1959).

APPENDIX

Table A-1. Cross Reference Listing of Catalysts.

<u>Number</u>	<u>Catalyst</u>	<u>Catalyst Group</u>
1	Lanthanum Strontium Cobalt Oxide	Cobalt-Based
2	Lanthanum Cobalt Oxide	"
3	Copper Cobalt Oxide	"
4	Barium Titanium Oxide	Other Non-Noble Metal
5	Cobalt Titanium Oxide	Cobalt Based
6	Nickel Zinc Ferrite	Other Nickel Based
7	Lanthanum Oxide-Strontium Oxide-Cobalt Oxide	Cobalt-Based
8	Lanthanum Strontium Cobalt Oxide	"
9	Lanthanum Cobalt Oxide	"
11	Cerium Oxide-Cobalt Oxide	"
15	Lanthanum Barium Cobalt Oxide	"
18	Lanthanum Cobalt Oxide	"
19	Lanthanum Barium Cobalt Oxide	"
20	Lanthanum Strontium Cobalt Oxide	"
22	Gadolinium Cobalt Oxide	"
23	Rare Earth Oxide	Rare Earth Oxide
24	Rare Earth Cobalt Oxide	Cobalt Based
24B	Rare Earth Cobalt Oxide	"
27	Lanthanum Oxide-Strontium Oxide-Cobalt Oxide	"
28	Tin Oxide	Other Non-Noble Metal
29	Strontium Cobalt Oxide	Cobalt-Based
30	Neodymium Cobalt Oxide	"
31	Dysprosium Cobalt Oxide	"
32	Cobalt Oxide	"
33	Cobalt Oxide	"
34A	Cobalt Oxide	"
34B	Cobalt Oxide	"

Table A-1. (Cont.)

<u>Number</u>	<u>Catalyst</u>	<u>Catalyst Group</u>
35	Lanthanum Nickel Oxide	Other Nickel-Based
37	Rare Earth Cobalt Oxide	Cobalt-Based
38	Rare Earth Cobalt Oxide	"
39	Rare Earth Cobalt Oxide	"
40	Rare Earth Cobalt Oxide	"
41	Rare Earth Cobalt Oxide	"
42	Rare Earth Cobalt Oxide	"
43	Bastnasite	Rare Earth Oxide
44	Copper Molybdenum Oxide	Copper Based
45	Lanthanum Manganese Oxide	Other Non-Noble Metal
46	Nickel Manganese Oxide	Other Nickel Based
47	Lanthanum Iron Nickel Oxide	Other Nickel-Based
49	Rare Earth Iron Nickel Oxide	" "
50	Rare Earth Nickel Oxide	" "
51	Lanthanum Iron Oxide	Other Non-Noble Metal
52	Monel Metal	Copper-Nickel
52U	Monel Metal	"
53	Lanthanum Copper Oxide	Other Copper-Based
54	Copper-Nickel Oxide	Copper-Nickel
56	Rare Earth-Chromium Oxide	Chromium-Based
57	Rare Earth-Nickel Cobalt Oxide	Other Nickel Based
58	Nickel Metal	Other Nickel-Based
58U	Nickel Metal	" "
60	Cobalt Manganese Oxide	Cobalt Based
61	Nickel Chromium Oxide Spinel	Nickel-Chromium
62	Rare Earth Copper Oxide	Other Copper-Based
63	Vanadium Chromium Oxide	Chromium-Based
64	Copper Vanadium Oxide	Copper Based
65	Nickel Vanadium Oxide	Other Nickel Based
66	Copper Chromium Oxide	Copper Based
67	Copper Nickel Vanadium	Copper Based
68	Bastnasite Nickel Oxide	Other Nickel-Based

Table A-1. (Cont.)

<u>Number</u>	<u>Catalyst</u>	<u>Catalyst Group</u>
71	Rare Earth Oxide	Rare Earth Oxide
73	Lanthanum Nickel Oxide	Other Nickel-Based
76	Lanthanum Rhodium Oxide	Noble Metal-Based
77	Lanthanum Rhodium Oxide	" "
78	Strontium Ruthenium Oxide	" "
79	Lanthanum Rhodium Oxide	" "
80	Lanthanum Rhodium Oxide	" "
81	Nickel Chromium Oxide Spinel	Nickel-Chromium
82	Strontium Ruthenium Oxide	Noble Metal-Based
83A	Bastnasite Nickel Chromium Oxide	Nickel-Chromium
83B	Bastnasite Nickel Chromium Oxide	"
84	Nickel Chromium Oxide Spinel	Nickel-Chromium
85	Nickel Chromium Oxide Spinel	"
86	Nickel Chromium Oxide Spinel	"
87	Nickel Chromium Oxide Spinel	"
89	Rare Earth Nickel Oxide	Other Nickel-Based
90	Strontium Yttrium Ruthenium Oxide	Noble Metal-Based
91	Nickel Chromium Oxide Spinel Lithium-doped	Nickel-Chromium
94	Nickel Oxide	Other Nickel-Based
96	Lanthanum Nickel Ruthenium Oxide	Noble Metal-Based
97	Nickel Chromium Oxide Spinel	Nickel-Chromium
98	Nickel Chromium Oxide Spinel	"
99	Nickel Chromium Oxide Spinel Platinum-doped	Noble Metal-Based
103	Zirconium Vanadium Oxide	Other Non-Noble Metal
104	Cerium Tungsten Oxide	" " "
106	Cerium Molybdenum Oxide	" " "
111	Cerium Oxide	Rare Earth Oxide
112	Copper Iron Oxide	Other Non-Noble Metal
113	Copper Chromium Oxide	Chromium-Based
114	Platinum-Doped Nickel	Noble Metal-Based

Table A-1. (Cont.)

<u>Number</u>	<u>Catalyst</u>	<u>Catalyst Group</u>
115	Unspecified	Other Non-Noble Metal
116	Copper Tungsten Bronze	Tungsten Bronze
117	Cerium Tungsten Bronze	" "
118	Sodium Tungsten Bronze	" "
119	Palladium	Noble Metal-Based
120	Ruthenium	" "
121	Platinum	" "
122	Rhodium	" "
123	Copper Oxide-Nickel Oxide	Copper-Nickel
124	Copper Oxide-Nickel Oxide	"
125	Copper Oxide-Nickel Oxide	"
126	Copper Oxide-Nickel Oxide	"
127	Nickel Oxide-Chromium Oxide	Nickel-Chromium
128	Nickel Oxide-Chromium Oxide	"
129	Nickel Oxide	Other Nickel-Based
131	Chromium Oxide	Chromium-Based

